

REF
620.169
1995
ABD

**EFFECT OF ORDER-DISORDER ON MAGNETIZATION AND
MAGNETIC PHASE TRANSITIONS OF SOME 3d TRANSITION
METAL ALLOYS**

BY

A.K.M.ABDUL HAKIM

**A THESIS SUBMITTED TO THE DEPARTMENT OF PHYSICS,
BANGLADESH UNIVERSITY OF ENGINEERING &
TECHNOLOGY IN PARTIAL FULFILLMENT OF THE
REQUIREMENT FOR THE DEGREE OF
DOCTOR OF PHILOSOPHY**



**BANGLADESH UNIVERSITY OF ENGINEERING &
TECHNOLOGY
DHAKA, BANGLADESH
NOVEMBER 1995**



#89369#

Bangladesh University of Engineering and Technology
Department of Physics

Certification of thesis work

A thesis on
"Effect of order-disorder on magnetization and magnetic phase transitions of
some 3d transition metal alloys"

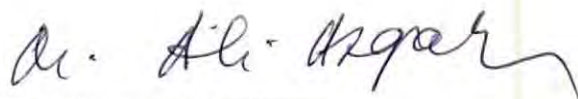
by

A.K.M. Abdul Hakim

has been accepted as satisfactory in partial fulfilment of the requirement
for the degree of Doctor of Philosophy in Physics and certify that the
student demonstrated a satisfactory knowledge of the field covered by this
thesis in an oral examination held on 17 December 1995.

Board of Examiners

1. **Prof. Dr. M. Ali Asgar**
Dept. of Physics
B.U.E.T, Dhaka
2. **Dr. Per Nordblad**
Assoc. Professor
Dept. of Solid State Physics
Institute of Technology
Uppsala University
Sweden.
3. **Prof. Dr. Gias Uddin Ahmad**
Head, Dept. of Physics,
B.U.E.T, Dhaka.
4. **Prof. Dr. Tafazzal Hossain**
Dept. of Physics,
B.U.E.T, Dhaka



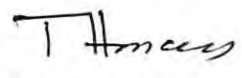
Supervisor and Chairman



Co-Supervisor



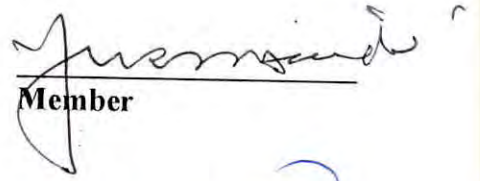
Member




Member

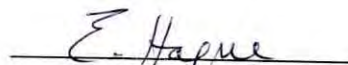
.....Contd.

5. **Prof. Dr. Yusuf Haider**
Dept. of Physics
University of Dhaka, Dhaka
6. **Dr. Mominul Huq**
Assoc. Professor
Dept. of Physics,
B.U.E.T, Dhaka
7. **Dr. S.M.M.R.Choudhury**
Ex.Member,(Physical Science)
Bangladesh Atomic Energy Commission
Dhaka
8. **Prof.Dr.Ehsanul Haque**
Dept. of Metallurgical Engineering
B.U.E.T, Dhaka
9. **Dr. B.K.Srivastava**
Assoc. Professor
Department of Physics
University of Rajasthan
Jaipur, INDIA


Member


Member


Member


Member


Member (External)

Dedicated to my beloved parents

CERTIFICATE

This is to certify that this thesis which the candidate has presented for a Ph.D.degree has been done by the candidate himself and does not contain any material extracted from elsewhere or from a work published by any body else. The work of this thesis has not been presented by the candidate for another degree or diploma in any other University. No other person's work has been used without due acknowledgement.



.....
Candidate



.....
Supervisor



.....
Co-Supervisor

Abstract

Department of Physics
Bangladesh University of Engineering and Technology

Doctor of Philosophy

Effect of order-disorder on magnetization and magnetic phase transitions of some 3d transition metal alloys

By

A.K.M.Abdul Hakim

This thesis describes the experimental investigation of the magnetic properties of $\text{Ni}_{1-x}\text{Pt}_x$, $0.14 \leq x \leq 0.57$, and pseudobinary $\text{Ni}_{1-x}\text{Fe}_x\text{Pt}$, $0.02 \leq x \leq 0.2$, and $\text{Ni}_{1-x}\text{Co}_x\text{Pt}$, $0.01 \leq x \leq 0.1$, alloys in the ordered and disordered states. The specimens are prepared, using arc furnace, with high purity constituent elements. The characterization of the samples are performed by X-ray diffraction and Scanning electron microscopy techniques. The measurements have been performed using Superconducting Quantum Interference Device (SQUID) magnetometer, Vibrating Sample Magnetometer (VSM) and AC Susceptometer.

Ni-Pt system undergo order-disorder transformation from face centered cubic structure in the disordered state to simple cubic ($L1_2$) and face centered tetragonal ($L1_0$) structure in the ordered state at stoichiometric ratios Ni_3Pt and NiPt respectively. The critical concentrations for the onset of ferromagnetism in the ordered and disordered states have been determined experimentally. A strong dependence of magnetic moment and Curie temperature is observed on ordering in Ni-Pt system. The depression of magnetic moment and Curie temperature on ordering in $L1_2$ phase and complete disappearance of ferromagnetism in $L1_0$ phase is revealed through the present study. The observed difference in the magnetic properties due to order-disorder transition in Ni-Pt alloys is explained as arising from the associated change of local environment. Clustering effects

have been found in the alloys near the critical concentrations in both the ordered and disordered phases.

A rapid increase in magnetic moment and Curie temperature is observed in the pseudobinary $\text{Ni}_{1-x}\text{Fe}_x\text{Pt}$ and $\text{Ni}_{1-x}\text{Co}_x\text{Pt}$ alloys in the ordered and disordered states when small amount of Fe or Co is substituted for nickel. Giant moments have been observed in both the ordered and disordered phases of Fe and Co doped systems. The observed giant moments depend sensitively on Fe and Co concentration, and have higher values per atom for lower concentration. Ordered pseudobinary alloys show hysteresis effect with large coercivities which increase very rapidly with decreasing temperature. The ordered Fe and Co doped pseudobinary alloys display unusual stepping behaviour in the initial magnetization process. The form of the initial magnetization characterized by critical field is explained in terms of domain wall pinning concept. The temperature dependence of magnetization for the ordered alloys has been measured which shows pronounced thermomagnetic history effect.

Acknowledgement

It is a great pleasure for me to express my sincere gratitude to my supervisor Prof.M.Ali Asgar, Department of Physics,BUET, for his keen interest, constant guidance and fruitful discussions and advice during the course of this thesis work. His generous support in moments of crisis as well as his profound scientific professionalism in the field of magnetism has enabled me to complete this thesis.

I am very much indebted to my co-supervisor Dr.Per Nordblad, Uppsala University, Sweden for his stimulating interest, excellent guidance and valuable assistance during the experimental work performed at the Solid State Physics Laboratory, Institute of Technology, Uppsala University,Sweden. His rigorous expertise and intuition in experimental work and generous support has contributed substantially to the completion of the present work.

I would like to express my sincerest gratitude to Prof.Gias Uddin Ahmad, Head, Department of Physics,BUET, for his interest and valuable suggestions in various stages of this work. It is my pleasure to express my grateful thanks to the members of the Doctoral Committee, Prof.Tafazzal Hossain, Department of Physics, BUET, Prof.Ehsanul Hoque, Department of Metallurgy, BUET, Prof.Yusuf Haider, Department of Physics, University of Dhaka, Dr.S.M.M.R.Choudhury, Ex.Member, Bangladesh Atomic Energy Commission and Dr.Mominul Huq, Associate Professor, Department of Physics,BUET, for their gracious help during the progress of my research work through their critical judgements, suggestions and kind appraisal of my work.

I am deeply grateful to Dr.M.A.Wazed Mia, Member Physical Science, Bangladesh Atomic Energy Commission for his interest and for his encouragement in this work.

I express my thanks and gratitude to Mr.M.A.Mazid, Head, Magnetic Materials Division, Atomic Energy Centre, Dhaka who first introduced me to the fascinating field of magnetism. His continuous support and interest in my work and the frequent stimulating scientific discussions that I had with him, have been most useful. I gratefully acknowledge all members of the Magnetic Materials Division, AECD, for their co-operation and inspiration during this work. I am thankful to Dr.Md.Feroz Alam Khan and Mr.Md.Shaif-UI-Alam of Physics Department, BUET for their valuable assistance.

I am indebted to Prof.Dr. Leif Lundgren for his help and assistance during my work at Uppsala

I wish to express my thanks to Dr.Peter Svedlindh, Dr.Per Granberg, Department of Solid State Physics, Uppsala University, Sweden for their heartfelt co-operation and stimulating discussions. Dr.Per Norling's assistance in electron microscopy and computer data analysis is highly acknowledged. I would like to thank Dr.Johan Mattsson, Mr.Johan Magnusson and Mr.Claes Djurberg for their fruitful co-operation and assistance in SQUID measurements and friendly gesture and Mr.Bengt Gotesson for technical assistance.

I am very much obliged to Dr.Yvonne Andersson of Inorganic Chemistry Department of Uppsala University for her generous assistance in the preparation of alloys and X-ray measurements.

I wish to thank Prof.Dr.Nguyen Chau, Dept of Physics, Hanoi University, Vietnam for fruitful and stimulating discussions.

I express my indebtedness and deep sense of gratitude to Dr.Lennart Hasselgren, Director, International Programme in Physical Sciences(IPPS), Uppsala University, Sweden for his keen interest and constant encouragement in this work.

Thanks are due to Dr.Garreth Bray, Asa Bergengren, Mona Thorwaldsdotter and Pravina Gajjar of International Science Programme (ISP),Uppsala University,Sweden for

their kind co-operation for having made my stay in Sweden comfortable.

I am obliged to express my gratitude to Bangladesh Atomic Energy Commission for giving me permission to carry out this work in Sweden on deputation.

I also wish to thank the authority of Bangladesh University of Engineering & Technology for providing me with the necessary permission and financial assistance for conducting this thesis work.

International Science Programme (ISP), Uppsala University, Sweden is thankfully acknowledged for providing me with the fellowship to perform part of this work in the Department of Solid State Physics, Institute of Technology, Uppsala University, Sweden for a period of two years.

The help and assistance from the Library of BUET and AECD is highly acknowledged.

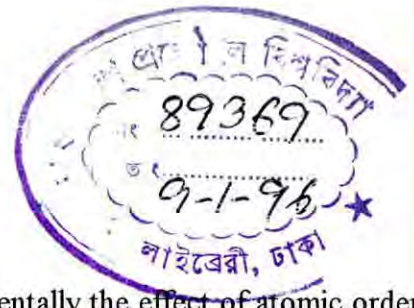
I am greatly in debt to my wife and members of my family for their constant encouragement and inspiration.

Thanks are due to Promila Rani Saha of Magnetic Materials Division, AECD for her skilful computer composing of my manuscript.

Contents

Chapter	Page No.
Chapter 1 Introduction	1
Reference	7
Chapter 2 Order-disorder phenomena and magnetic order	9
2.1 Order-disorder phenomena	9
2.1.1 General characteristics	9
2.1.2 Long range order and short range order	11
2.1.3 Crystallography	12
2.1.4 Kinetics of ordering	14
2.2 Effect of atomic order-disorder on magnetic ordering	16
2.2.1 Introduction to magnetic ordering	16
2.2.2 Magnetic properties of transition metal alloys	18
2.3 Purpose of this thesis	25
Reference	26
Chapter 3 Sample preparation and characterization	29
3.1 Preparation of samples	29
3.1.1 Ni _{1-x} Pt _x	29
3.1.2 Ni _{1-x} Fe _x Pt	31
3.2 Ordering of the sample	31
3.3 X-ray investigations	33
Reference	43
Chapter 4 Magnetization measurement techniques	44
4.1 Introduction	44

4.2	Vibrating Sample Magnetometer	44
4.3	SQUID Magnetometer	47
4.4	AC Susceptometer	52
	Reference	57
Chapter 5	Measurements on Nickel-Platinum alloys	58
5.1	Introduction	58
5.2	Experimental	60
5.3	Results and Discussion	62
5.3.1	Disordered alloys	62
5.3.2	Ordered alloys	74
	Reference	85
Chapter 6	Measurements on Ni_{1-x}Fe_xPt alloys	87
6.1	Introduction	87
6.2	Experimental	88
6.3	Results and Discussion	90
6.3.1	Disordered alloys	90
6.3.2	Ordered alloys	97
	Reference	121
Chapter 7	Measurements on Ni_{1-x}Co_xPt alloys	123
7.1	Introduction	123
7.2	Experimental	124
7.3	Results and Discussion	125
7.3.1	Disordered alloys	125
7.3.2	Ordered alloys	132
	Reference	154
Chapter 8	Conclusion	155



CHAPTER 1

Introduction

The aim of this thesis has been to investigate experimentally the effect of atomic order-disorder on the magnetic properties of nickel-platinum alloys and iron and cobalt doped equiatomic nickel-platinum alloys.

A large number of binary substitutional alloys are ordered at low temperatures and disordered at high temperatures[1-7]. A binary alloy which is in the ordered state, the constituent atoms A and B occupy definite lattice sites, but in a disordered state the constituent atoms occupy the available lattice sites at random. In the disordered state, like atoms are often adjacent to each other (AA or BB pairs), where as ordering commonly makes all nearest neighbours unlike. The order-disorder transition in magnetic alloys is interesting because atomic ordering and magnetic ordering are closely related phenomena characterized by well defined transition temperatures. Atomic ordering in alloys and compounds changes the local environment and consequently affect the intrinsic magnetic properties like magnetic moment, Curie temperature and single ion anisotropy[3,4,7]. The extrinsic magnetic properties like coercive field, remanence, permeability etc. are also affected by order-disorder transformation[8-12]. The study of order-disorder phenomena is therefore important in understanding magnetic properties of alloys as well as in tailoring magnetic characteristics for technological uses.

Many important magnetic materials have their magnetic hardness originating from lattice transformations. Both KS steel [13] and MT magnet steel [14] belong to this category. The former is composed of iron, cobalt and tungsten, while the latter is composed of iron, carbon and Aluminium. The real mechanism of high coercivity is related to order-disorder transformations in these cases. More over, the equiatomic alloys of Fe and Co with Pt show high coercivity and remanence which are the characteristic properties of hard magnetic materials and arise from complete ordering of the alloys[8,10,12]. The maximum magnetic

hardness occurs when the alloy is fully tetragonal. The interaction of domain walls with lamellae boundaries coupled with high anisotropy and the associated internal strains due to lattice transformations are thought to be responsible for the magnetic hardness of these alloys. The degree of magnetic softness depends essentially on the freedom of the movement and rotation of 180° and 90° magnetic domain walls. If the domain walls in a material can move easily under the influence of an external magnetic field, the material is said to be magnetically soft. On the otherhand when the freedom of the movement of domain walls is constrained by inhomogeneities, precipitates, imperfections, internal strains or due to magnetocrystalline anisotropy or magnetostriction, magnetically hard materials result.

The state of development and the present interest in understanding the effect of atomic ordering on magnetic properties and the kinetics of the mechanism of ordering phenomena is reviewed in chapter 2. This includes the general characteristics of the ordering processes, short range and long range order parameters, formation of superlattices and thermodynamic considerations of the transformations in relation to different alloy compositions.

Sample preparation and their characterization is a vital part in the investigation of the magnetic properties in the ordered and disordered states. Small amount of impurity can affect the true evaluation of magnetic properties. Therefore, high purity constituent elements with purity 5 N have been used to prepare good quality samples.

Ordering of the samples is another important parameter for comparing the magnetic properties of the ordered and disordered phases quantitatively. Ordering of the Ni-Pt alloys and their doped system have been done on the basis of the phase diagram and the information available from previous reports[7,15-18]. The knowledge of the ordering kinetics of similar systems have been made use of in the preparation of ordered and disordered samples. Ordered and disordered phases can be identified by X-ray, neutron and electron diffraction[19,20]. In the present work X-ray investigations have been employed to identify the ordered and

disordered phases. The presence of sharp superlattice lines in the X-ray photograph and diffractogram conclusively determines the ordered structure of the alloys. Scanning electron microscope (SEM) has been used to detect if there is any surface defect, imperfection or precipitated phase. Black precipitates, identified as second phase, have been observed for the ordered Fe and Co doped NiPt system in this SEM studies. These findings have the compatibility with the magnetization and susceptibility measurements in which the effect of these defects are manifested and have fruitfully been exploited to interpret the magnetic behaviour of the alloys concerned.

A series of $\text{Ni}_{1-x}\text{Pt}_x$ alloys with $x = 0.14, 0.24, 0.30, 0.44, 0.5$ and 0.57 and the pseudobinary $\text{Ni}_{1-x}\text{Fe}_x\text{Pt}$ ($0.02 \leq x \leq 0.2$) and $\text{Ni}_{1-x}\text{Co}_x\text{Pt}$ ($0.01 \leq x \leq 0.1$) alloys have been prepared in an arc furnace. The alloy compositions have been shown to be very close to the nominal values considering the negligible small losses during melting. These are described in detail in chapter 3.

In order to determine the magnetic property of a substance, magnetization and susceptibility measurements are the powerful techniques for their relative simplicity and flexibility. From the magnetization measurements it is possible to evaluate quantitatively magnetic moment per atom, Curie temperature, susceptibility of the material, permeability, exchange and anisotropy energy and qualitatively the spin and the domain structures. AC susceptibility is a special technique to identify unambiguously magnetic phase transitions in a variety of magnetic materials, particularly for the alloys in which the transition from the ferromagnetic state to the paramagnetic state occurs gradually, and also for multiphase materials and the alloys near the critical concentration where the statistical concentration variations are present. Atomic-scale experiments, such as neutron diffraction and Mossbauer spectroscopy are required to reveal the detailed microscopic structure.

In the present thesis susceptibility and magnetization measurements have been

employed to investigate the magnetic properties of $\text{Ni}_{1-x}\text{Pt}_x$ and pseudobinary $\text{Ni}_{1-x}\text{Fe}_x\text{Pt}$ and $\text{Ni}_{1-x}\text{Co}_x\text{Pt}$ alloys. DC magnetization and susceptibility have been measured with Vibrating Sample Magnetometers (VSM) and also with a Superconducting Quantum Interference Device (SQUID) magnetometer. AC susceptibility measurements are carried out with a Lake Shore Susceptometer and a laboratory built AC susceptibility measuring system based on mutual induction method. By using this technique magnetic phase transition temperatures for the multiphase Co doped NiPt system have been determined. Description of the various techniques used in this thesis work for measuring the magnetic properties are described in chapter 4.

Binary $\text{Ni}_{1-x}\text{Pt}_x$ and pseudobinary $\text{Ni}_{1-x}\text{Fe}_x\text{Pt}$ and $\text{Ni}_{1-x}\text{Co}_x\text{Pt}$ alloys have been studied for their magnetic properties covering a wide range of composition, temperature and magnetic field. The nickel-platinum binary alloy system has been chosen for its continuous range of solid solubility for all concentrations and for having order-disorder transitions affecting magnetic properties[7,21,22]. The spontaneous magnetization and the Curie temperature of this interesting system can be measured in the disordered and ordered phases directly without changing the degree of order, since the Curie temperatures of the alloys with different compositions are much lower than the order-disorder transition temperature.

Atomic ordering changes the spatial distribution of atoms in the lattice sites. Due to this change of the local environment magnetic moments and the Curie temperatures of the alloys are affected. The aim of this investigation is to measure and compare the magnetic moment and Curie temperature in the two extreme situations; i.e. the most ordered state obtained after a long time annealing at a temperature below the order-disorder transition temperature, and the most disordered state obtained by drastic quenching of the alloy from disordered solid solution phase. A strong dependence of magnetic properties on atomic ordering is observed, specially near the equiatomic composition. A depression of magnetic moment and Curie temperature is observed near the Ni_3Pt composition where the fcc (A1)

structure in the disordered phase changes to L1₂ structure in the ordered phase. Around equiatomic composition of nickel and platinum this effect becomes prominent and can even change the type of magnetic ordering associated with the change from fcc (A1) structure to fct (L1₀) on ordering. This is explained as due to the change in the number of nearest neighbours of Ni atoms that is affected by the order-disorder phenomena. The disappearance of ferromagnetism in L1₀ phase indicates that a nearest-neighbour number of Ni atoms greater than four is necessary to give rise to ferromagnetism in the Ni-Pt System.

The concentration dependence of magnetic moment and Curie temperature of the disordered alloys show that the critical concentration, the concentration of Pt at which Ni-Pt system loses its ferromagnetism at zero kelvin, is approximately 57at.% Pt and is close to the reported values of ≈ 58 at.% Pt[23-25]. For the ordered Ni-Pt system it appears from the magnetization versus field curves and their Arrott Plots [26-28] that the alloy with Pt concentration 44at.% is also very close to the critical concentration. Similar value has been quoted in the recent study of the Ni-Pt phase diagram[22].

A detail study of the magnetization as a function of magnetic fields at different temperatures for the alloys near the critical concentrations suggest that clusters are formed in the critical alloys in the ordered and disordered phases. It appears that magnetization is inhomogeneously distributed in the alloys near the critical concentrations for both the ordered and disordered phases. These are in agreement with[29] but disagree with[23-25] for the disordered phases. The latter authors claimed that magnetization is homogeneously distributed for the disordered alloys near the critical concentration. In chapter 5 detail magnetization measurements for Ni_{1-x}Pt_x alloys are illustrated with results and discussion.

Pseudobinary Ni_{1-x}Fe_xPt and Ni_{1-x}Co_xPt system in the disordered states show that magnetic moment and Curie temperature increase continuously with increasing Fe and Co concentration. This increase is faster at lower concentration and become slower with

increasing x . The saturation magnetization is observed for magnetic field $H < 4$ kOe and there is no hysteresis. Substitution of Fe and Co for Ni induce giant moments and the giant moment inducement is larger for low concentrations of Fe and Co than for high concentrations.

Ordered $\text{Ni}_{1-x}\text{Fe}_x\text{Pt}$ and $\text{Ni}_{1-x}\text{Co}_x\text{Pt}$ alloys show unusual critical field behaviour in magnetization process at low temperature in the zero field cooled condition i.e. stepping behaviour in the initial magnetization process. The magnetization could not be saturated even with magnetic field of 50 kOe in contrast with the behaviour of the disordered alloys. Hysteresis effects are observed with high coercivity. This coercivity has a strong temperature dependence which increases very rapidly with decreasing temperature. The critical field is found to be equal to the coercive field for all the Fe doped alloys. These phenomena have been interpreted in terms of domain wall pinning effect, high anisotropy and multiphase formation. This type of behaviour has been observed in many other systems and explained as due to domain wall pinning effect[30-34]. But for Co doped alloys some anomalous results are obtained. In the ordered Fe and Co doped systems giant moments have also been observed which decrease with increasing x . This is explained as due to the polarization of the host matrix by Fe or Co atoms. The giant moment is considered as the sum of the bare localized moment of Fe or Co atom and the induced moment of the matrix. One way to interpret the results is to attribute the total moment to the Fe or Co atom. Giant moments of about 4-6 μB associated with Fe and Co atoms have been found in the dilute alloys of PtFe and PtCo due to the polarization of Pt matrix[35-39]. Magnetic moment and Curie temperature increase with increasing x as in the case of disordered phase. Chapter 6 and 7 describes the magnetic properties of $\text{Ni}_{1-x}\text{Fe}_x\text{Pt}$ and $\text{Ni}_{1-x}\text{Co}_x\text{Pt}$ systems respectively in the disordered and ordered states together with the possible interpretation of the unusual magnetic behaviour observed in ordered phases of both the systems.

The major conclusions are presented in chapter 8.

Reference

1. Van Deen, J.K. and F. Van Der Woude *Acta Metallurgica* (1981) Vol. 29, 1255
2. Oyedele, J.A. and M.F. Collins, *Phys. Rev.* (1977), B16, 3208
3. Sanchez, J.M., J.L.Moran-Lopez, C. Leroux and M.C. Cadeville, *J.de. Phy..* (1988), C8, Tome 49, 107.
4. Sumiyama, K., M. Shiga, Y. Kobayashi, K. Nishi and Y. Nakamura, *J. Phys.* F8, 1978, 1281
5. Shunk, F.A., *Constitution of Binary Alloys*, 2nd Supplement, McGraw-Hill (1969), P.335.
6. *Metals Handbook*, 1973a,b, Vol.8 (Am. Soc. Met.,Metals Park OH), P.306
7. Dahmani, C.E., M.C. Cadeville, J.M. Sanchez and J.L. MoranLopez,*Phys.Rev.Letters*, (1985), 55, 1208
8. Hadjipanayis,G.C. and P.Gaunt, *J.Appl.Phys.* 1979, 50, 2358
9. Tsoukatos, A.,H.Wan, G.C. Hadjipanayis, Y.J. Zhang, M.Waite,and S.I.Shah, *J.Mag.& Mag.Mat.* 1993,118, 387
10. Craik, D.J., *Plat. Metals Rev.* 1972, 16, 129
11. Martin,D.C., *J.Phys.* F5, 1975, 1031
12. Elcock,E.W., *Order-disorder phenomena*, John Wiley and Sons, Inc., 1956, 34.
13. Honda,K. and S.Saito., *Sci., Rept., Tohuku Imp. Univ*, 1920, 9,417
14. Mishima,T, and N,Makino, *Iron & Steel*, 1956, 43, 557,726
15. Hansen,M., *Constitution of Binary Alloys*, 2nd edn. P.493, McGraw-Hill, NewYork (1958)
16. Dahmani,C.E., M.C.Cadeville and V.Pierron-Bohnes, *Acta Metallurgica*, (1985), Vol. 33, P. 369-377
17. Greenholz,M., A.Kidron and U. Shimony, *J. Appl: Crystallography*, 7, (1974), 83
18. Esch,V. and Schneider, A.I, *Z. Electrochem.*,1944, 50,268

19. Cullity, B.D., Elements of X-ray diffraction, edited by Addison-Wesley Pub. Co. Inc., 1956, P.363
20. Tsoukatos, A., H.Wan, G.C.Hadjipanayis, Y.J. Zhong, M.Waite and S.I.Shah. J. Mag. and Mag. Mat. 118, (1993), 387-393
21. Massalski, T.B., H.Okamoto, and P.K.Subramanion, Binary Alloy Phase Diagram (ASM Int. Materials Park, 1990), vol.2, page 1744
22. Cadeville, M.C., C.E.Dahmani and F.Kern. J. Mag. Mag. Mat., 1986, 54-57, 1055
23. Alberts, H.L., J.Beille and D.Bloch, Phys. Rev., 1974, B9, 2233
24. Besnus, M.J. and A. Herr Phys. Lett., 1972, 39A, 83
25. Beille, J., D.Bloch and E.P.Wohlfarth, Phys. Lett., 1973, 43A, 207
26. Arrott, A., Phys. Rev. 1957, 108, 1394
27. Kouvel, J.S. Gen., Elec., Research Lab., Report 1957, 57-RL-1799
28. Belov, K.P., and A.N.Goryaga, Fizika Metall., 1956, 2, 3
29. Ododo, J.C. and W.Howarth, Solid State Comm., 1978, 26, 39
30. Barbara, B., C.Becle, R.Lemaire and D.Paccard, J. De Phys. (Paris), 1971, 32, C1-299
31. Folks, L., C.D.Milham and R.Street, Proc. 7th Int. Symposium on Magnetic Anisotropy & Coercivity in RE-TM alloys, 1992, Canberra, Australia, 274
32. Oesterreicher, H., J. Appl. Phys., 1971, 42, 5137 and 1973, 34
33. Yang, Y.C. and Zhang, X.D., J. Appl. Phys., 1990, 67, 4765
34. Nesbitt, E.A., G.Y.Chin, G.W.Hull, R.C.Sherwood, M.L.Green and J.H.Wernick, Proc. 1972, Conf. on Magn. Magn. Mat., AIP Conf. Proc. 1973
35. Crangle, J., and W.R.Scott, J. Appl. Phys. 1965, 36, 921
36. Bozorth, R.M., D.D.Davis, and J.H.Wernick, J. Phys. Soc. Jpn, 1962, 17, Suppl. B1, 112
37. Foner, S., E.J.McNiff Jr., and R.P.Guertin, Phys. Letters, 1970, 31A, 466
38. Swallow, G.A., G.Williams, A.D.C.Grassi, and J.W.Loram, Phys. Rev., 1975 B11, 330
39. Ododo, J.C. J. Phys. 1982, F12, 1821

CHAPTER 2

Order-disorder phenomena and magnetic order

2.1 Order-disorder phenomena

2.1.1. General characteristics:

Order-disorder phenomena, in metallic alloys and compounds, belong to the class of cooperative' phenomena of considerable intrinsic interest to physicists. There has been much interest in alloys which undergo a critical phase transition from ordered to disordered states since most of the physical properties of the alloys strongly depend on the atom distribution on the lattice sites. In many binary alloys, usually those which exhibit complete or nearly complete miscibility, at particular compositions there can exist below a critical temperature, T_C , an "ordered" lattice (superlattice) and above T_C a "disordered" lattice [1-7].

First order-disorder phenomena was predicted by G.Tammann in 1919 [8] on CuAu alloy on the basis of chemical evidence and latter on in 1925 Johansson and Linde [9] confirmed the ordered structure of CuAu from X-ray pattern. In the disordered state in most substitutional solid solutions, the two kinds of atoms A and B are arranged more or less at random on the atomic sites of the lattice. By "ordered" is meant that the lattice sites are grouped into sublattices, each of which is occupied predominantly by one species of atoms. Simple superlattices in binary alloys with cubic structure occur near composition corresponding to stoichiometric ratios of atoms like A_3B , AB , AB_3 etc. Ideally, at sufficiently low temperatures this long range order should extend throughout each single crystal. However, at low temperature the ordering process is too slow and at high temperature the disturbing thermal agitation is too large to allow the ideal condition ever to be attained. The ordered state in an actual single crystal (or grain) should be imagined as consisting of many small volumes within which the order is very high but varying in a discontinuous manner at the boundary between these volumes. Each of these volumes can be thought of as separately nucleated during the transition from a random to an ordered solid solution. Clearly, the overall degree of order in a crystal at equilibrium depends upon the size of these blocks of high

order and it changes with temperature and with deviation from the stoichiometric composition which corresponds to an ideal complete order.

For sometime it was believed that the order-disorder transformation is a homogeneous transformation; i.e., the two states cannot coexist in equilibrium. Now mounting evidence [3,10,11] points to the conclusion that this is not true and that many, if not all, ordering reactions are heterogeneous and similar to the conventional phase transitions.

The ordering process is very conveniently described in terms of a change in the number of nearest neighbours of each kind of atoms. The ordering usually leads to a preferential formation of mixed bonds AB rather than AA or BB. In the disordered state like atoms are often adjacent to each other i.e., they prefer AA or BB bonds. On the basis of thermodynamics it can be shown that an ordered arrangement of atoms in an alloy may produce a lower internal energy compared to a disordered arrangement, particularly if the segregation of atoms to designated atomic sites occurs at relatively low temperatures where entropy, associated with randomness, plays a lesser role. The thermodynamic criterion for an alloy to be orderable is

$$E_{AB} < \frac{1}{2}(E_{AA} + E_{BB}) \quad (2.1)$$

where E_{AA} and E_{BB} represent energies of like pairs of atoms and E_{AB} represents the energy of the unlike pair. The physical significance of this criterion is that atomic ordering is feasible only when the bond energy of the unlike atom pair is less than the mean bond energy of the two kinds of like atom pairs. On the other hand, if $E_{AB} > \frac{1}{2}(E_{AA} + E_{BB})$, the alloy system will tend to form mixtures of two A- and B-rich solid solutions, in which like atom pairs dominate.

2.1.2. Long range order and short range order

With perfect order at a low temperature the mathematical probability of finding an A atom on an A site and a B atom on a B site is unity. At higher temperatures, however, the probability that an A site is occupied by an A atom will be reduced to a fraction of unity, say p . This departure from perfect order can be described, according to Bragg and Williams by means of the long range order parameter, S ,

$$S = (p-r)/(1-r) \quad (2.2)$$

where r is the fraction of A atoms in the alloy. According to expression(2.2), S varies from one to zero as order decreases.

The order-disorder transition, like the magnetic phase transition, is a cooperative phenomena. As more atoms find themselves in wrong atomic sites due to thermal agitation the energy difference indicated by (2.1) decreases and it becomes easier to produce further disorder. Eventually a critical temperature, T_c , is reached at which all distinction between different sites is lost.

This simple approach does not allow for the possibility of the existence of magnetic domains and other types of interruptions in the ordered array of atoms that may cause a departure from perfect order which makes it possible for a high degree of local order to exist even though its perfection is not absolute on a large volume scale.

In order to describe such situations an alternative method of defining the state of order is possible which, instead of considering the probability of finding A or B atoms on designated A or B sites, takes into account the number of unlike nearest neighbours around a given atom. The Bethes, short range order parameter σ is defined by,

$$\sigma = q-q_r/q_m-q_r \quad (2.3)$$

where q denotes the fraction of unlike nearest neighbours at a given temperature and q_r and q_m correspond to the fractions of unlike nearest neighbours at conditions of maximum randomness and maximum order. So σ is defined in such a way that it would become unity for

perfect order and zero for randomness. Actually, instead of reaching zero on disordering σ usually remains a definite value above T_C . In terms of the relationship between atoms σ measures the state of order in the immediate vicinity of a given atom unlike the long range order parameter, S , which deals with the whole lattice.

2.1.3 Crystallography

Atomic ordering changes the crystal structures of the alloys and compounds. FeCo alloy is bcc in the disordered state and forms ordered L2₀(superlattice) structure after atomic ordering. The ordered L2₀ structure corresponds to CsCl structure in which iron atoms occupy only corner sites and Co atoms only the cube center sites. In this ordered structure, each atom has eight unlike nearest neighbours. Again Ni₃Fe, Fe₃Pt, Co₃Pt and Ni₃Pt alloys are fcc in the disordered state and form superlattices corresponding to L1₂ structures on ordering. This structure is equivalent to four inter-penetrating simple cubic lattices. In L1₂ ordered structure all A atoms are accommodated at the corners of the unit cells and all B atoms at the face centres of the unit cells. Another type of ordered structure L1₀ is found in alloys of FeNi, FePt, CoPt and NiPt and they are all fcc in the disordered state. Ordering of all these equiatomic AB alloys in the fcc lattice necessitates the segregation of atoms of each species alternately on the (001) planes leading to a change in the original structure from fcc to an ordered face-centered tetragonal (fct) L1₀ superlattice. Each atom has eight nearest neighbours of opposite kind in the adjacent (001) planes, and four of the same kind in its own (001) plane at a slightly greater distance, since the axial ratio, c/a , is usually less than unity. Another type of superlattice DO₃, is found in ferromagnetic Fe₃Al and Fe₃Si alloys in which the bcc lattice is accompanied by an enlargement of the unit cell by a factor of 8, i.e, unit cell of an ordered alloy in the bcc lattice contains 8 original unit cells of the disordered bcc structure. Four common types of superlattices found in ferromagnetic alloys are given in table 2.1[12].

TABLE 2.1
Four common types of superlattices observed in ferromagnetic alloys

Type	Crystal structure	No. of atoms per unit cell	Coordinates of atoms in the unit cell	No. of possible distinct domains	Examples
L1 ₀	Face-centered tetragonal	4	2A in (000, $\frac{1}{2}\frac{1}{2}0$) 2B in ($\frac{1}{2}0\frac{1}{2}$, $0\frac{1}{2}\frac{1}{2}$)	6	FePt, CoPt, NiPt:FePd
L1 ₂	Face-centered cubic	4	1B in (000) 3A in ($0\frac{1}{2}\frac{1}{2}$, $\frac{1}{2}0\frac{1}{2}$, $0\frac{1}{2}\frac{1}{2}$)	4	Ni ₃ Fe, Ni ₃ Mn, Fe ₃ Pt, Pt ₃ Fe, Pt ₃ Co, Ni ₃ Pt, Pd ₃ Fe
L2 ₀	Body-centered cubic	2	1A in (000) 1B in ($\frac{1}{2}\frac{1}{2}\frac{1}{2}$)	2	FeCo
DO ₃	BCC with unit cells 8 times larger than those in the disordered lattice	6	4B in (000) f.c. 4A in ($\frac{1}{2}\frac{1}{2}\frac{1}{2}$) f.c. 8A in $\pm(\frac{1}{4}\frac{1}{4}\frac{1}{4})$ f.c.	4	Fe ₃ Al, Fe ₃ Si

2.1.4. Kinetics of ordering

The knowledge of the kinetics of the order-disorder transition has been provided by the investigation of the ordering processes of under cooled disordered alloys or the disordering processes of overheated ordered alloys. The kinetics may be inferred from the evolution of heat, the change of some line on an X-ray photograph, or the variations of electrical resistance, magnetic susceptibility, or some other physical property [13]. The time at which the equilibrium state is approached has been observed to vary markedly from one system to another and to depend on the actual temperature T and on the difference between T and critical temperature, T_c of the system.

An alloy as a thermodynamic system will tend to make its free energy minimum. It will do so if sufficient time is given for this equilibrium to be attained. Now at finite temperature, the enthalpy H is greater than the free energy G of the system by an amount given by absolute temperature T times the entropy S' .

$$G = H - TS' \quad (1.4)$$

At high temperature the increase in entropy, hence the corresponding disorder will be favoured so long as the associated increase in the internal energy is more than compensated by the reduction of free energy by the entropic part.

A disordered state can be obtained if the alloy is cooled rapidly enough from the high temperature so as to inhibit the formation and growth of ordered regions. The nucleation for ordered regions involves the diffusion of atoms. In order to overcome local energy barriers of the disordered alloy which is in a metastable state the atoms must get sufficient thermal energy. The number of atoms available with necessary activation energy is controlled by the Boltzman factor $\exp(-E_a/kT)$, where E_a is the appropriate activation energy for diffusion. The time required for ordering should thus vary exponentially with temperature.

This is expressed by the Arrhenius law,

$$\tau(T) = \tau_0 \exp E\alpha/KT \quad (2.5)$$

where τ_0 is a constant of the order of 10^{-13} - 10^{-14} second. Dahmani et al [14] and Berg et al [15] found $\tau_0 = 1.3 \times 10^{-13}$ and 6×10^{-14} sec and $E\alpha = 2.48$ and 3.12 eV for $Ni_{0.5}Pt_{0.5}$ and $Co_{0.25}Pt_{0.75}$ respectively. The exponential dependence of relaxation time on temperature makes the choice of annealing temperature very critical. The annealing time on the other hand has a linear relation with ordering. This is because annealing time is proportioned to the number of attempts made by an atom to overcome the local energy barriers.

For a particular alloy number of distinct domains that can be formed plays an important role in sustaining a metastable microstructure. An aggregate can not sustain a metastable state when the number of different types of domains is less than four. When this number exceeds four the system is more likely to maintain the metastable microstructure according to Bragg [16].

In order to prepare an ordered magnetic alloy properly we must know the time rate at which the equilibrium state of order or disorder is approached, since there are marked variations in the rates at which superlattices form in different alloys. If the ordered state is preferred for the product of the alloy, the temperature and time for the ordering treatment must be chosen according to the specific kinetics. On the other hand if a disordered state is desired, we have to know first whether or not the ordering transition can be suppressed by quenching. So the knowledge of the kinetics of order-disorder transition is thus extremely important in the preparation of the alloy product.

2.2 Effect of atomic order-disorder on magnetic ordering

2.2.1 Introduction to Magnetic Ordering

The onset of magnetic order in solids have two basic requirements:

- (i) individual atoms should have magnetic moments (spins)
- (ii) exchange interactions should exist that couple them together.

Magnetic moments originate in solids as a consequence of overlapping of the electronic wave functions with those of neighbouring atoms. This condition is best fulfilled by some transition metals and rare-earths. The exchange interactions depend sensitively upon the interatomic distance and the nature of the chemical bonds, particularly of nearest neighbour atoms. When the positive exchange dominates, which corresponds to parallel coupling of neighbouring atomic moments (spins), the magnetic system becomes ferromagnetic below a certain temperature T_C called the Curie temperature. The common spin directions are determined by the minimum of magnetocrystalline anisotropy energy of the crystal. Therefore, ferromagnetic substances are characterized by spontaneous magnetization. But a ferromagnetic material in the demagnetized state displays no net magnetization in zero field because in the demagnetized state a ferromagnet of macroscopic size is divided into a number of small regions called domains spontaneously magnetized to saturation value and the directions of these spontaneous magnetization of the various domains are such that the net magnetization of the specimen is zero. The existence of domains is a consequence of energy minimization. The size and formation of these domains is in a complicated manner dependent on the shape of the specimen as well as its magnetic and thermal history. When negative exchange dominates, adjacent atomic moments (spins) align antiparallel to each other, and the substance is said to be anti-ferromagnetic below a characteristic temperature, T_N , called the Neel temperature. In the simplest case, the lattice of an antiferromagnet is divided into two sublattices with the magnetic moments of these in antiparallel alignment. This results in zero net magnetization. A special case of antiferromagnetism is ferrimagnetism. In ferrimagnetism there are also two

sublattices with magnetic moments in opposite directions, but the magnetization of the sublattices are of unequal strength resulting in a non-zero magnetization and therefore has net spontaneous magnetization. At the macroscopic level of domain structures, ferromagnetic and ferrimagnetic materials are therefore similar. The Curie and Neel temperatures characterize a phase transition between the magnetically ordered and disordered (paramagnetic) states. From these simple cases of magnetic ordering various types of magnetic order exists, particularly in metallic substances. Because of long range order and oscillatory nature of the exchange interaction, mediated by the conduction electrons, structures like helical, conical and modulated patterns might occur. Examples of different types of magnetic order are shown in Fig.2.1.

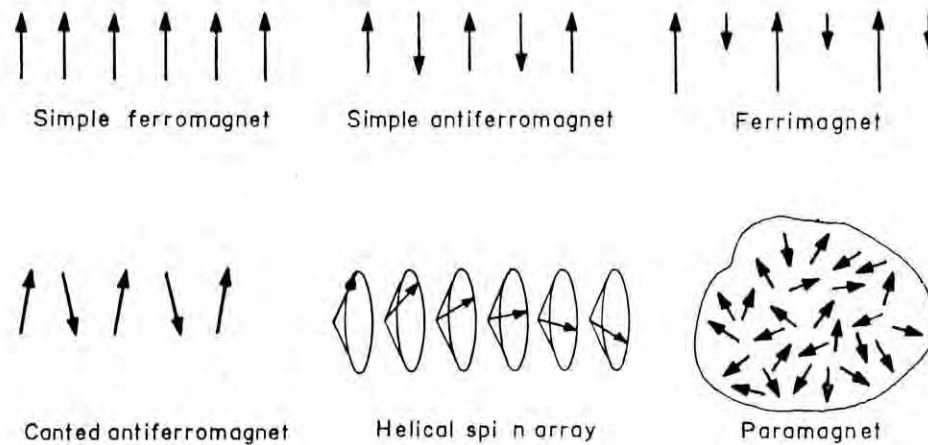


Fig. 2.1. Examples of different types of magnetic order using a linear array of localized moments, including paramagnet.

2.2.2 Magnetic Properties of Transition Metal Alloys

Transition metals iron, cobalt and nickel are three archetypal ferromagnets and the existence of partially filled 3d electron shells is the origin of the magnetic properties. The magnetic properties of these three ferromagnetic metals have extensively been studied for many decades, but even now it is by no means the case that iron, cobalt and nickel are fully understood [17]. The experimental observed values of the fundamental properties are as follows : magnetic moments in Bohr magneton

$\text{Fe} = 2.216\mu_B, \text{Co} = 1.716\mu_B, \text{Ni} = 0.616\mu_B$ and Curie temperatures, $T_C, \text{Fe} = 1043\text{K},$
 $\text{Co} = 1400\text{K}, \text{Ni} = 631\text{K}$ [18].

Transition metals and their alloys display a rich variety of magnetic properties. Among them alloys of 3d transition metals notably iron, cobalt and nickel with palladium and platinum has drawn considerable attention since the first reports of their magnetic properties by Crangle et al [19-21] and Bozorth et al [22].

Although Pd and Pt do not exhibit any ferromagnetism in the pure metallic state but seem capable of ferromagnetic interaction when alloyed with elements of iron group transition metals. Small concentrations (approximately 1 at.% or even much less) of Fe, Co or Ni are sufficient to give rise to ferromagnetism in the alloys and the moment per 3d atom considerably exceed the values characteristic of the ferromagnetic elements themselves. The moment per 3d atom is of the order of 5-10 Bohr magnetons in the Pd or Pt alloys and is larger than the 3d shell itself can possess. Neutron diffraction experiments have shown that this giant moment arises from the polarization of the Pd or Pt atoms in the vicinity of a 3d atom with a range of about 10\AA and so includes about 200 host atoms [23]. This effect of polarization is stronger in Pd matrix than in Pt matrix. It is because pure Pd is a nearly ferromagnetic metal sometimes called an incipient ferromagnet [24,25]. Their paramagnetic susceptibility is rather high and accordingly easily polarized. Both Pd and Pt are exchange enhanced and the enhancement factor for Pd ≈ 10 while for Pt ≈ 3 [26]. Among these two

elements Pt has special interest. Alloys of Pt with transition metals like Fe,Co,Ni,Mn and Cr form wide range of solid solutions with the face centered cubic structure (A1) at high temperature and undergo atomic ordering below a critical temperature, T_C , forming superlattices as those found in Cu-Au system [3,4,7,27]. Therefore the alloys of 3d transition metals with Pt has considerable interest in the study of their magnetic properties in the ordered and disordered states.

Atomic or chemical ordering is strikingly analogous to magnetic ordering. Both are cooperative phenomena characterized by a sharp critical temperature and both are controlled by interactions between atoms or spins. Atomic ordering change the local environment or the relative number of different kinds of nearest neighbouring atomic pair in a large number of alloys. The nature of the nearest neighbours in a particular alloy can influence magnetic moments, single ion anisotropy and the exchange integral, and through the variation of these parameters the magnetic properties like magnetization, magnetic phase transition temperature and anisotropy can be changed dramatically. The magnetic moment of an atom in an alloy matrix is not only determined by its chemical nature but also by its atomic environment through the loss or gain of orbital electrons and the polarization effect of the conduction electrons. This is observed in the manifestation of giant magnetic moment in the alloys of 3d transition metal with Pt or Pd [22,28-30]. Besides the effect of order-disorder on primary magnetic properties, the secondary properties of a magnetic alloy is also drastically influenced by the state of ordering. Thus the permeability, remanence, coercivity, hysteresis loop etc. which characterize a magnetic material suitable for technological applications are influenced by atomic ordering [31-35]. The understanding of the mechanism of coercivity and remanence in terms of domain distribution, domain-wall pinning & domain nucleation can be facilitated by investigating how the order-disorder affects the movement of the domain walls and the magnetic hardness of an alloy.

Saturation magnetization

The saturation magnetization is known to change with order in many transition metal alloys and compounds. In Fe-Co binary system in the composition range 30-70 at.% Fe show an order-disorder transition at $\approx 1000\text{K}$ [36]. The disordered alloys have bcc and ordered ones have B2 (CsCl) structure. An increase of 4% of the saturation magnetization on ordering is observed [37,38]. Ni_3Fe has order-disorder transition temperature of $\approx 820\text{K}$ [39] having fcc structure in the disordered state and cubic $L1_2$ (Cu_3Au) structure in the ordered state. Atomic ordering of Ni_3Fe increases saturation magnetization by about 6% as compared to the disordered state [40].

Similarly an increase in saturation magnetization in Fe_3Al and Fe_3Si occurs on ordering. Both of them have DO_3 type of structure in the ordered state and bcc structure in the disordered state. In Ni_3Mn , which orders like Ni_3Fe , ordering has a profound effect. The disordered alloy is paramagnetic or weakly ferromagnetic depending on the degree of disorder and slight compositional variation around stoichiometric ratio while the ordered alloy is ferromagnetic [41-44]. The disordered samples of this alloy show an average moment of $0.1\mu\text{B}$ per atom. After ordering the moment increases to $1.02\mu\text{B}$ per atom. This large increase in magnetization caused by atomic ordering in Ni_3Mn has been interpreted in terms of the coupling of magnetic moments.

The Heusler alloys Cu_2MnSn and Cu_2MnAl , like Ni_3Mn , are paramagnetic when disordered and ferromagnetic when ordered. Noteworthy the Heusler alloys were the first group of ferromagnets discovered to display sensitive dependence of saturation magnetization and Curie temperature upon the degree of long-range chemical order [45]. The occurrence of ferromagnetism on ordering in all these three alloys are based on the fact that ordering makes the Mn-Mn distance large enough for the exchange interaction to become positive.

Fe-Pt system orders like $\text{Cu}_3\text{Au}(\text{L}1_2)$, $\text{CuAu}(\text{L}1_0)$ and $\text{Cu}_3\text{Au}(\text{L}1_2)$ structures at the stoichiometric composition A_3B , AB and AB_3 and their ordering temperatures are 1109K, 1573K and 1625K respectively. Saturation magnetization decreases on ordering for both Fe_3Pt and FePt alloy [4,46]. The compound Fe_3Pt is well-known for its Invar characteristics and studied extensively. The results of magnetization measurements showed that both magnetization and high field susceptibility decrease with increasing degree of order. In case of equiatomic FePt ordering decreases saturation magnetization by 15% but increases the magnetic hardness of the alloy. A coercivity as high as 1.5 kOe has been observed [35]. It is suggested that the high coercivity is associated with large internal strain due to lattice distortion and inhomogeneities of composition which decrease the freedom of movement of the magnetic domain walls. The disordered FePt_3 is ferromagnetic and becomes antiferromagnetic on ordering and again upon cold working becomes strongly ferromagnetic [47-48].

Similarly Co-Pt system has face centered cubic structures throughout entire range of solid solutions. Ordering changes the crystal structures in the sequence of $\text{L}1_2$, $\text{L}1_0$ and $\text{L}1_2$ for the concentration ratios Co_3Pt , CoPt and CoPt_3 [3]. Their ordering temperature is between 840 K and 1100 K. CoPt alloys have been thoroughly studied especially in the composition range with $x=0.5\pm 0.1$ [49,50] because of their importance as permanent magnet materials. Long annealing below order-disorder transition temperature impart magnetic hardness to the alloy characterized by high magnetocrystalline anisotropy ($\approx 5 \times 10^7$ erg/cm³ at 4 K) and high coercivity (≈ 6.3 kOe at 4 K and 4 kOe at 300K) [31,33,34]. The ordered tetragonal ($\text{L}1_0$) phase is formed from the disordered fcc($\text{A}1$) phase by the nucleation within it of a lamellar system of twin-oriented regions. Maximum magnetic hardness is obtained when the alloy is fully tetragonal. It is assumed that the interaction of the domain walls with lamellae boundaries coupled with high anisotropy is responsible for the permanent magnet properties of this compound.

Chen and Buttry [51] measured the saturation magnetization of the ordered and disordered $\text{Co}_{1-x}\text{Pt}_x$ ($x=0.5\pm 0.05$) alloys. It is observed that the saturation magnetization decreases on ordering by about $\approx 30\%$. CoPt_3 alloy is ferromagnetic in both the ordered ($L1_2$) and disordered state ($A1$). Magnetic moment per formula unit decreases with the increase of degree of order [52]. For fully ordered material magnetic moment per formula unit is $2.43 \mu_B$ and for the disordered one magnetic moment per formula unit is $2.65 \mu_B$.

NiPt system is isomorphous with CoPt and CuAuI system, having face centered cubic ($A1$), structure at high temperature in the disordered phase and simple cubic, $L1_2$ (Cu_3Au), face centered tetragonal, $L1_0$ (CuAu), and simple cubic, $L1_2$ (Cu_3Au), structures below order-disorder transition temperature of approximately 900K at the stoichiometric compositions Ni_3Pt , NiPt and NiPt_3 respectively [7,27,53]. It was found that the disordered alloys are ferromagnetic up to platinum concentration of $58\text{at.}\%$. [54-59]. Cadeville et al [60] and Dahmani et al [7] determined the equilibrium chemical and magnetic phase diagram of NiPt system in both the ordered and disordered states and found that in the ordered phase magnetism disappears with appearance of $L1_0$ phase at platinum concentration of $44 \text{at.}\%$ instead of $58\text{at.}\%$ Pt in the disordered phase. $L1_0$ ordered structure exists between approximately $44\text{-}60 \text{at.}\%$ Pt.

Watanabe et al [61] found by magnetization measurement that $\text{Ni-}46.7 \text{at.}\%$ Pt is ferromagnetic when disordered and paramagnetic when ordered. The moment calculated from saturation magnetization of the disordered alloy is only $0.06 \mu_B$ per atom and the effective moment, P_{eff} of disordered and ordered alloys calculated from temperature dependence of susceptibility are 1.9 and $1.7 \mu_B$ respectively per formula unit. The information available until now on the magnetic behaviour and magnetization data are inadequate to understand the effect of atomic ordering on the composition variation of magnetic properties of this interesting system.

Curie Temperature

The Curie temperature, T_C , of a ferromagnetic alloy depend on the strength of the exchange interaction which arises from the overlapping of the electronic wave functions of the interacting magnetic atoms. The atomic ordering changes the local environment or the relative number of different kinds of nearest neighbouring atomic pair, and thus is expected to affect the Curie temperatures of the alloys. Although there is a close relationship between the increasing effect of atomic order on saturation magnetization and that on the Curie temperature, there are cases in which such a relationship breaks down. This is particularly true for the alloys whose Curie temperature are much higher than the order-disorder transition temperatures. For example Ni_3Fe and its neighbouring alloys have Curie temperatures much higher than the order-disorder transition temperatures. So the Curie temperatures of these Ni-Fe alloys are independent of the state of atomic order.

Curie temperature of the disordered Ni_3Fe phase has been determined by resistivity measurement and found to be $\approx 860K$ which is slightly higher than order-disorder transition temperature of $\approx 820K$ [39]. The Curie temperature of the ordered phase is also higher than the order-disorder transition temperature. But its measurement is difficult since some randomness take place in the ordered phase before the Curie temperature is reached. Similar is the situation with Fe-Co alloys whose Curie temperatures are above the order-disorder transition temperature of $1000K$. Therefore the Fe-Co and Ni-Fe alloys, it is unrealistic and insensible to discuss the effect of atomic order on Curie temperature.

Curie temperature of disordered and ordered Ni_3Mn lies below the order-disorder temperature of $750 K$. Curie temperature of the disordered alloy is $130 K$ but jumps to $690 K$ after ordering [62]. This large increase in T_C is consistent with the unusually large increase in magnetization discussed previously. The resistivity measurements performed on highly ordered alloy show an anomaly both at T_C and at the order-disorder transition temperature and the measurements are extremely sensitive to the thermal history and order [39].

The effect of atomic ordering on the Curie temperature in Fe₃Pt has been studied by Suzuki et al [63], Mizoguchi et al [64], Sumiyama et al [4], and Sasaki et al [46]. The former author found that the Curie temperature of the disordered alloy is 280K and that of the ordered alloy is 430K. The results of other investigators are comparable slight deviation is due to compositional variation and degree of long range order parameter S. Similar increase in T_C from 540K in the disordered state to 750K in the ordered state has been found for the equiatomic FePt alloy [12]. The alloy with the stoichiometric composition FePt₃ chemical disorder can only be achieved by the application of severe cold work. Curie temperature measured on powdered specimen of FePt₃ produced by filing is about 425K. The alloy orders antiferromagnetically on ordering below T_N=200K [47,48,65]. An increase in T_C is also observed in Pd₃Fe from 497K to 529K on ordering [12].

The Curie temperatures of Co-rich ferromagnetic side of Co-Pt alloys (around Co₃Pt) are independent of the state of atomic order, since their T_C are much higher than order-disorder transition temperature. The Curie temperature of disordered CoPt₃ is 460 K and upon ordering T_C decreased to 320 K [52]. Similarly T_C decreases on ordering for CoPt alloy.

The Curie temperatures of Ni_{1-x}Pt_x alloys are much lower than the order-disorder transition temperature of about 900 K. Therefore, it is convenient to measure the dependence of Curie temperature on the degree of long range order of NiPt alloys. A qualitative picture regarding the depression of Curie temperature in the ordered L1₂ phase and complete disappearance of ferromagnetism in L1₀ phase has been reported in the phase diagram of the NiPt system[7,60].

2.3. Purpose of this thesis

Magnetic properties of $\text{Ni}_{1-x}\text{Pt}_x$ system have been studied mainly for the disordered phases. The effect of atomic ordering on the magnetic properties of $\text{Ni}_{1-x}\text{Pt}_x$ system has not been studied in detail and the information available in this regard is less than satisfactory to understand the role of atomic ordering on the magnetization and magnetic phase transition of this system.

The main purpose of this thesis is to investigate in detail the effect of atomic order-disorder on the crystal structure, magnetization and magnetic phase transition temperature of $\text{Ni}_{1-x}\text{Pt}_x$ system covering a wide range of composition upto the critical concentration, x_c (concentration where Curie temperature goes down to absolute zero). It would be interesting to see the effect of substituting Fe or Co for Ni keeping Pt 50 at.% throughout on the magnetic properties in ordered or disordered phases. Replacement of Ni by Fe or Co is supposed to introduce magnetic disturbance in terms of magnetic moment and exchange integral. PtFe and PtCo are well known giant moment ferromagnets [29]. So the substitution of small amount of Fe or Co for Ni in the NiPt alloy in both the ordered and disordered states is expected to induce giant moment associated with Fe or Co atom. In the pseudobinary $\text{Ni}_{1-x}\text{Fe}_x\text{Pt}$ and $\text{Ni}_{1-x}\text{Co}_x\text{Pt}$ alloys role of Fe and Co atom for the changes in magnetization and Curie temperature as the matrix goes to ordered or disordered state would be determined and the expected giant moment associated with Fe or Co atom due to polarization of the host matrix would be calculated in both states of order.

Reference

1. Van Deen, J.K. and F. Van Der Woude *Acta Metallurgica* (1981) Vol. 29, P.1255-1262
2. Oyedele, J.A. and M.F. Collins, *Phys. Rev.* (1977), B16, 3208
3. Sanchez, J.M., J.L.Moran-Lopez, C. Leroux and M.C. Cadeville, *J.de. Phy..* (1988), C8, Tome 49, 107.
4. Sumiyama, K., M. Shiga, Y. Kobayashi, K. Nishi and Y. Nakamura, *J. Phys.* F8, 1978, 1281
5. Shunk, F.A., *Constitution of Binary Alloys*, 2nd Supplement, McGraw-Hill (1969), P. 335.
6. *Metals Handbook*, 1973a,b, Vol.8 (Am. Soc. Met.,Metals Park OH), P.306
7. Dahmani, C.E., M.C. Cadeville, J.M. Sanchez and J.L. MoranLopez,*Phys.Rev.Letters*, (1985), 55, 1208
8. Tammann, G., *Z. anorg. chem.*,107, 1(1919); "*Lehrbuch der Metallographie*", P. 325 L. Voss, Leipzig, 1921.
9. Johansson,C.H. and J.O.Linde,*Ann.Physik* [4],78,439 (9125)
10. Raynor, G.V. in *Physical Metallurgy*, R.W.Cahn edition (North Holland Pub. Co.), 1970, P. 374.
11. Calvayrac, Y. and M.Fayard, *Mate. Res. Bull.* (1972), 7, 891
12. Chen,C.W, *Magnetism and Metallurgy of Soft Magnetic Materials*, (North-Holland Pub. Co.), 1977, 322.
13. Muto, T. and Y. Takagi, "The theory of order-disorder transitions in alloys". *Solid State Physics.Vol.I. Advances in research and applications*, edited by F.Seitz and D. Turnbull. (1955), P.250.
14. Dahmani, C.E., M.C. Cadeville and V.Pierron-Bohnes, *Acta Metallurgica*(1985), Vol.33,P.369-377
15. Berg, H. and J.B. Cohen, *Metall Trans.* (1972), 3, 1797.
16. Bragg, W.L., *Proc. Phys. Soc.* (1940), 52, 105
17. Wohlfarth, E.P.,in *Ferromagnetic Materials*, edited by E.P.Wohlfarth, Vol.1, (North Holland Pub. Co.), 1980,20
18. Danan,H., A.Herr and A.J.P.Meyer,1968, *J.Appl.Phys.*39, 669
19. Crangle,J. and D. Parsons, *Proc. Roy. Soc.*, 1960, A 255,509
20. Crangle, J., in *electronic structure and alloy chemistry of the transition elements*, edited by P.A. Beck (John Willey & Sons. Inc. NY), 1963, 64
21. Crangle,J., 1960, *Phil. Mag.*, 5, 335

22. Bozorth, R.M., P.A.Wolf, D.D.Davis, V.B.Compton and J.H.Wernick, Phys. Rev. 1961, 122, 1157
23. Bagguley, D.M.S. and J.A. Robertson, J. Phys. F, Metal Phys. 1974, 4, 2282
24. Lederer, P. and Blandin A., Phil. Mag/, 1966, 14, 363
25. Takahashi, T. and M. Shimizu, J. Phys. Soc. Jap., 1965, 20, 26
26. Mydosh, J.A. and G.J. Nieuwenhuys, in Ferromagnetic Materials, edited by E.P. Wohlfarth, Vol. 1, (North Holland Pub. Co.), 1980, 82
27. Hansen, M., Constitution of Binary alloys. McGraw Hill, NY, 2nd edition, 1958.
28. Nieuwenhuys, G.J., Adv. Phys. 1975, 24, 515
29. Crangle, J. and W.R. Scott, J. Appl. Phys. 1965, 36, 921
30. Clogston, A.M., B.T. Matthias, M. Peter, H.J. Williams, E. Corenzwit and R.C. Sherwood, Phys. Rev. 1962, 125, 541,
31. Hadjipanayis, G.C. and P. Gaunt, J. Appl. Phys. 1979, 50, 2358
32. Tsoukatos, A., H. Wan, G.C. Hadjipanayis, Y.J. Zhang, M. Waite, and S.I. Shah, J. Mag. & Mag. Mat. 1993, 118, 387-393
33. Craik, D.J., Plat. Metals Rev. 1972, 16, 129
34. Martin, D.C., J. Phys. F5, 1975, 1031
35. Elcock, E.W., Order-disorder phenomena, John Wiley and Sons, Inc., 1956, 34.
36. Oyedele, J.A. and M.F. Collins, Phys. Rev. 1977, B16, 3208
37. Bardos, D.I., J. Appl. Phys. 1969, 40, 1371
38. Collins, M.F. and J.B. Forsyth, Phil. mag/ 1963, 8, 401
39. Orehotsky, J., J.B. Sousa and M.F. Pinheiro, J. Appl. Phys. 1982, 53, 7939
40. Chin, G.Y. and J.H. Wernick, in Ferromagnetic Materials, edited by E.P. Wohlfarth, Vol. 2, (North Holland Pub. Co.), 1980, 129
41. Goldfarb, R.B. and C.E. Patton, Phys. Rev. B, 1981, 24, 1360
42. Abdul-Razzaq, W. and J.S. Kouvel, J. Appl. Phys. 1984, 55, 1623
43. Shull, C.G. and M.K. Wilkinson, Phys. Rev. 1955, 97, 304
44. Kouvel, J.S., Material Research Symposium Proceedings, 1983 (Elsevier, (New York), 19, 353
45. Cullity, B.D., Introduction to Magnetic Materials, Addison-Wesley Pub. Co., 1972, 149
46. Sasaki, T. and S. Chikazumi, J. Phys. Soc. Jap, 1979, 46, 1732
47. Bacon, G.E. and J. Crangle, Proc. Roy. Soc. London, 1963, A272, 387
48. Suda, T., M. Shirane and K. Motizuki, Proc. Int. Conf. Darmstadt, Germany on transition metals, 1992, Vol. II, 765,

49. Darling, A.S., *Plat. Metals Rev.*, 1963, 7, 96
50. MacGuire, R.A. and P. Gaunt, *Phil. Mag.* 1966, 13, 567
51. Chen, C.W. and R.W. Buttry, *AIP Conf. Proc.*, 1974, 24, 437
52. Menzinger, F. and A. Paoletti, *Phys. Rev.*, 1966, 143, 365
53. Massalski, T.B., H. Okamoto, and P.K. Subramanian, *Binary Alloy Phase Diagram* (ASM Int. Materials Park, 1990), vol. 2, page 1744
54. Beille, J., D. Bloch, and M. Besnus *J. Phys. F: Metal Phys.*, 1974, 4, 1275
55. Alberts, H.L., J. Beille and D. Bloch, *Phys. Rev.*, 1974, B9, 2233
56. Besnus, M.J. and A. Herr *Phys. Lett.*, 1972, 39A, 83
57. Fischer, G. and M.J. Besnus, *Solid State Comm.*, 1969, 7, 1527
58. Marian, V., *Ann. Phys.*, 1937, 7, 459
59. Para, R.E., and J.W. Cable, *Phys. Rev. B*, 1980, 21, 5494.
60. Cadeville, M.C., C.E. Dahmani and F. Kern, *J. Mag. Mag. Mat.*, 1986, 54-57, 1055
61. Watanabe, M. and S. Miyahara *J. Phys. Soc. Jap.*, 1967, 23, 451.
62. Kouvel, J.S., C.D. Graham, and J.J. Becker, 1958, *J. Appl. Phys.*, 29, 518
63. Suzuki, Y., H. Miyajima, G. Kido, N. Miura and S. Chikazumi, *J. Phys. Soc. Jpn.*, 1981, 50, 817
64. Mizoguchi, T., M. Akimitsu, and S. Chikazumi, *J. Phys. Soc. Jpn.*, 1973, 34, 932
65. Kohigi, M., Y. Ishikawa and Radhakrishna, *Solid State Comm.*, 1978, 27, 409.

CHAPTER 3

Sample preparation and characterization

3.1 Preparation of samples

3.1.1 $\text{Ni}_{1-x}\text{Pt}_x$

A series of polycrystalline $\text{Ni}_{1-x}\text{Pt}_x$ alloys with $x=0.14, 0.24, 0.30, 0.44, 0.50$ and 0.57 have been prepared from appropriate proportions of Ni of 99.999% purity and Pt of 99.99% purity in an arc furnace on a water-cooled copper hearth under an atmosphere of pure argon. The required amounts of the constituent elements were taken from pure metal bars or wires and weighed carefully with a sensitive electronic balance and were placed inside the furnace. Before melting the furnace chamber has been evacuated (10^{-3} torr) and flashed with argon gas, the process was repeated several times to get rid of residual air and finally kept in an argon atmosphere. A substantial amount of pure titanium getter placed in one side of the chamber was melted first in order to absorb any oxygen present in the furnace chamber. The constituent elements were then melted in the shape of buttons and turned upside down and remelted three times to ensure homogeneous mixer and eliminate segregation. The button shaped alloys were then taken out of the furnace and weighed. The samples were then sealed in evacuated quartz tubes and heat treated at 1050 C for seven days for further homogenization and water quenched. The weight loss after melting was less than 1% except for the concentrated alloys, and weight loss for the alloys with higher percentages of nickel have higher melting loss. However the actual composition of each alloy must be very close to the nominal values, which are shown in Table 3.1

From each alloy small amount of powder was filed for X-ray measurements and the remaining part was used for making spherical sample for magnetic measurements. The spheres of diameter 2-3mm weighing about 50-100mg are fabricated by the grinding procedure in a rotating device.

Table 3.1 Composition of Ni_{1-x}Pt_x alloys

Platinum Content X	Weight % Ni	Weight % Pt	At. % Ni	At. % Pt	% weight loss after melting
0.14	64.58	35.42	85.83	14.17	1.43
0.24	48.82	51.18	76.02	23.98	1.32
0.30	41.25	58.75	70.00	30.00	1.04
0.44	27.67	72.31	56.00	44.00	0.73
0.50	23.08	76.92	49.93	50.07	0.51
0.57	18.54	81.46	43.06	56.94	0.26

Table 3.2 Composition of Ni_{1-x}Fe_xPt alloys

Iron Content X	Weight % Ni	Weight % Fe	Weight % Pt	At. % Ni	At. % Fe	At. % Pt	% weight loss after melting
0	23.08		76.92	49.93		50.07	0.51
0.02	22.66	0.44	76.90	48.99	1.0	50.01	0.30
0.05	21.98	1.09	76.93	47.5	2.49	50.01	0.42
0.10	20.85	2.19	76.96	45.02	4.98	50.0	0.32
0.20	18.56	4.40	77.04	40.03	9.99	49.98	0.87

Table 3.3 Composition of Ni_{1-x}Co_xPt alloys

Cobalt Content X	Weight % Ni	Weight % Co	Weight % Pt	At. % Ni	At. % Co	At. % Pt	% weight loss after melting
0	23.08		76.92	49.93		50.07	0.51
0.01	22.9	0.23	76.86	49.50	0.50	50.00	0.60
0.20	22.67	0.46	76.87	49.02	1.00	49.98	1.18
0.05	22.00	1.16	76.94	47.51	2.49	50.00	0.88
0.07	21.51	1.63	76.86	46.49	3.50	50.01	0.59
0.1	20.82	2.32	76.86	45.14	4.99	49.87	0.86

3.1.2 $\text{Ni}_{1-x}\text{Fe}_x\text{Pt}$ and $\text{Ni}_{1-x}\text{Co}_x\text{Pt}$

A series of pseudobinary alloys $\text{Ni}_{1-x}\text{Fe}_x\text{Pt}$ with $x=0.02, 0.05, 0.1, 0.2$ and $\text{Ni}_{1-x}\text{Co}_x\text{Pt}$ with $x=0.01, 0.02, 0.05, 0.075, 0.1$ based on equiatomic nickel-platinum have been prepared by arc melting in an argon atmosphere as described. The purity of the starting material was 99.999% for Ni, Fe and Co and 99.99% for Pt. In these alloy preparation platinum was taken in powder form and pressed with a hydraulic press in the form of pellets. Iron and cobalt was placed inside the platinum powder before pressing. It was done so to prevent any loss of Fe and Co during arc melting since the amount of Fe and Co was very small. By arc melting button shaped ingots were prepared. The ingots were remelted at least four times in order to achieve homogeneity. Weight loss during the melting was much less than 1% in weight. The compositions of $\text{Ni}_{1-x}\text{Fe}_x\text{Pt}$ and $\text{Ni}_{1-x}\text{Co}_x\text{Pt}$ alloys are given in Tables 3.2 and 3.3 respectively. The ingots were then heat treated for homogenization at 1050 C for ten days and subsequently quenched in water. Spherical samples of 2-3 mm diameter weighing approximately 50-100 mg were made for magnetic measurements. Powders for X-ray diffraction have been taken from each ingot.

3.2 Ordering of the sample

To get atomically disordered samples the spheres were sealed in evacuated quartz tubes and annealed at 1000 C for 24 hours and were quenched rapidly by crushing the quartz tubes in the iced water or salt water. This annealing also helps to eliminate the effects of plastic deformation resulting from grinding for shaping. By this drastic quenching method it is assumed that the maximum degree of atomic disorder is attained although upon quenching it is reasonable to expect the formation of some short-range chemical order[1]. This is a quite general effect. Any solid solution which exhibits long-range order below a certain temperature exhibits some short-range order above that temperature. Moreover another kind of departure from randomness in a solid solution is often found known as clustering in which a tendency of

like atoms to be close neighbours is observed. In fact, there is probably no such thing as a perfectly random solid solution. All real solid solutions probably exhibit either short-range ordering or clustering to a greater or lesser degree simply because they are composed of unlike atoms with particular forces of attraction or repulsion operating between them. Bardos et al [2] pointed out that to inhibit the ordering process, a quenching rate of approximately 6000°C per second must be employed.

Kinetics of ordering in Ni-Pt and pseudobinary (Ni-Fe)-Pt and (Ni-Co)-Pt alloys is slow since their superlattices have four and more than four distinct domains and hence quenching has been proved effective to suppress ordering. In view of the above fact it is plausible to assume that the alloys are disordered to a high degree which has indeed been confirmed by X-ray diffraction.

Ordering of the Ni-Pt alloys have been done by prolong annealing of the disordered spheres in a vacuum furnace (10^{-6} torr) at 525°C for 27 days and then cooled to room temperature with the furnace cooling rate. The furnace enabled to maintain the temperature of the specimens within an accuracy of $\pm 2^\circ\text{C}$ of the set temperature. When for (Ni-Fe)-Pt and (Ni-Co)-Pt alloys annealing has been done at 580°C in vacuum (10^{-6} torr) for 2 days, then slowly cooled down to 525°C at the rate of approximately 10°C/hr, kept at this temperature for 12 days and then cooled to room temperature. Ni₃Pt and NiPt have an ordering temperature of 585°C and 645°C[3]. The annealing temperature for ordering was chosen at 525°C on the basis of the knowledge of kinetics of order-disorder transformation of NiPt and similar systems [4-7]. According to Greenholz et al [7] ordered NiPt was obtained for 30 days annealing at 450°C with an order parameter, S, above 0.98. It was observed that up to $592 \pm 3^\circ\text{C}$ there exist a single phase ordered alloy. Between 592°C and $625^\circ\text{C} \pm 3^\circ\text{C}$ a two-phase region in which the ordered and disordered phases were in equilibrium. Above $625 \pm 3^\circ\text{C}$ a disordered fcc structure exists. In an earlier experiment Esch and Schneider [8] obtained an ordered NiPt phase after very long annealing of 54 days at 610°C and 135 days at

400 C. Similarly Gillespie et al [9] made a long time annealing of 37 days at 600 C to get ordered NiPt phase. But Watanabe et al [10] found ordered NiPt by annealing at 580 C for 9 days. Dahmani et al [4] found that kinetics of ordering in NiPt system is much faster than predicted by many earlier experimentalists. He claimed that 30 days annealing at ≈ 450 C is reasonably long time to get ordered NiPt alloys. Sasaki et al [11] obtained an order parameter of $S \approx 1$ for Fe₃Pt alloy by annealing the specimen at 600 C for 30 hours, at 550 C for a week and slowly cooled down to 450 C during 20 days. In the present work it was observed that equiatomic NiPt alloy after 15 days of annealing at 525 C ordered state was identified with the appearance of superlattice lines on the X-ray diffraction pattern but to be more confident about the attainment of maximum order annealing was continued for 27 days. But for (Ni-Fe)-Pt and (Ni-Co)-Pt alloys annealing was done initially at 580 C in order to make the ordering kinetics faster since it has been reported [12,13] that ordering temperature increases with addition of these two elements. Ordered structures were confirmed by X-ray diffraction.

3.3 X-ray investigations

A direct way of investigating the ordering is by X-ray, neutron or electron diffraction [14-16]. In these methods, long range ordering manifests itself by the appearance of extra (superlattice) lines or ring on the X-ray, neutron or electron diffraction pattern in addition to the fundamental lines or rings. According to the theory of X-ray diffraction by crystals, the waves scattered by the A atoms in an ordered alloy will all be exactly in phase with each other and exactly out of phase with those scattered by the B atoms. If the scattering factors of the two kinds of atoms are different, the scattered waves will not cancel and hence a superlattice line will appear on the X-ray pattern. On the other hand, if the atoms are distributed at random over the lattice points, each point gives rise to a scattered wave whose amplitude is the average for A and B atoms according to their atomic concentrations. Then the

waves scattered by the successive net planes cancel each other completely owing to equal amplitudes and no X-ray line is observed in the diffraction pattern.

The presence of superlattice lines on an X-ray or neutron diffraction pattern is the decisive proof of the existence of the ordered arrangement of atoms in the alloys. X-ray investigations have been done on $\text{Ni}_{1-x}\text{Pt}_x$ alloys with $x=0.24, 0.50, 0.57$ to determine lattice parameters, crystal structures and also to confirm ordered lattice. X-ray measurements were performed on alloy powders taken from the ordered and disordered samples by filing. A Guiner-Hagg type focusing camera with $\text{CuK}\alpha$ radiation ($\lambda=1.540598 \text{ \AA}$) calibrated with Si powder ($a=5.431065 \text{ \AA}$) was used for recording the powder pattern of all NiPt alloys at room temperature. More over X-ray diffractogram was recorded at room temperature with a Siemens D-5000 diffractometer in wide range of 2θ values ($10 < 2\theta < 140$) using a step scanning mode with step size 0.02 and time per step 2 seconds. The X-ray diffraction lines were indexed in terms of hkl reflections. The lattice parameters were determined by least squares method using a standard computer programme.

X-ray measurements show that all the disordered NiPt alloys have face centered cubic (fcc), $A1$, structures and the lattice parameters increase with increasing platinum concentration. The ordered alloy with $x=0.24$ crystalizes in the simple cubic, $L1_2$ (isomorphous with Cu_3Au) structure and the lattice parameters are almost same in the ordered and disordered states. There are average four atoms per unit cell distributed at random at 000 , $\frac{1}{2}\frac{1}{2}0$, $\frac{1}{2}0\frac{1}{2}$ and $0\frac{1}{2}\frac{1}{2}$ in the complete disordered state. On ordering each unit cell contains one Pt atom at 000 , and three Ni atoms at $\frac{1}{2}\frac{1}{2}0$, $\frac{1}{2}0\frac{1}{2}$ and $0\frac{1}{2}\frac{1}{2}$. The alloys with $x=0.50$ and 0.57 in the ordered states crystalize in the face centered tetragonal (fct), $L1_0$ structure (prototype CuAu). Each unit cell for equiatomic NiPt contains two Pt atoms, at $000, \frac{1}{2}\frac{1}{2}0$ and two nickel atoms, at $\frac{1}{2}0\frac{1}{2}$ and $0\frac{1}{2}\frac{1}{2}$. The structure is built up of (001) planes alternately containing only Ni or only Pt atoms. Each atom has eight nearest neighbours of the opposite kind in the adjacent (001) planes and four of the same kind in its own (001) plane at a slightly

greater distance, since the axial ratio c/a , is usually less than one. Fig. 3.1 (a,b) show the unit cell of $L1_2$ and $L1_0$ ordered phases of Ni_3Pt and $NiPt$ respectively. The alloys are found to be single phase.

Fig. 3.2 (a,b) show the X-ray diffraction patterns of equiatomic $NiPt$ alloy powders in the disordered and ordered states respectively at room temperature. In the diffraction pattern of disordered $NiPt$ (fig.3.2a), it is observed that no reflections of mixed indices are present. The diffraction lines (111), (002), (022), (113), (222) etc corresponds to any face centered cubic lattice. The diffraction pattern of ordered $NiPt$ is shown in Fig. 3.2(b), where the mixed index lines (001), (110), (201), (112), (221) etc correspond to superlattice reflections are obtained. The structure of the ordered alloys have lower symmetry than those of the corresponding disordered fcc alloys and their diffraction patterns have, therefore, extra Bragg reflections. The presence of superlattice lines (mixed hkl) and their sharpness and no diffuse intensity between the fundamental lines (200) and (002) and around the (001) line together with the knowledge of the kinetics of ordering of this alloy system has convinced that maximum degree of order has been attained. Similar extra lines have also been observed on the X-ray powder photograph for the ordered powder. The lattice parameter of disordered (fcc) $NiPt$ alloy as calculated from powder photograph is $a=3.751\text{\AA}$ and a little smaller value of $a=3.741\text{\AA}$ is calculated from X-ray diffractogram. This difference may be due to experimental uncertainty. Similarly the lattice constants a and c determined by both the techniques of the ordered fct phase of $NiPt$ is comparable. It is observed that the $c/a= 0.943$ for both the cases. In spite of structural change, the unit cell volume of the fct $NiPt$ (52.564\AA^3) is very close to

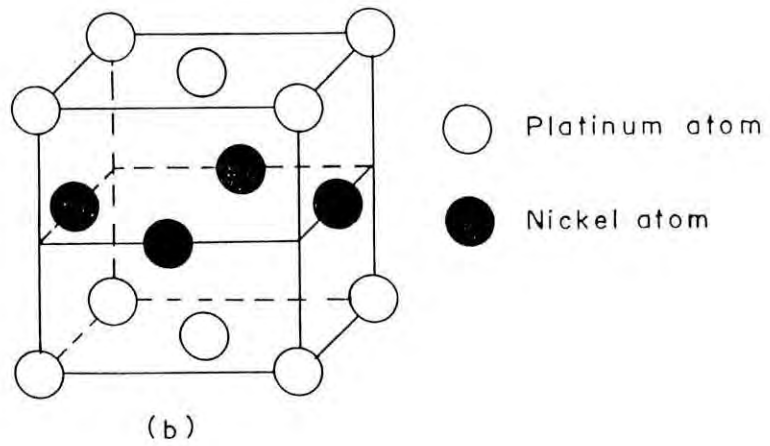
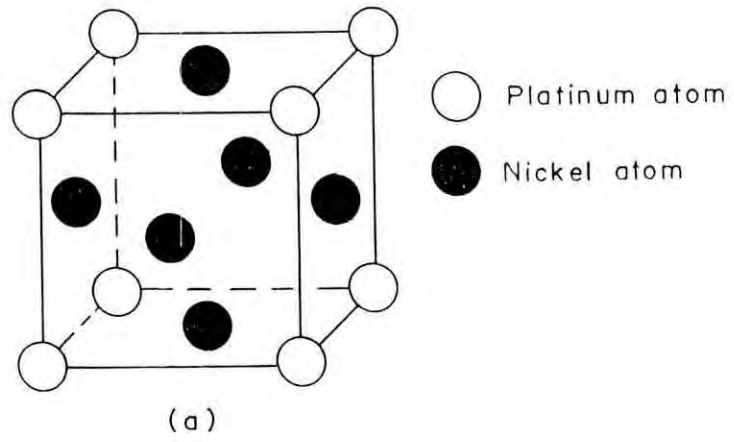


Fig. 3. 1. Unit cell of (a) $L1_2$ type of superlattice found in Ni_3Pt and (b) $L1_0$ type found in $NiPt$

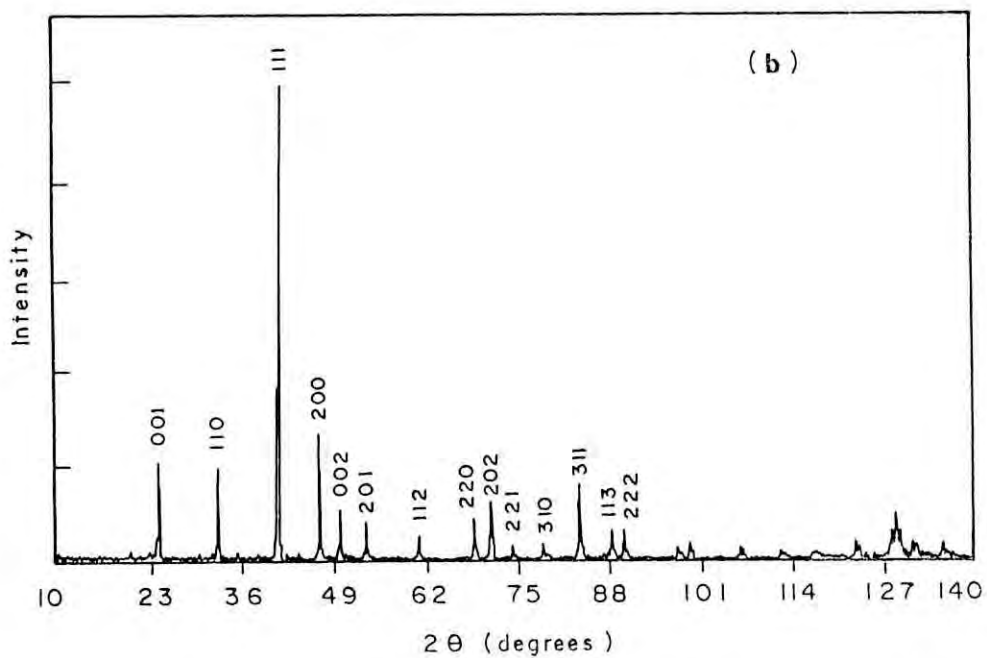
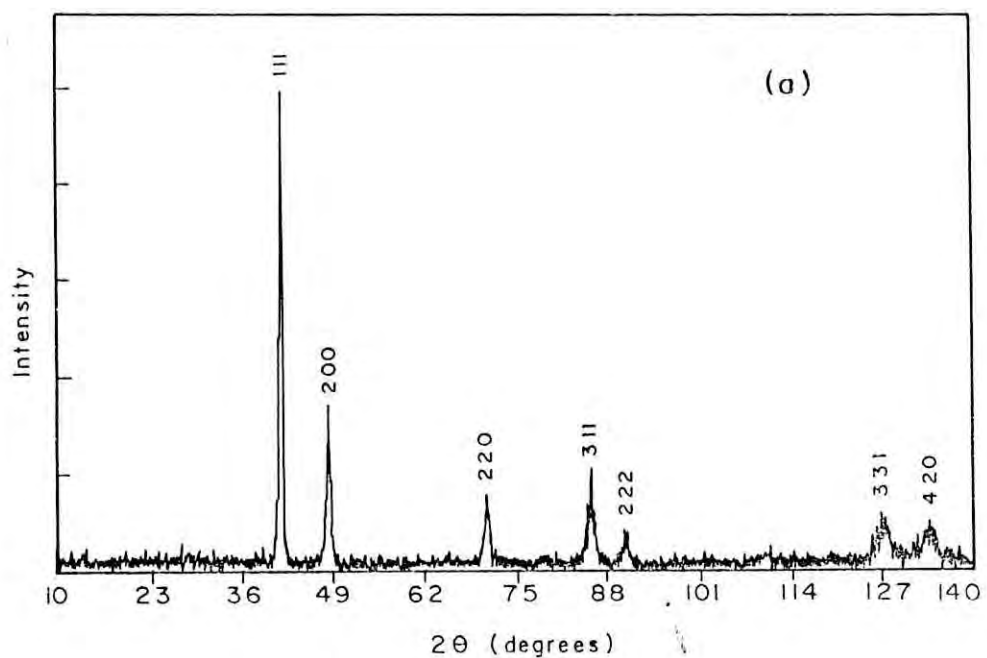


Fig. 3.2 X-ray diffraction pattern for $\text{Ni}_{1-x}\text{Pt}_x$ with $x = 0.50$ of (a) disordered and (b) ordered alloys.

that of the fcc (52.780\AA^3). In case of non-stoichiometric alloy with $x=0.57$ lattice constant and c/a ratio increase in both ordered and disordered states. Results are shown in Table 3.4. The results of the present X-ray measurements are in reasonable agreement with those reported earlier [3,7,17]. According to the second author NiPt alloy has $c/a=0.941$, where $c=3.594\text{\AA}$ and $a=3.819\text{\AA}$. The corresponding values for the CoPt and CuAu are $c/a=0.981$ and $c/a=0.931$ respectively with the same crystal structure[14,16,18]. It is calculated that in the ordered (fct) NiPt alloy a Ni atom has 4 Ni and 8 Pt nearest neighbours and a Pt atom has 4Pt and 8Ni nearest neighbours at a distance of 2.701\AA and 2.625\AA respectively.

Similarly X-ray diffraction has been done on $\text{Ni}_{1-x}\text{Fe}_x\text{Pt}$ with $x=0.05$ by both diffractometer and powder diffraction photographic techniques using $\text{CrK}\alpha$ radiation ($\lambda = 2.89976\text{\AA}$). The Guinier-Hagg camera with $\text{CrK}\alpha$ radiation was used in vacuum in order to reduce air absorption. A detail X-ray analysis shows that the disordered alloy is face centered cubic with $a = 3.7542 \pm 0.003\text{\AA}$. The ordered alloy is face centered tetragonal with a certain amount of disordered phase present. Moreover two reflection peaks on either side of (111) line could not be indexed either by fcc or fct. This might belong to a very small amount of complex phase. Fig 3.3 (a,b) shows the diffraction pattern recorded for both ordered and disordered Ni-Fe-Pt powder. It is observed that the reflections are not so sharp as that of fct NiPt alloy. So the alloy is not perfectly ordered and single phase. The fct phase has $c/a=0.944$, where $c=3.6096\pm 0.0004\text{\AA}$ and $a = 3.8220\pm 0.0003\text{\AA}$. Values calculated from both the techniques are comparable. Table 3.5 shows results of X-ray measurements. The lattice constants increase slightly with substitution of Fe for Ni in either states of order and a slight reduction ($\approx 0.3\%$) in cell volume occurs on ordering.

For the $\text{Ni}_{1-x}\text{Co}_x\text{Pt}$ alloys X-ray measurements have been performed on alloys with $x=0.01,0.02,0.05,0.07,0.1$ with siemens D-5000 diffractometer at room temperature in the ordered and disordered states. For comparison a single composition with $x=0.05$, a

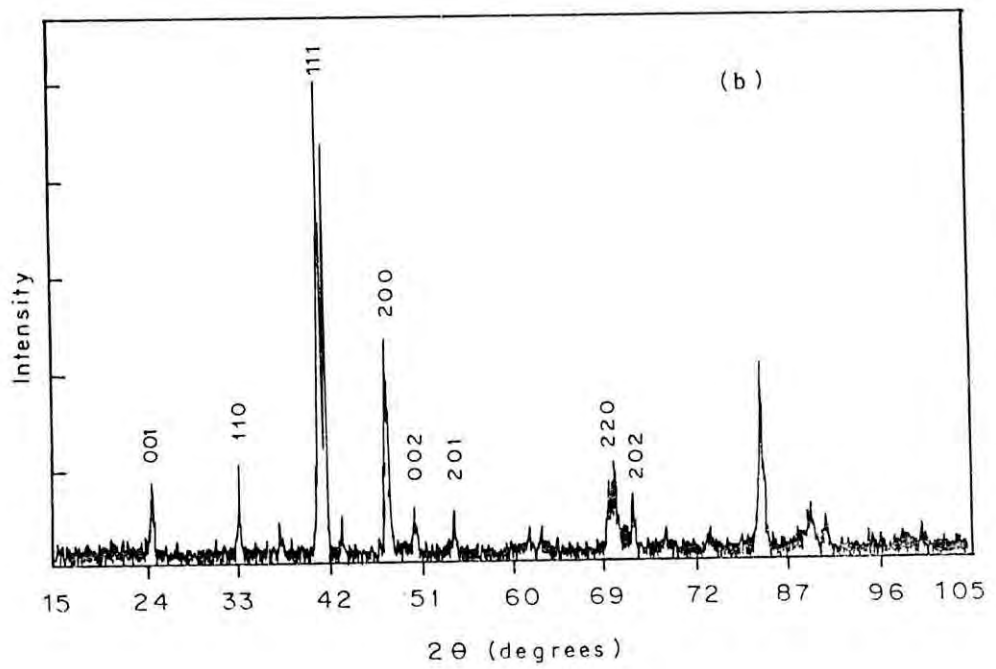
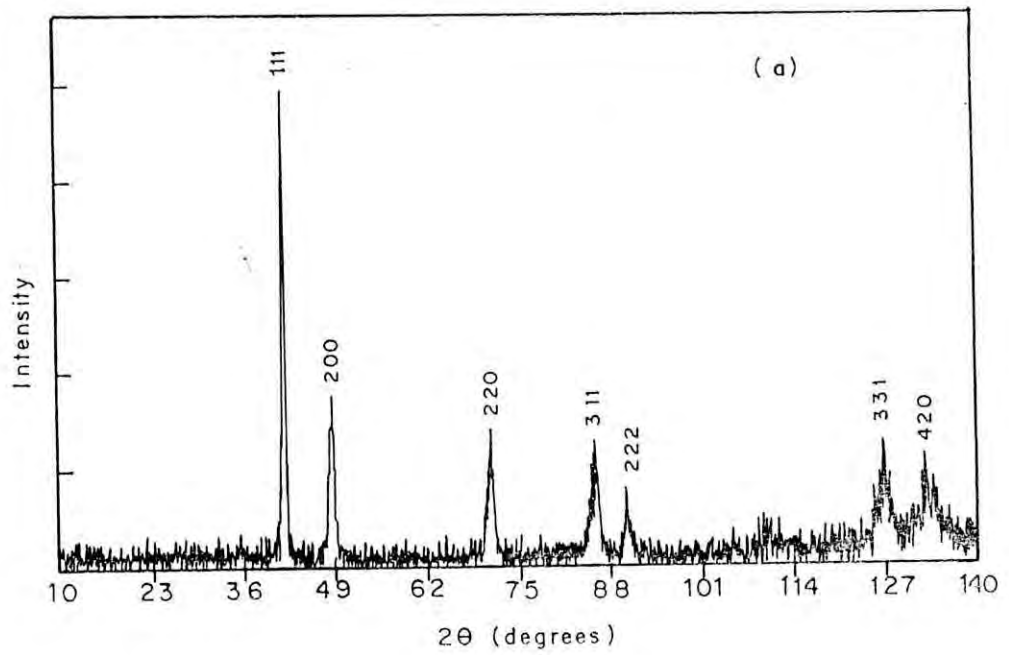


Fig. 3.3 X-ray diffraction pattern for $Ni_{1-x}Fe_xPt$ with $x = 0.05$ of (a) disordered and (b) ordered alloys.

Guiner-Hagg focusing camera is used to take X-ray powder photograph with $\text{CrK}\alpha$ radiation only for the ordered alloy powder. X-ray diffraction pattern recorded on diffractometer is shown in Fig 3.4(a,b) for an alloy with $x=0.05$. It is observed that all the disordered alloys are single phased with fcc structures. But the ordered ones are face centered tetragonal with some disordered phases in an ordered matrix. Like $\text{Ni}_{1-x}\text{Fe}_x\text{Pt}$, the alloys may contain small amount of second phase the composition of which could not be identified. Extra reflections with weak intensity occurs on either side of (111) line. So the ordered alloys are not single phase. There is little increase in the lattice parameters with addition of cobalt in the both ordered and disordered states. A small reduction ($\approx 0.3\%$) in cell volume occurs on ordering for the (Ni-Co) Pt alloys as in the case of (Ni-Fe)Pt alloys. Similar reduction (0.3%) in cell volume has also been reported for the similar systems[12,13] with much higher concentrations of Fe and Co. Table 3.5 summarizes the results of X-ray investigations.

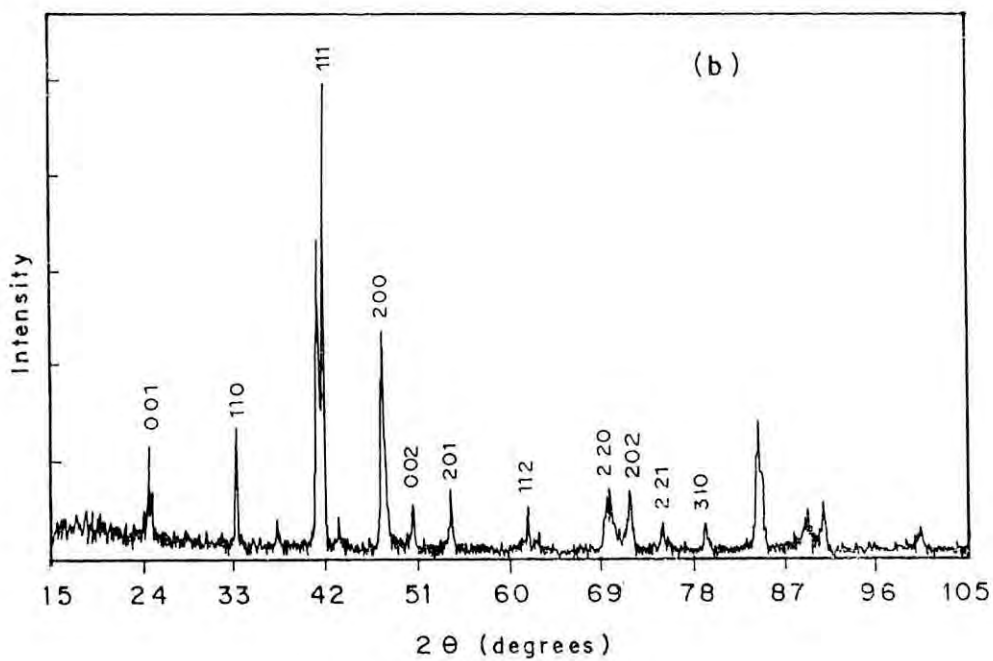
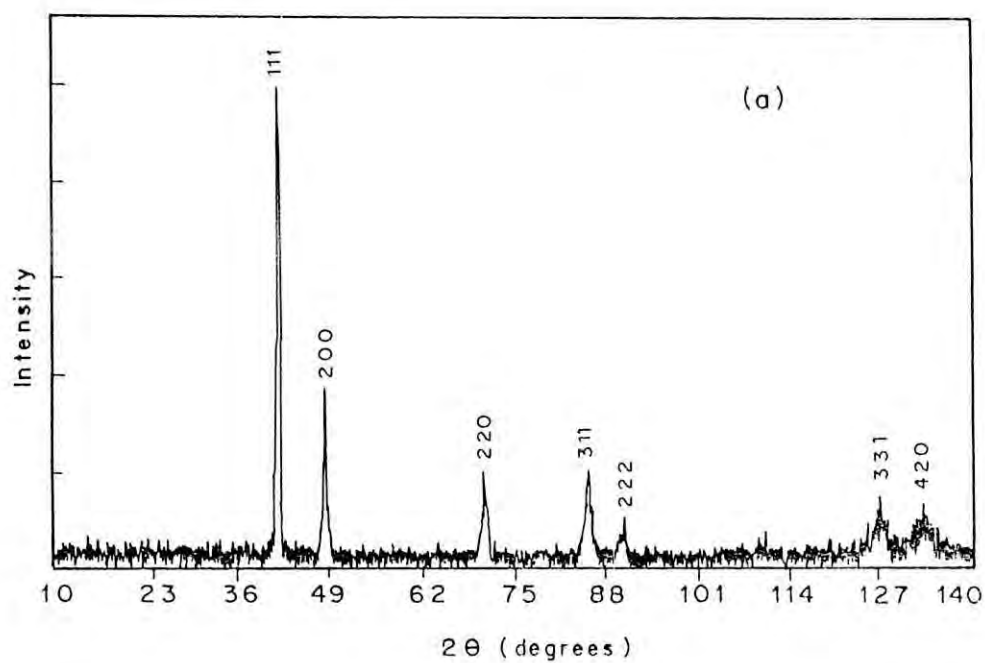


Fig. 3.4 X-ray diffraction pattern for $Ni_{1-x}Co_xPt$ with $x=0.05$ of (a) disordered and (b) ordered alloys.

Table 3.4 X-ray results of Ni_{1-x}Pt_x alloys

Platinum Content X		Crystal Structure	Lattice Parameter			Unit Cell Volume Å ³
			a(Å)	c(Å)	c/a	
0.24	dis	FCC	3.6449±0.0005			48.423±0.022
	ord	SC	3.6440±0.0001			48.388±0.007
0.50	dis	FCC	3.7511±0.0005			52.780±0.021
	ord	FCT	3.8192±0.0001	3.6036±0.0002	0.943	52.564±0.006
0.57	dis	FCC	3.7598±0.0004			53.148±0.018
	ord	FCT	3.8194±0.0004	3.6285±0.0005	0.95	52.932±0.012

Table 3.5 X-ray results of Ni_{1-x}Fe_xPt and Ni_{1-x}Co_xPt alloys

Content X		Crystal Structure	Lattice Parameter			Unit Cell Volume Å ³
			a(Å)	c(Å)	c/a	
0.05(Fe)	dis	FCC	3.7542±0.003			52.911±0.121
	ord	FCT	3.8220±0.0003	3.6096±0.0004	0.944	52.728±0.011
0.05(Co)	dis	FCC	3.7525±0.0007			52.842±0.032
	ord	FCT	3.8201±0.0008	3.6115±0.001	0.945	52.704±0.028

Reference

1. Crane, S. and H. Claus, *Solid State Commun* 35, 461, 1980
2. Bardos, D.I., A.T. Aldred and P.A. Beck, *J. Appl. Phys.* 38, 1260, (1967)
3. Hansen, M., *Constitution of Binary Alloys*, 2nd edn. PP.493, McGraw-Hill, New York (1958)
4. Dahmani, C.E., M.C. Cadeville, J.M. Sanchez, J.L. Moran-Lopez. *Phy. Rev. Lett.* (1985), 55, 1208-1211
5. Dahmani, C.E., M.C. Cadeville and V. Pierron-Bohnes, *Acta Metallurgica*, (1985), Vol. 33, P. 369-377
6. Greenholz, M., A. Kidron and U. Shimony, *J. Mater. Sci.*, (1972), 7, 1285-1291
7. Greenholz, M., A. Kidron and U. Shimony, *J. Appl. Crystallography*, 7, (1974), 83
8. Esch, V. and Schneider, A.I, *Z. Electrochem.*, 1944, 50, 268
9. Gillespie, D.J. and Schneider, A.I., *AIP Conf. Proc.*, 1971, 5, 461
10. Watanabe, M. and Miyahara, S., *J. Phys. Soc. Japan*, 1967, 23, 451
11. Sasaki, T. and S. Chikazumi, *J. Phys. Soc. Japan*, 1979, 46, 1732
12. Martin, D.C., *J. Phys. F: Metal Phys.*, 1975, 5, 1031
13. Woolley, J.C. and B. Bates, *J. Less Comm. Met.*, 1959, 1, 382 and Woolley, J.C. and B. Bates, *J. Less Comm. Met.*, 1960, 2, 11
14. Cullity, B.D., *Elements of X-ray diffraction*, edited by Addison-Wesley Pub. Co. Inc., 1956, P. 363
15. Elcock, E.W., *Order-disorder phenomena*, edited by John Wiley & Sons, Inc., 1956 P. 15-25
16. Tsoukatos, A., H. Wan, G.C. Hadjipanayis, Y.J. Zhong, M. Waite and S.I. Shah. *J. Mag. and Mag. Mat.* 118, (1993), 387-393
17. Para, R.E and J.W. Cable, *Phys. Rev. B*, 1980, 21, 5494
18. Darling, A.S., *Plat. Metals Rev*, 7, (1963), 96

CHAPTER 4

Magnetization Measurement Techniques

4.1 Introduction:

There are various means of measuring magnetization of a substance. The magnetization of a substance is usually determined by measuring its magnetic moment divided by the volume or mass of the substance. In the present thesis magnetization and susceptibility measurements have been performed using a Vibrating Sample Magnetometer (VSM), a Superconducting Quantum Interference Device (SQUID) magnetometer and a Lake Shore AC Susceptometer covering a wide range of temperature and magnetic field. A laboratory built AC susceptibility measurement technique based on mutual induction method has been extensively used for quick determination of the magnetic phase transition temperature (T_c) of the investigated samples in the temperature range 4.2-300K.

Most of the magnetic measurements have been carried out at the Department of Solid State Physics (magnetism group), Uppsala University, Sweden. A few measurements at room temperature and above are performed with the VSM designed and fabricated at Magnetic Materials Division, Atomic Energy Centre, Dhaka[1]. In this chapter a brief description of different equipment are given below.

4.2 Vibrating Sample Magnetometer (VSM)

Vibrating Sample Magnetometer is a versatile and sensitive method of measuring magnetic properties developed by S.Foner[2-3] and is based on the flux change in a coil when the sample is vibrated near it. The sample usually a sphere or small disc, is attached to the end of a rod, the other end of which is fixed to a loudspeaker cone or to some other kind of mechanical vibrator. The current through the loudspeaker vibrates the rod and the sample in a direction perpendicular to the applied magnetic field. The flux change from the sample induces an e.m.f in two pick-up coils connected in series and placed symmetrically on both sides of the sample. The vibrating rod also carries a small permanent magnet near its

upper end. The oscillation of this permanent magnet induces another e.m.f as a reference signal in the two reference coils connected in series. This voltage is fed through a voltage divider to a lock-in amplifier. The voltages from the two sets of coils are compared in the lock-in amplifier. The voltage divider is set in such a way that its output becomes equal to the sample signal and the lock-in amplifier shows zero output.

The VSM that has been used in this thesis work at the Department of Solid State Physics, Uppsala University, has a primary coil as a reference instead of a permanent magnet. The primary coil is glued on the sample rod. The primary coil oscillates with the same frequency and amplitude as the sample. A magnetic moment is produced by this coil when the current passes through it and this induces an e.m.f (reference signal) in the stationary secondary coils connected in series. The reference signal is compared with the sample signal in a lock-in amplifier. The output of the lock-in amplifier is fed to a Proportional Integrating Differentiating (PID) device which sends a current that compensates the sample signal to the primary coil of the reference. This current is used to measure the magnetization of the sample [4]. This procedure makes the measurement insensitive to changes in vibration amplitude and frequency. A schematic diagram of the VSM is shown in fig. 4.1

The sensitivity of the VSM's used in the present work is $\approx 10^{-4}$ emu and all of them have the same working principle with slight deviation in their constructions. The applied magnetic field can be varied between 0 and 5.5 KOe.

A helium cryostat is used for measuring magnetization in the temperature range 4.2 K to room temperature using Au(0.07% Fe)- chromel and copper-constantin thermocouple as thermometers. From room temperature and above a high temperature oven [5] with a PID temperature controller has been used. The temperature is measured by a chromel-constantin thermocouple placed adjacent to the sample. In order to keep good thermal contact between the sample and the thermocouple, continuous flow of helium exchange gas is maintained. The temperature gradient over 10mm of length in the warmest part of the oven is

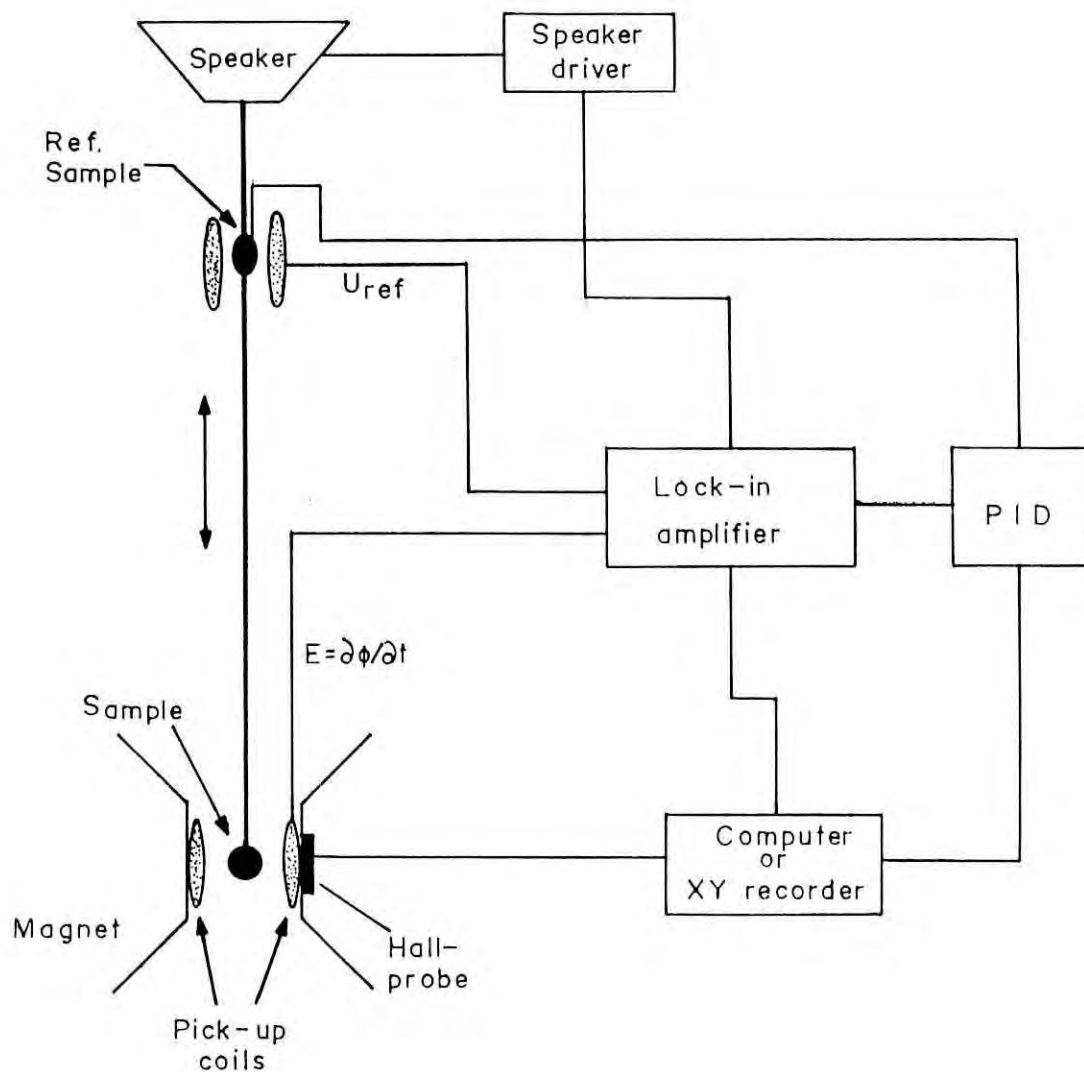


Fig. 4.1. A schematic diagram of VSM

approximately 0.1% and independent of temperature. The oven can be heated from room temperature to 1043 K in less than 15 minutes with a temperature difference between the thermocouple and the sample of less than 1 K at final temperature. Moreover, a temperature difference of the order of 1 K is established at a constant heating or cooling rate of 5 K/minute. The applied magnetic field has been measured using Hall probe. The calibration coefficient of the magnetometers have been determined using a standard sphere of pure nickel available from the National Bureau of Standards (NBS), USA.

For measuring magnetization at very high field and low temperature a VSM in conjunction with a helium cryostat and a superconducting magnet, capable of producing 70 kOe field, has been used[6]. The results of the experiment has been taken as continuous graph in X-Y recorder or as data points in the computer. The available softwares Kaleidagraph, Statview and Cricketgraph have been used for analyzing data and plotting graphs.

4.3 SQUID Magnetometer

The Magnetic Property Measurement System or MPMS is a sophisticated analytical instrument configured specifically for the study of the magnetic properties of small samples over a broad range of temperatures and magnetic fields. This standard system, made by Quantum Design Inc.U.S.A, can measure the magnetic moment of a sample with a differential sensitivity of 10^{-8} emu and has a maximum signal size of 1.25 emu[7]. A general view of the MPMS with its system components is shown in Fig.4.2

The system hardware has two major components.

- (1) The dewar and probe assembly: the dewar is a 56 litre insulated vacuum vessel filled with liquid helium; the probe is a cryogenic insert, suspended in the helium

SYSTEM COMPONENTS

- 1. Sample Rod
- 2. Sample Rotator
- 3. Sample Transport
- 4. Probe
- 5. Helium Level Sensor

- 6. Superconducting Solenoid
- 7. Flow impedance
- 8. SQUID Capsule
- 9. Dewar Cabinet
- 10. Dewar
- 11. HP Thinkjet Printer
- 12. Magnet Power supply
- 13. Model 1802 Temperature Controller

- 14. Console Cabinet
- 15. Power Distribution Unit
- 16. Model 1822 MPMS Controller
- 17. Gas/Magnet Control Unit
- 18. HP Vectra Computer
- 19. Monitor

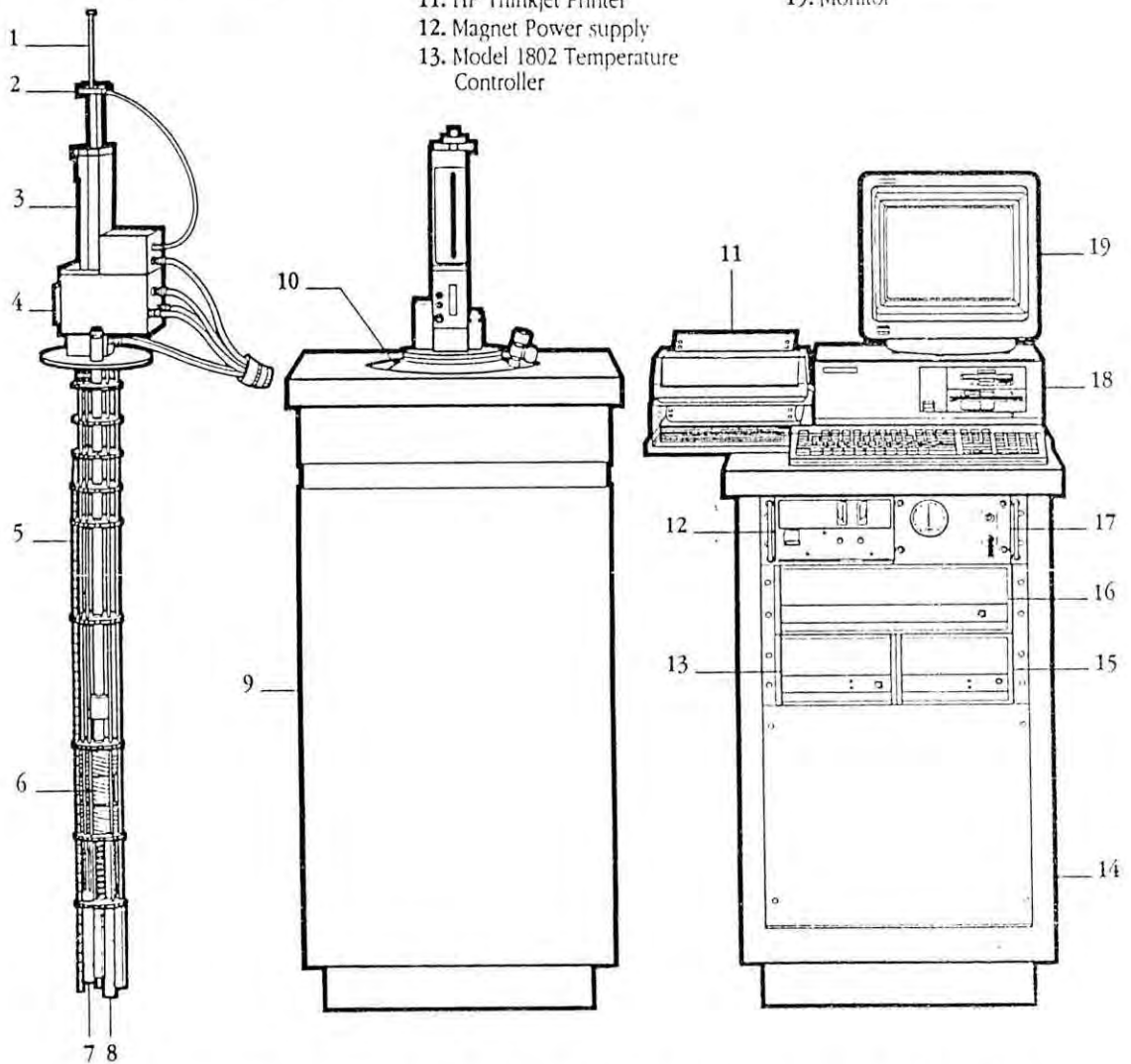


Fig.4.2 A general view of the SQUID magnetometer with its system components

vessel, containing the magnet, the temperature control module and the SQUID detection system.

- (2) The associated control system: automatic control and data collection are provided by an HP computer and two independent subsystem controllers; most of the gas control and other ancillary functions in the system are also automated.

The main component of the MPMS is the SQUID detection system. The SQUID consists of a superconducting ring with a small insulating layer known as the 'weak link' or Josephson junction [8] as shown in Fig. 4.3a. The SQUID, is a sensor of magnetic flux, providing an output voltage that is periodic in units of the flux quantum Φ_0 in units of 2.067×10^{-15} Wb. Connected to appropriate feedback circuitry, it becomes a linear sensor of magnetic flux (Fig. 4.3b). The operating principles of SQUIDs combine the properties of Josephson weak links or junctions with the phenomenon of flux quantization in a superconducting ring.

The magnet is a solenoid, made of superconducting wire. The magnetic field can be set within a range of -55000 gauss to 55000 gauss (± 5.5 tesla). In the high resolution mode, the field is set to 0.1 gauss resolution for fields below 5000 gauss, and to 1 gauss resolution above 5000 gauss.

The magnetic fields can be changed either by "oscillate mode" or "no overshoot mode". The "oscillate" mode is used to minimize the remanent field of the magnet, whenever an accurate value of the magnetic field is needed, e.g. in case of zero field cooling. In the hysteresis measurement the "no overshoot" mode has been selected, in which the field is changed directly from one value to another, and the magnet is returned to its persistent mode.

The temperature control unit is residing in the bore of the superconducting magnet. The temperature of the sample chamber can be set within a range of 1.9 K to 400 K. For operation above 4.4K the system uses a combination of cold helium gas flow and heaters. Responsible for the temperature measurements are two sensors: a germanium thermometer

and a platinum thermometer. The temperature stability is within ± 0.1 K.

The MPMS uses a second derivative detection coil as shown in Fig.4.4b. In this coil the upper and the lower single turns are counterwound with respect to the two-turn centre coil. This configuration strongly rejects interference from nearby magnetic background sources and uniform gradients to first order.

When changing the magnetic field or the temperature, the machine rests the sample at the lower end of its scan. To generate the SQUID output signal, the sample is pulled upwards through the pick-up coils by the sample transport unit. The induced current in the pick-up coils is transformed to give the typical SQUID output signal as displayed in fig. 4.4a. The curve shows the ideal output voltage as a function of the sample position assuming a dipole point source. In a real scan the signal is only measured at a finite number of data points along the z-axis. To fit a curve through these data points the "linear regression" mode is used. This method calculates an emu value by attempting to fit a theoretical signal to the actual measured signal and using the amplitude of the point response to calculate the emu. Such a method filters out noise more effectively. The number of data points in one scan should be at least five times the scan length in centimetres to supply enough data to the regression formula for accurate calculation of the response. In the present work consistently 32 data points were used at a scan length of 6 centimetres.

The data points are evenly spaced over the total scan length. Every time the system stops to record a data point, it averages a pre-set number(in this case 15) of voltage readings from the SQUID output. This yields the average voltage at that point. An individual reading of the SQUID output can be made in about 5 milliseconds.

The transformation from the SQUID voltage output curve to the magnetic moment (in emu) has been determined in the factory by measuring a palladium standard over a range of magnetic fields, and adjusting the system calibration factors to obtain the correct moment for the standard.

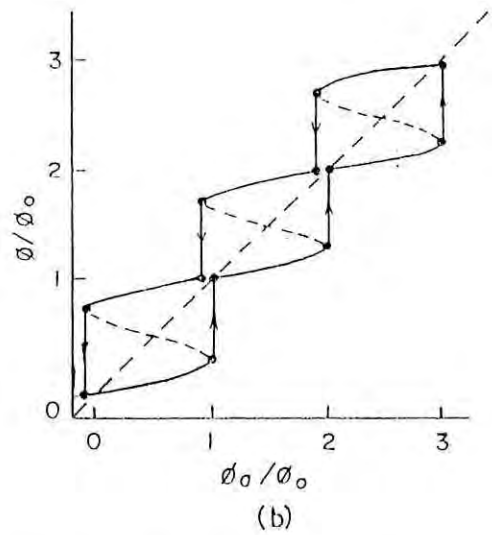
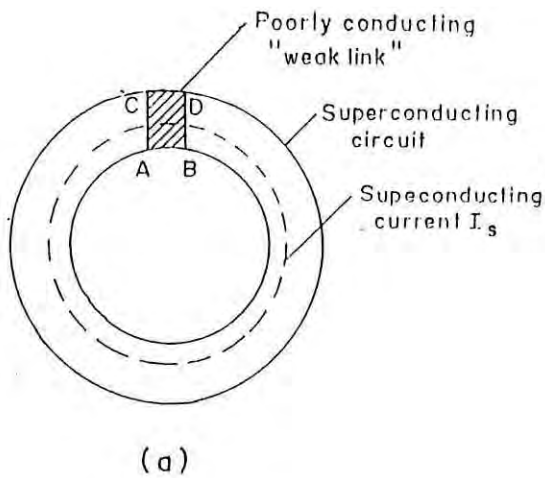


Fig. 4.3. (a) A Josephson junction device, which consists of a superconductor with a poorly conducting "weak link" ABCD, and (b) The relation between ϕ , the flux in the ring, and ϕ_a , the flux due to the applied field, in a SQUID magnetometer.

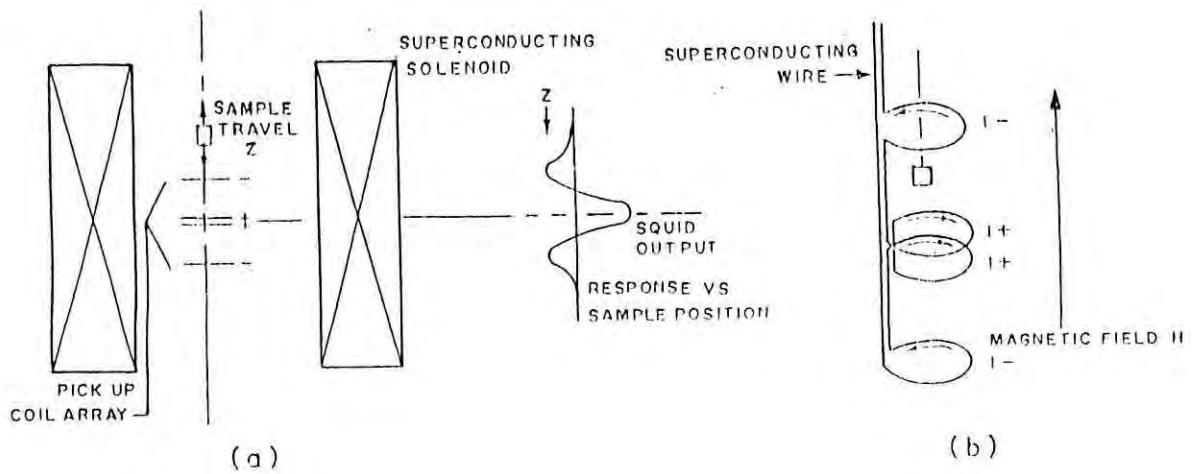


Fig. 4.4(a) A typical SQUID output signal versus sample position and (b) A second derivative coil configuration in SQUID.

A sophisticated computer operation system is used to control the measurements and to perform adjustment. By means of a program sequence it was possible to instruct the system to execute a sequence of system operations. In this way, highly automated measurements could be performed.

The measured data were recorded into a data file. Such a file generally exists of 5 numbers for each measurement: the system temperature, the magnetic field value (in gauss), the measured magnetic moment (in emu) and the time at which the measurement started and ended.

4.4 AC Susceptometer

Lake Shore AC Susceptometer/DC Magnetometer Model 7225 is the most versatile magnetic measurements system. It has the capability to perform both AC and DC magnetization measurements in a single instrument. The system provides an absolute measurement of both the real (χ') and imaginary (χ'') components of magnetic susceptibility as a function of temperature, amplitude and frequency of an applied AC field, with or without DC bias fields of ± 50 kOe. The equipment has sensitivity of 10^{-8} emu in terms of equivalent magnetic moment for AC susceptibility measurement. The susceptometer can be operated in the temperature range 4.2 K to 325 K with AC fields from 0.00125 Oe to 20 Oe and frequencies from 1 Hz to 10 KHz. The temperature stability is within ± 0.1 K [9].

Lake Shore susceptometer allows the calibration coefficient to be determined without the use of standard materials. The calibration can be determined directly from physical geometry of the susceptometer coils. The calibration of the susceptometer has been checked with a chromium potassium alum supplied by Lake Shore which obey Curie's Law. Figure 4.5 shows that the mass susceptibility of this paramagnetic salt is inversely proportional to temperature. The measurements are performed automatically through data acquisition and control software packages.

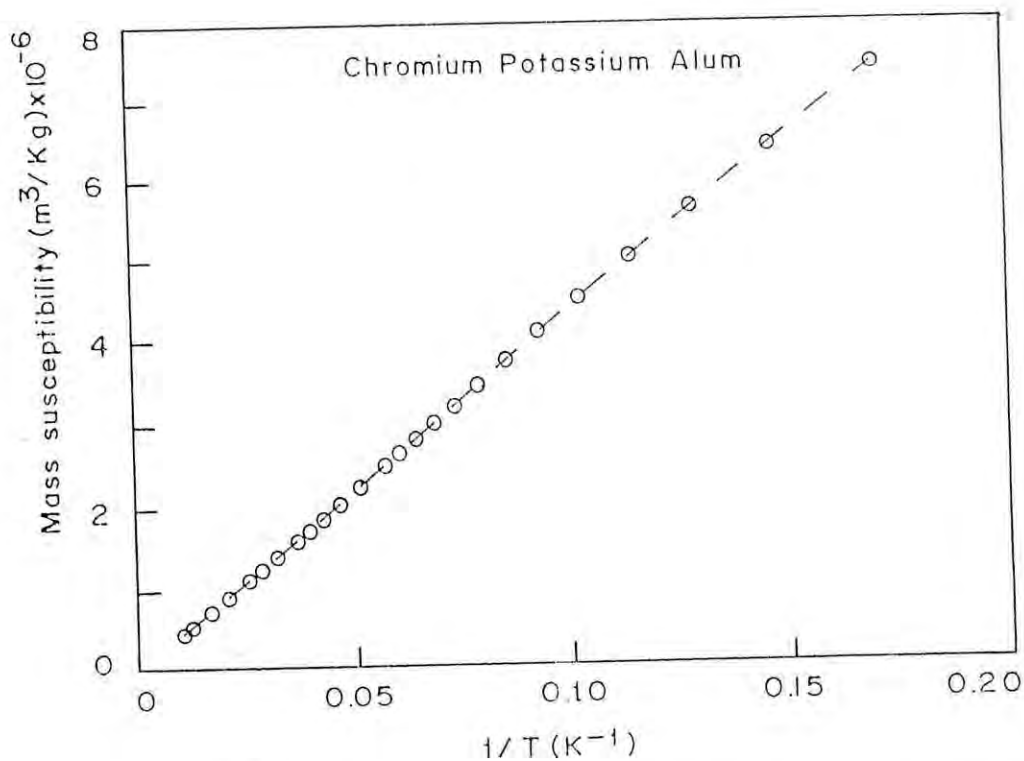


Fig. 4.5 Mass susceptibility of Chromium Potassium Alum as a function of inverse temperature.

Principles of Operation

The principle of operation of AC susceptometer involves subjecting the sample material to a small alternating magnetic field. The flux variation due to the sample is picked up by a sensing coil surrounding the sample and the resulting voltage induced in the coil is detected. This voltage is directly proportional to the magnetic susceptibility of the sample. Fig.4.6 shows schematically how the principles of AC susceptometry are incorporated in the Lake Shore AC Susceptometer Model 7225. The alternating magnetic field is generated by a solenoid which serves as the primary in a transformer circuit. The solenoid is driven with an AC current source with variable amplitude and frequency. Two identical sensing coils (S₁ and S₂) are positioned symmetrically inside of the primary coil and serve as the secondary coils in

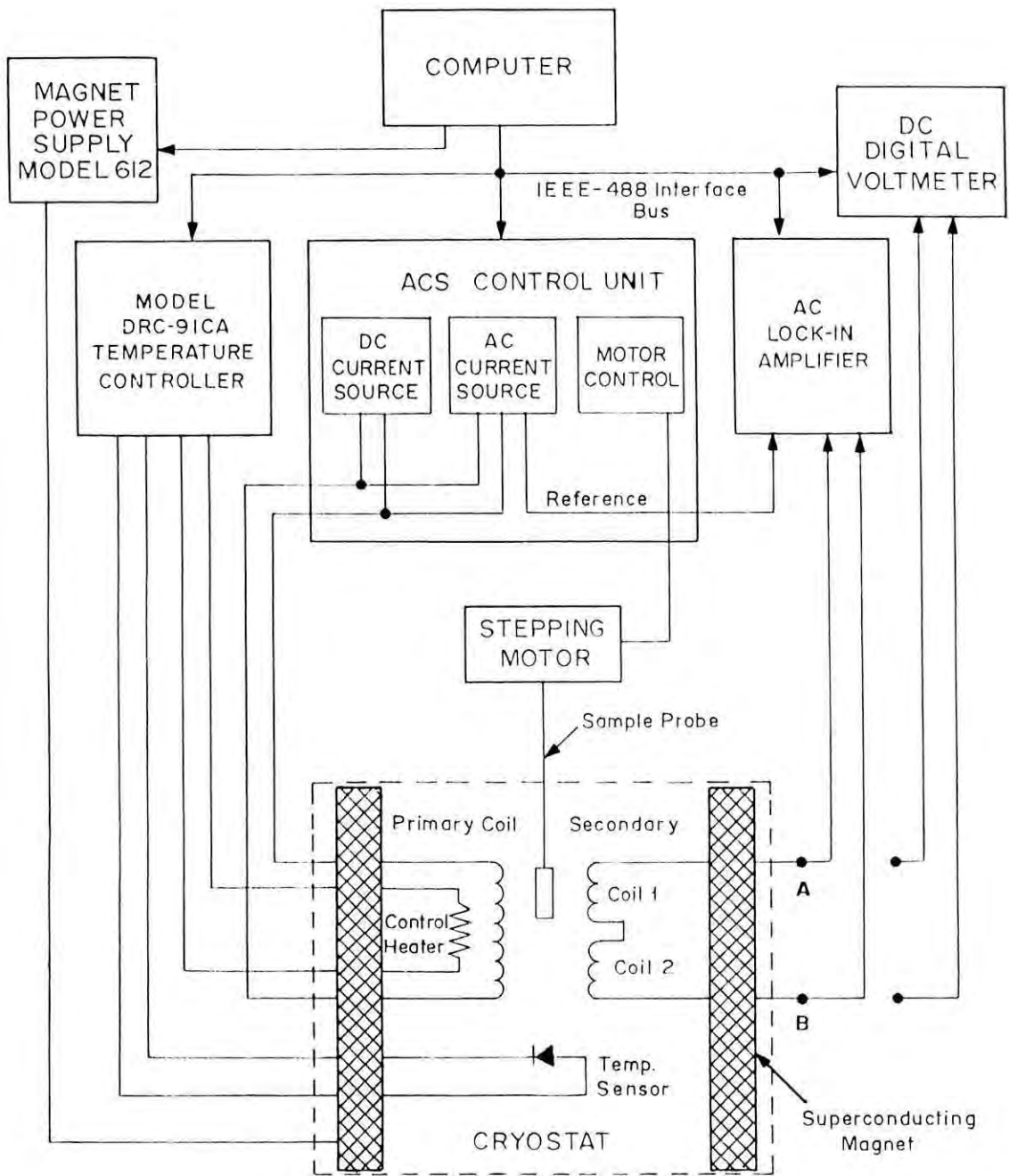


Fig. 4.6. AC Susceptometer / DC Magnetometer Block Diagram Model 7225

the measuring circuit. A cross-sectional view of the coil assembly is demonstrated in Fig.4.7. The two sensing coils are connected in opposition in order to cancel the voltages induced by the AC field itself or voltages induced by unwanted external sources. Assuming perfectly wound sensing coils and perfect symmetry, no voltage will be detected by the Lock-in amplifier when the coil assembly is empty.

When the sample is now placed within one of the sensing coils, the voltage balance is disturbed. The measured voltage is proportional to the susceptibility of the sample. In order to obtain the internal susceptibility of the sample demagnetization corrections are made. The true internal susceptibility, χ_{int} is given by the following relationship,

$$\chi_{int} = \frac{\chi}{1 - D\chi}$$

where D is the shape-dependent demagnetization factor and χ is the measured susceptibility of the sample.

One of the most useful features of the AC Susceptometer is that both the real or in phase component χ' and the imaginary or out of phase component χ'' of the susceptibility can be measured. The proper separation of the two components requires an understanding of how phasing is handled in a lock-in amplifier and how to make the appropriate adjustment for the sample being studied. The control software associated with AC susceptometer is designed to make this separation with minimal effort.

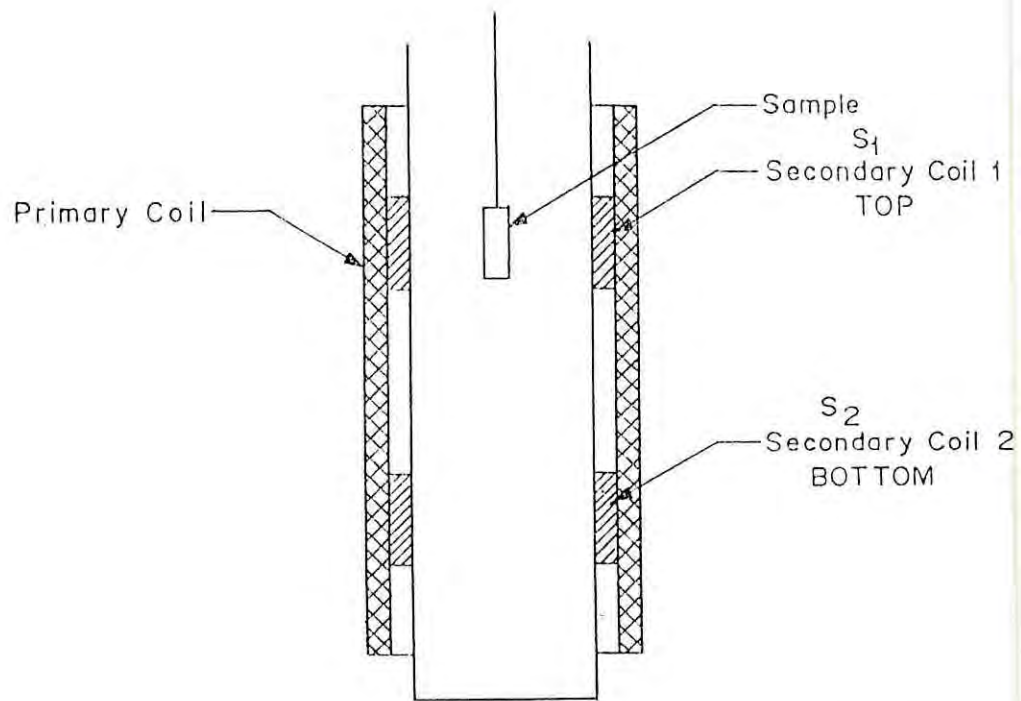


Fig. 4.7 Cross-sectional View of Primary and Secondary Coils.

Reference:

1. Mazid, M.A., M. Amanullah Chowdhury and Shireen Akhter, Internal report, 1986, Atomic Energy Centre, Dhaka
2. Foner, S., Rev. Sci. Instr., 1959, 30, 548
3. Foner, S., Rev. Sci. Instr., 1955, 27, 578
4. Ramaswamy, S., and L. Lundgren, Uppsala University report, UPTEC, 8345R, May, 1983
5. Nordblad, P. and L. Lundgren, Uppsala University report, UPTEC, 8003R, Jan, 1980
6. Figueroa, E. and S. Hornfeldt, Uppsala University report, UPTEC, 80 20R, March, 1980
7. MPMS User's Manual, Quantum Design Inc., U.S.A. August, 1990
8. Josephson, B.D., Phys. Lett., 1962, 1, 251
9. Lake Shore 7000 Series System Users Manual, U.S.A.

CHAPTER 5

Measurements on Nickel-Platinum alloys

5.1 Introduction

NiPt system exhibits complete solubility for all concentrations. Therefore, Nickel and Platinum can be mixed in all proportions to form disordered solid solutions having face centered cubic (A1) structure at high temperature. This high temperature disordered phase (fcc) can be retained at room temperature by rapid quenching ignoring slight tendency for segregation[1-2] and atomic ordering. It is in fact possible because the atomic mobility in this alloy system is very sluggish. These disordered phases transform via first-order transitions to ordered phases below about 900K in the sequence of simple cubic (L1₂), face centered tetragonal (L1₀), and simple cubic (L1₂) structures at the stoichiometric compositions Ni₃Pt, NiPt and NiPt₃ respectively, like in the prototype Cu-Au system[3-6]. The NiPt phase diagram is almost symmetrical versus concentration. Spin-orbit interactions have been accounted for ordering in NiPt alloys [7]. Temperature dependence of atomic relaxation time in both ordered and disordered states have been measured for the Ni-Pt system [8]. In the vicinity of the order-disorder transition, important slowing down effects are observed.

Ni-Pt alloys in the disordered phases have been investigated in detail earlier by several investigators[9-14] and it was observed that the ferromagnetic-paramagnetic transition takes place at a critical concentration $x_c \approx 58\text{at.}\% \text{ Pt}$ [10,11,14]. Alloys with Pt concentration higher than 58at.% appear to be exchange enhanced paramagnets [11]. From detailed analysis of the magnetization data the alloys near the critical concentration have been characterized as homogeneous weak itinerant ferromagnets in the sense of Edwards-Wohlfarth [15] and Mathon[16]. Such conclusion has been drawn from the observed linearity and parallelism of Arrott plots (M^2 against H/M) of the magnetization M as a function of magnetic field H over a wide range of concentrations, temperature and pressures and the proportionality of M_{00}^2 ($H=0, T=0$), $\frac{1}{\chi_0}$ and T_c^2 to concentration (where χ_0 is the initial susceptibility and T_c is the Curie temperature)[9-12,14]. But Ododo and Howarth [17] argued that these relationship

(other than for T_c) are a general property of any magnetic system in vicinity of the critical concentration, x_c , to which Landau's theory of phase transitions applies and are not restricted to homogeneous itinerant magnets. It has been shown that the magnetization appears inhomogeneously at the critical concentration in NiPt in conformity with the isoelectronic NiPd [18] and other Ni-based system [19-22] which exhibit distinctly inhomogeneous-moment distribution in the form of ferromagnetic clusters near the critical concentration. Acker and Huguenin [23] found that the experimental variation of magnetization at zero field and zero temperature, M_{00} , and of the Curie temperature T_c , with concentration and pressure does not agree with the predictions of the Edwards-Wohlfarth [15] and Mathon [16]. He has also proposed a model for NiPd alloys (where the local moments are formed by clusters of Ni atoms only) and demonstrated that rather straight Arrott plots may be expected in spite of obvious inhomogeneity. Therefore, one should be aware that a straight Arrott plot can not be considered as a decisive proof for the material to be magnetically homogeneous.

The results of neutron diffuse scattering on disordered NiPt alloys indicate that both Ni and Pt are magnetic. The average Ni moment decrease with increasing Pt concentration, while Pt has an average moment of about half that of Ni [24]. It has also been shown that moment disturbances are caused by the chemical-magnetic environment corresponding to inhomogeneous moment distribution which may be described as ferromagnetic clusters. The polarized neutron diffraction measurements showed inhomogeneous distribution of magnetization persists from 50at.%Pt to higher percentages [25]. However, magnetization measurement by Gillespie et al [9,26] did not reveal any magnetic clusters in Ni-Pt alloys near the critical concentration.

Although many properties of NiPt alloys by several investigators are in agreement with the Edwards-Wohlfarth model some inconsistencies with experimental results remain. The major disagreement of the earlier experimentalists with Edwards and Wohlfarth

theory is that the inverse of the paramagnetic susceptibility follows Curie-Weiss law

$\frac{1}{\chi} = (T - T_C)/C$ rather than the predicted $\frac{1}{\chi} = (T^2 - T_C^2)/C$. More over for the disordered Ni-Pt

alloys some inconsistent values of the Curie temperatures near the critical concentration exist.

Beille et al [14] reported a Curie temperature of 12K for Ni-58.6at.% Pt while his quoted

critical concentration is $x_C = 57.9\text{at.}\%$. Bolling [27] found $T_C = 45\text{K}$ for Ni-60at.%Pt. For Ni-

57.1at.%Pt $T_C \approx 23\text{-}25\text{K}$ [10,11,14], $14\text{-}16\text{K}$ [28,29].

The effect of atomic ordering on magnetic properties has been measured [6,30] to determine the chemical and magnetic phase diagram and found a strong dependence of magnetism on chemical order. Atomic order in Ni-Pt alloys around equiatomic composition is associated with magnetic disorder. The study of the magnetic behaviour of Ni-Pt system in the ordered phases has not been studied in much detail. Due to this reason and some of the discrepancies of the reported results it is felt encouraging to measure magnetic properties of this system in the most ordered and disordered states to understand the role of spatial order on the magnetic behaviour of the system.

5.2 Experimental

A series of $\text{Ni}_{1-x}\text{Pt}_x$ alloys in the polycrystalline form have been studied for magnetization and Curie temperature as affected by order-disorder mechanism. Measurements have been performed on six disordered with $x = 0.14, 0.24, 0.30, 0.44, 0.50$ and 0.57 and five ordered samples with $x = 0.24, 0.30, 0.44, 0.50$ and 0.57 .

Alloy specimens are prepared by arc melting in an argon atmosphere on a water-cooled copper hearth. Disordered samples are obtained by rapid quenching from 1000°C into water and long range atomic ordering is attained by long annealing below order-disorder transition

temperature. The structural analysis is made and the ordered-disordered states are confirmed by X-ray diffraction. A detail description of the sample preparation and characterization is given in chapter 3.

Magnetization has been measured with a vibrating sample magnetometer (VSM) at different temperatures in magnetic fields up to 5 kOe and a SQUID magnetometer in the temperature range 2-300K and magnetic fields up to 50 kOe. All measurements are done on sphere shaped samples whose demagnetizing factor is $4\pi/3$. In order to estimate the effective internal fields, demagnetizing corrections are estimated and subtracted from the values of the applied field according to the relation $H_i = H_a - 4\pi M d/3$, where H_i and H_a is the internal and applied magnetic fields respectively, M is the magnetization per gram and d is the density of the specimen.

A liquid helium cryostat has been used in conjunction with VSM for measurements in the temperature range 4.2K to 300K using calibrated Copper-constantin and gold (0.07%Fe)-chromel thermocouple. From room temperature and above, a high temperature oven has been used with a calibrated chromel-constantin thermocouple.

Curie temperatures are determined from low field DC magnetization data by kink point method [31,32]. In addition, an AC susceptibility measurement technique based on mutual induction method has been used to measure the Curie temperature. In this method Curie temperature is taken as the temperature where the rate of change of susceptibility with temperature is maximum. A platinum resistor is used as thermometer. Arrott plots are also utilized to determine Curie temperature. The isotherm that passes through the origin defines the Curie temperature.

5.3 Results and discussion

5.3.1 Disordered alloys

Magnetization as a function of internal magnetic fields for all the disordered samples of $\text{Ni}_{1-x}\text{Pt}_x$ at 4.2 K measured with a VSM is shown in Fig. 5.1. Magnetization curves show a good saturation under an internal magnetic field of 4 kOe, except for $x=0.5$ (not readily visible in Fig.5.1) and 0.57. The sample with $x=0.57$ do not show any spontaneous magnetization even at $T=2$ K as discussed latter. Magnetization measurement up to magnetic field of 50 kOe with a SQUID magnetometer could not saturate the sample with $x=0.5$ and 0.57. Magnetization increases almost linearly from 7 emu/g at 5 kOe to 7.72 emu/g at 50 kOe for $x=0.5$. This supports the results of Beille et al [9], who could not saturate them even with applied magnetic field of 150 kOe. From the magnetization curves of Fig.5.1, spontaneous magnetization (M_0) for each alloy is determined. The spontaneous magnetization of a ferromagnet is the value of its intrinsic, or domain, magnetization in zero applied field. Because of the complications associated with the domain structure, it is not possible to measure this quantity directly. Therefore some extrapolation procedure is adopted. Spontaneous magnetization (M_0) at 4.2 K is estimated by linear extrapolation of the magnetization curves obtained in strong fields to zero internal field ($H=0$). The estimated values of the spontaneous magnetization at 4.2K is found to be very close to the value of spontaneous magnetization at zero kelvin, the difference being insignificantly small. The magnetic moment μ per formula unit is calculated using the mean field theory and spontaneous magnetization (M_0) data at 4.2K with the equation

$$\mu = AM_0/N\mu_B, \quad (5.1)$$

where A is the molecular weight of the sample, N is the Avogadro's number and μ_B is the Bohr magneton. The results are given in Table 5.1, together with spontaneous magnetization at 4.2K and saturation magnetization M_s , at 4.2K, 77.3K and 293K. For the $x=0.50$ sample,

magnetic moment, μ , is calculated from the magnetization value obtained at 50 kOe magnetic field because the magnetization is not saturated and the extrapolated value of the spontaneous magnetization may underestimate the value of magnetic moment in Bohr magneton.

Variation of magnetic moment with Pt concentration in atomic percent is shown in Fig.5.2. Suitable extrapolation of the magnetic moment μ to $\mu=0$ leads to a critical concentration of approximately 57at.%Pt and that to $x=0$ gives a magnetic moment of pure nickel comparable with the accepted value. This value of critical concentration of 57at.%Pt for the disordered Ni-Pt alloys in the present study is in reasonable agreement with the reported values of 58at.%Pt [10,11,14] and 56at.%Pt [30]. From Fig.5.2 it is observed that magnetic moment decreases continuously and nonlinearly with Pt concentration. These results are in good agreement with those of Fisher et al[12] but disagree with those of Marian[13] who found a linear dependence up to 40 at.%Pt. Such type of curvature of magnetic moment with concentration has also been observed in Ni-Pd alloys with Pd concentration higher than 50at.% and is interpreted as a phenomenon of depolarization[33-35]. In case of Ni-Pd magnetic moment vanishes at 97.3at.%Pd [36]. The lower value of critical concentration for Pt is probably due to the fact that Pt is not so near to be in ferromagnetic state as Pd, because of its lower density of state [37,38]. Fig.5.3 shows the magnetic isothermals of the alloy with $x=0.57$ up to 50 kOe magnetic field. The magnetization isotherm for 2 K rises sharply at low fields and then gradually bends over but still rising up to the maximum applied field of 50 kOe where magnetization of 3.75 emu/g is reached. This situation persists up to high temperature. The magnitude of the rate of change of magnetization with field indicates that this is not an ordinary paramagnetic state. Even at 80 K magnetization is not a linear function of field. The nonlinearities of the M vs H curves may be attributed to the ferromagnetic clusters present in the sample. The clusters are randomly oriented in the absence of any magnetic field. Application of a magnetic field partially orients them in the field direction. The size of the

89369

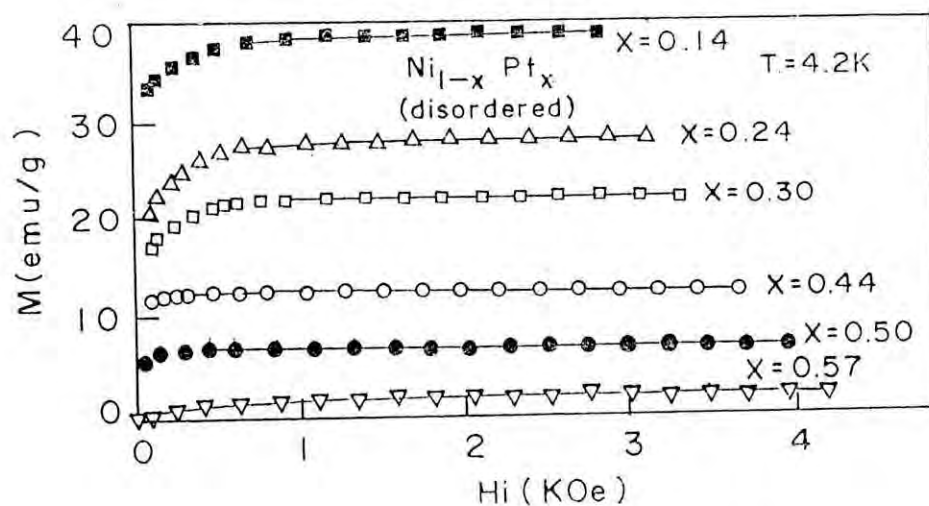


Fig.5.1. Magnetization per gram as a function of internal magnetic field of the disordered $\text{Ni}_{1-x}\text{Pt}_x$ alloys at 4.2 K.

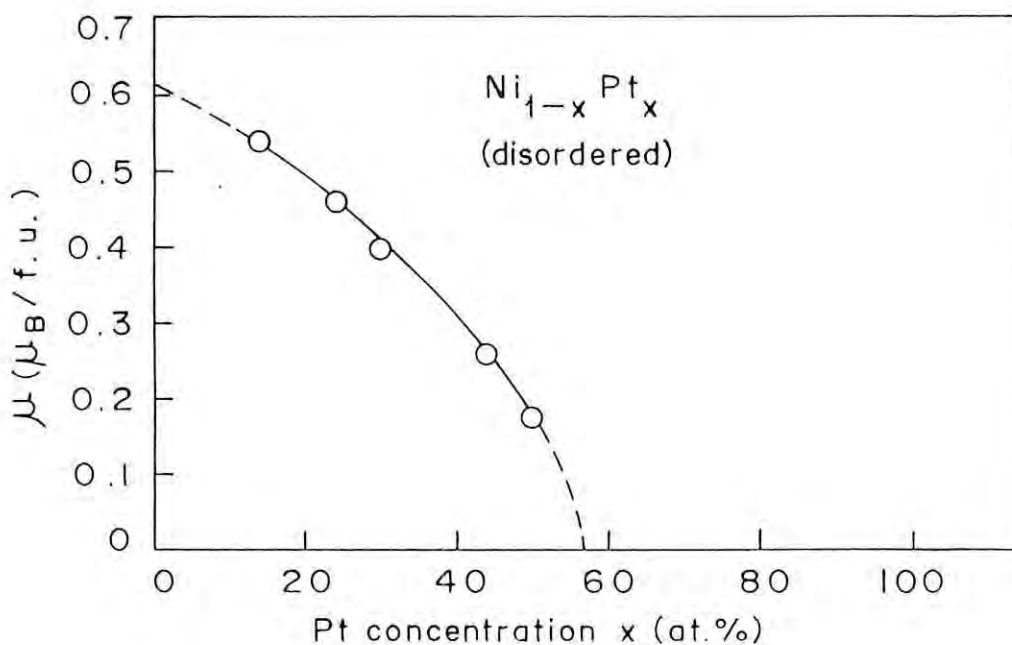


Fig.5.2. Variation of magnetic moment μ per formula unit versus platinum concentration of the disordered $\text{Ni}_{1-x}\text{Pt}_x$ alloys.

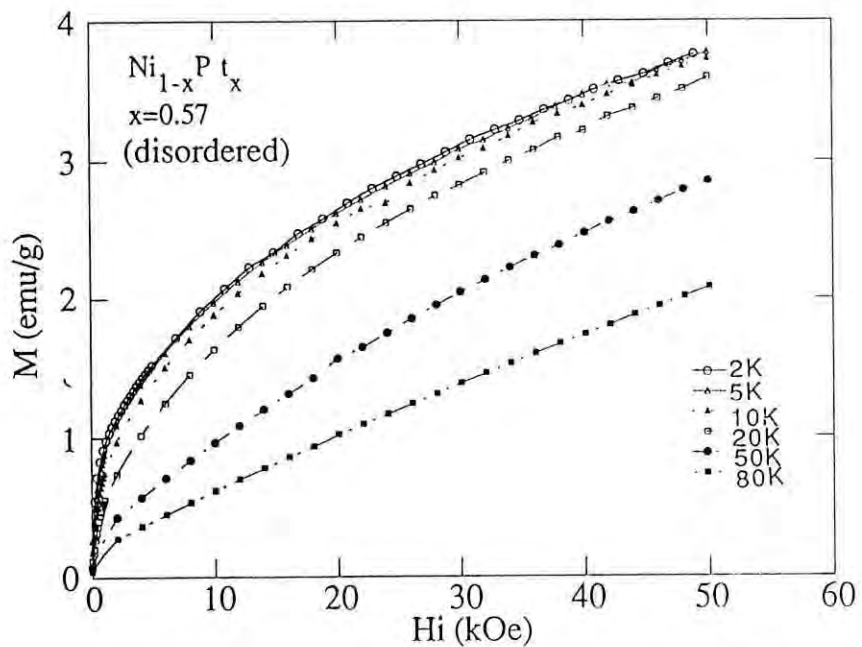


Fig. 5.3. Magnetic isotherms (M vs H) of the disordered $\text{Ni}_{1-x}\text{Pt}_x$ with $x=0.57$

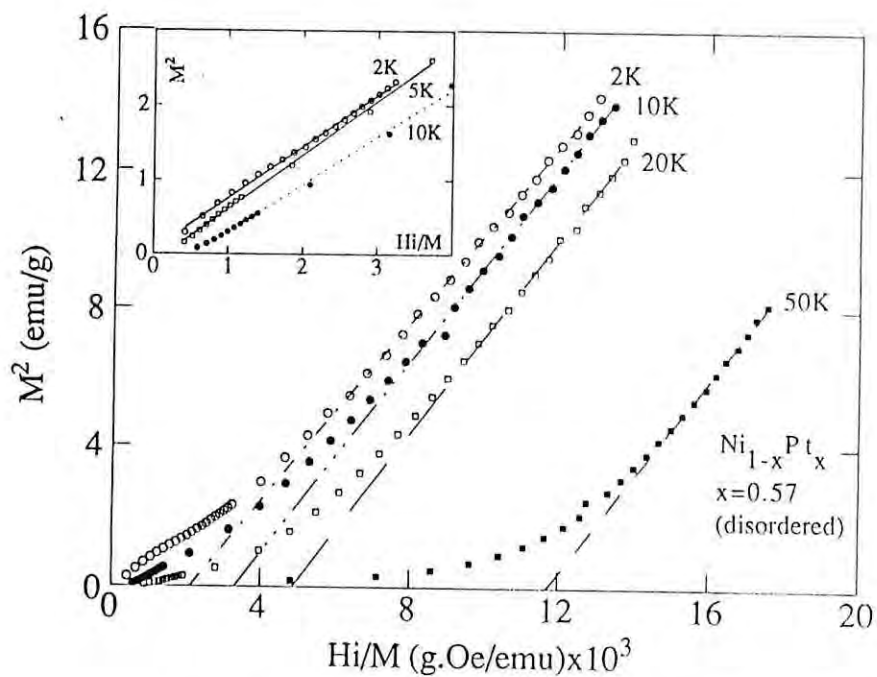


Fig. 5.4. Arrott plots from the magnetic isotherms of Fig. 5.3.; inset: Arrott plots with low magnetic fields.

ferromagnetic clusters give the characteristic curvature to the magnetization curve. It is noticed that the curvature is less pronounced at higher temperature magnetic isotherms due to decreasing the cluster size with temperature.

Arrott plots have been utilized in an attempt to determine the spontaneous magnetization. Arrott plots are based on straight line criterion and the extrapolation of the straight M^2 vs H/M curves to $H/M=0$ gives square of the spontaneous magnetization (M_0^2) and $M^2=0$ gives inverse of the initial susceptibility ($\frac{1}{\chi_0}$). Arrott plots are demonstrated in

Fig.5.4. It is evident that no spontaneous magnetization is observed even at 2 K when the Arrott plots are extrapolated from high field as well as low field magnetization data (in set of Fig 5.4) indicating the alloy to be paramagnetic at 2 K. But it seems quite reasonable to assume from the experimental evidence that this alloy is very close to the critical composition for the onset of ferromagnetism.

The Curie temperature, T_C , is a basic quantity in the studies of magnetic phase transitions of ferromagnetic materials. Low field DC and AC magnetization measurements as a function of temperature have been performed on Ni-Pt alloys to determine the Curie temperatures. Temperature dependence of low field DC magnetization measured with a VSM is shown in Fig.5.5a for the sample with $x=0.14$ and 0.24 in the magnetic field of 58 Oe which is the remanent field of the electromagnet. This low field magnetization is essential in determining the presence of a "kink point" in the magnetization [32]. Demagnetizing field limits the magnetization to a value of $M=H_a/D$ (where H_a is the applied magnetic field and D is the demagnetization factor), producing a magnetization that is temperature independent below the kink point. This kink point is considered as ferromagnetic Curie temperature. The measurements have been performed for all Ni-Pt alloys and Curie temperatures are determined during warming and cooling and the T_C values are reproducible within ± 1 K.

Low frequency (37 Hz), low field (10^{-3} Oe) AC susceptibility measurements as a

function of temperature have been carried out for the samples in the temperature range 4.2 K-300 K. In this method the set up with the sample is inserted into liquid helium dewar and susceptibility has been recorded during warming and cooling the sample. Fig.5.5b shows a representative curve with $x=0.44$ sample. The maximum of $\frac{d\chi}{dt}$ has been taken as the Curie temperature of the sample and found to be $T_C = 155\text{K}$. This value is very close to that of 156K determined by kink point method. In spite of back-ground signal from the applied field in the AC measurements the transition temperature is found to be equally well defined as in the Low field DC measurements.

The results of low field (20 Oe) DC magnetization taken with a SQUID magnetometer for the alloy $x=0.50$ are demonstrated in Fig.5.6 together with the AC susceptibility measurements (in set of Fig.5.6). The Curie temperatures are 77K for DC measurement and 80K for AC measurement. This is to note that DC magnetization measurements have been performed on this disordered sample with a time gap of three years to look for any possible ordering effect due to aging at ambient temperature. It is not clear whether this small difference in T_C is due to some atomic ordering that might take place during this period of time or due to different techniques used including experimental errors. But magnetization per gram at 4.2 K with magnetic field of 50 kOe have almost the same value of 7.75 and 7.72 before and after aging respectively. The Curie temperatures of the alloys with $x=0.14$, 0.24 and 0.30 have also been determined by Arrott plots and are found to be in good agreement ($\pm 1\text{K}$) with other methods. The results of all Curie temperature determinations are given in Table 5.1. Since the thermocouples in all methods of measurements are not directly attached to the sample and the reproducibility of the data is within $\pm 1\text{ K}$, it is felt that the absolute value of the Curie temperature may be considered as $T_C \pm 2\text{K}$. When all the various T_C data for disordered Ni-Pt alloys are collected as in Fig.5.7, a linear variation of T_C with Pt concentration is observed. Linear extrapolation of the Curie temperatures T_C to $T_C = 0$,

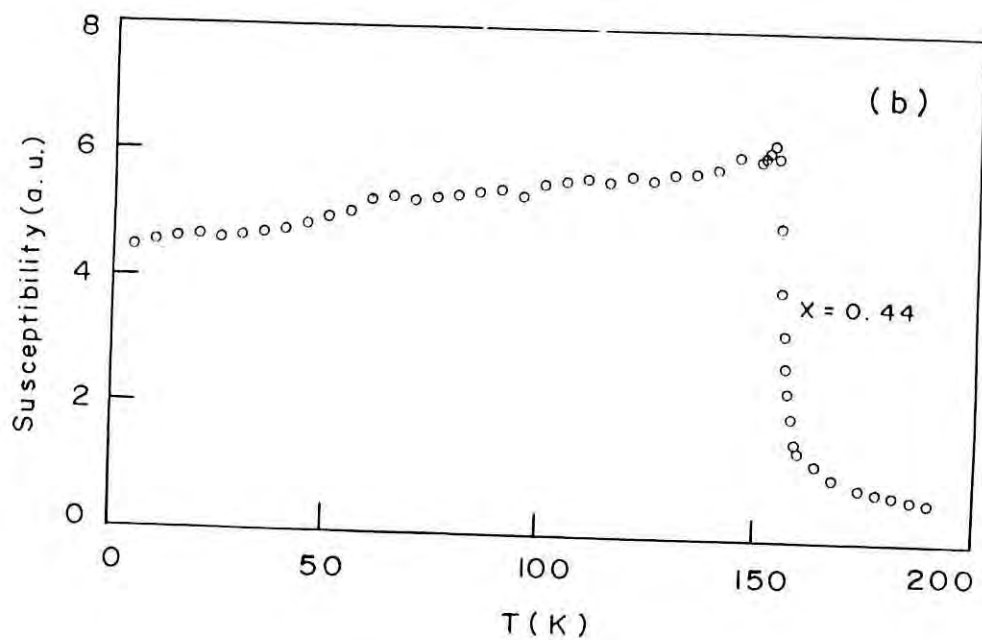
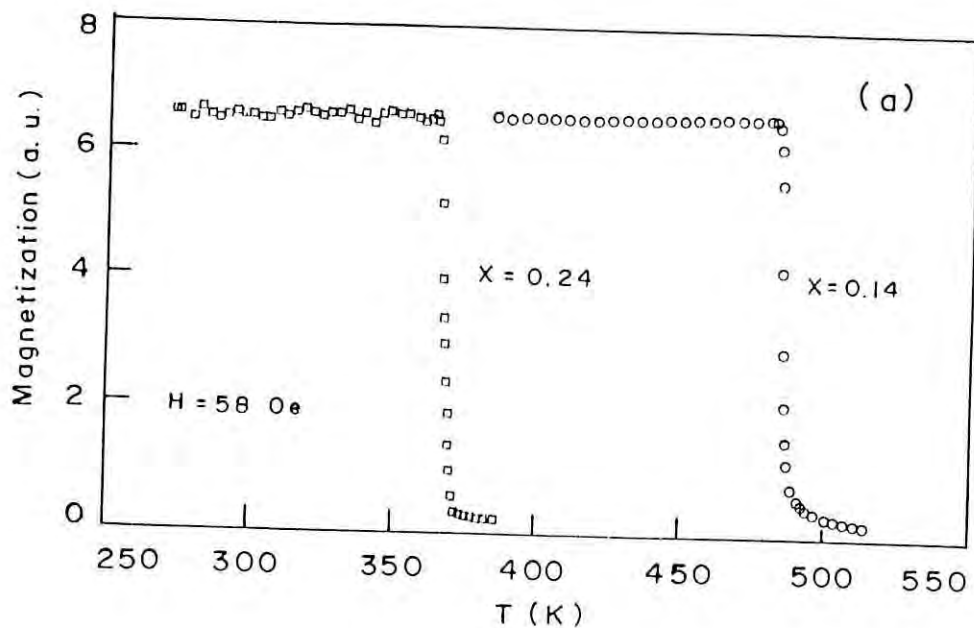


Fig.5.5. Temperature dependence of (a) low field DC magnetization with $x=0.14$ and 0.24 and (b) AC susceptibility with $x=0.44$ of the disordered $\text{Ni}_{1-x}\text{Pt}_x$ alloys.

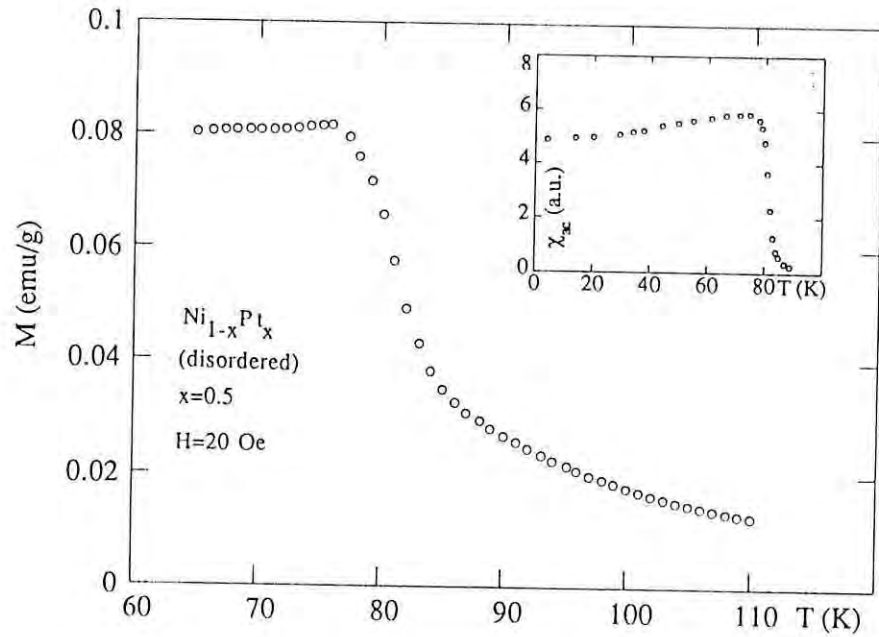


Fig.5.6. Temperature dependence of low field DC magnetization of the disordered alloy with $x=0.50$; inset: AC susceptibility for $x=0.50$

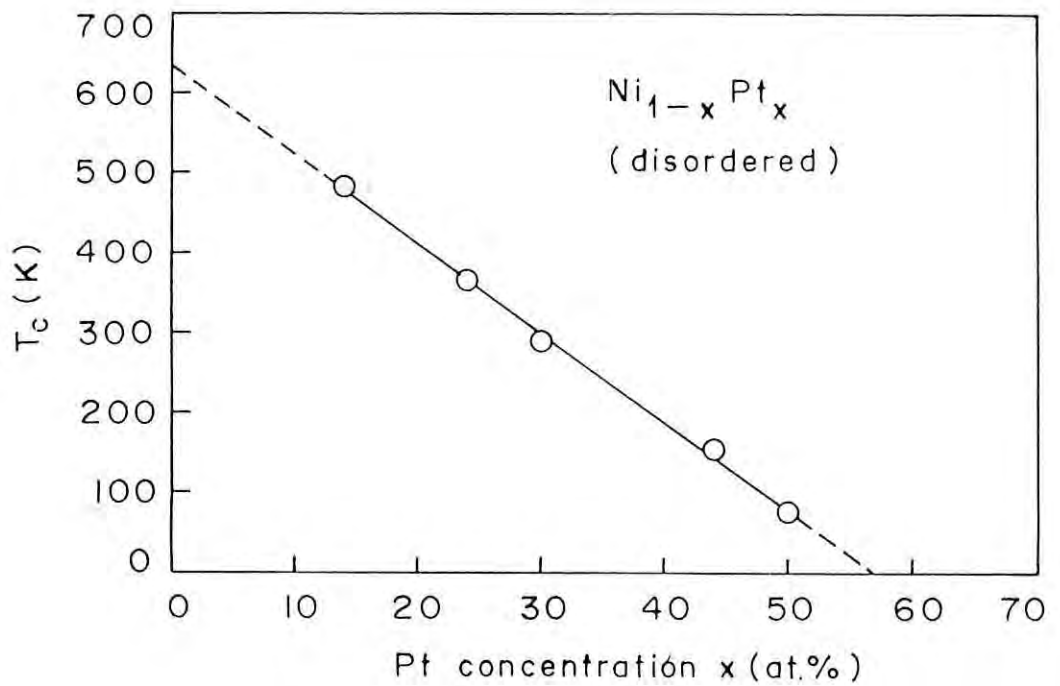


Fig.5.7. Concentration dependence of the ferromagnetic Curie temperature of the disordered $Ni_{1-x}Pt_x$ alloys.

Table.5.1 Magnetic properties of disordered Ni_{1-x}Pt_x

Platinum content x	0.14	0.24	0.30	0.44	0.50	0.57
M ₀ (H=0),T=4.2K (emu/g)	38.54	28.10	22.2	12.5	6.82	
M _S (emu/g)						
4.2K	39.09	28.50	22.39	12.69	7.72 ^a	3.75 ^a
77.3K	38.15	27.45	21.15	10.65	3.03	
293K	32.37	18.65	5.07 ^b			
μ (μ _B /f.u.)	0.54	0.46	0.40	0.27	0.176	
T _C (K)	484	367	292	156	79	

^a Value corresponding to H=50 kOe

^b Value corresponding to H=5 kOe

indicates a critical concentration of 57.2at.%Pt which is in good agreement with the critical concentration determined by extrapolation of magnetic moment $\mu = 0$ in the present work and previous reported results [10,11,14,30,39]. A least squares fit to the present Ni-Pt data shows that T_C with concentration is given by the empirical relation

$$T_C = 11.06 (57.2-x) \quad (5.2)$$

where x is the concentration of Pt in atomic percent. This linear dependence is valid over the whole ferromagnetic regime extrapolated to pure nickel indicating $T_C = 633\text{K}$, agrees quite well with the accepted value of 631K [40]. This is also what Albert et al [10] have pointed out that for a localized model of ferromagnetism Curie temperature should vary linearly with concentration, i.e. $T_C = K(x_C-x)$, where K is an arbitrary constant and x_C is the critical concentration of Pt in atomic percent. Ododo [36] collected the existing experimental data on Curie temperatures of disordered Ni-Pt alloys including that of weakly ferromagnetic alloys and demonstrated a linear dependence of Curie temperature with concentration appropriate for the localized model as proposed by [10] and in contrast with the square-root dependence, i.e. $T_C = K(x_C-x)^{1/2}$ proposed for an weak itinerant model [16] and claimed by previous authors [10,11].

Temperature dependence of magnetization and reciprocal susceptibility measured with magnetizing field of 10 kOe in the temperature range 5-300 K for $\text{Ni}_{1-x}\text{Pt}_x$ alloys with $x=0.50$ and 0.57 are depicted in Fig.5.8 and 5.9. From the general shape of the M vs T curves for $x=0.50$ sample, it seems likely that the transition occurs between a ferromagnetic and paramagnetic state around 80 K. If high field (10 kOe) M vs T data in Fig 5.9 for $x=0.57$ is scrutinized carefully one can identify an inflexion point around 15 K which may mistakenly be taken as the Curie point. But low-field (20 Oe) DC magnetization (see inset Fig.5.9) from 2-20 K does not show any inflexion or kink and its temperature dependence is typical for a paramagnet. AC susceptibility measurement down to 4.2 K did not

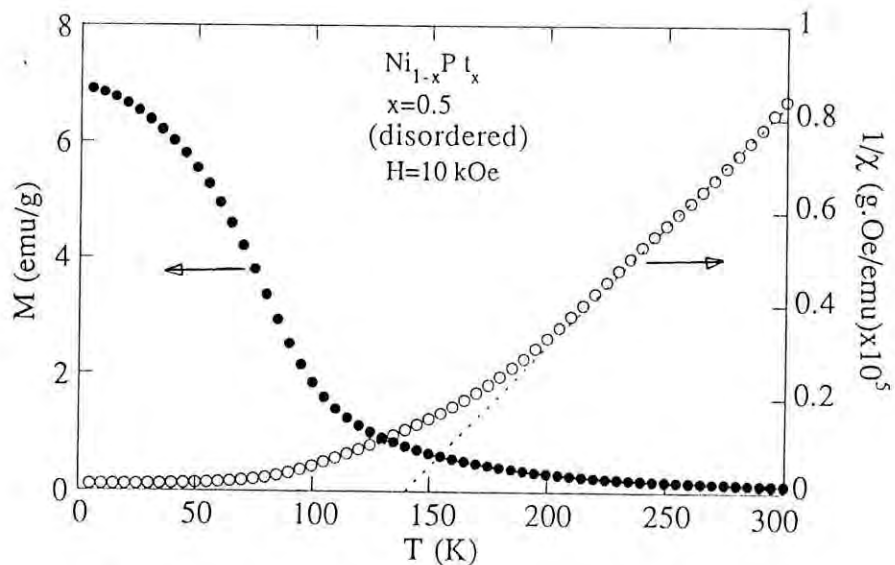


Fig.5.8. Temperature dependence of the magnetization and the reciprocal susceptibility of the disordered $\text{Ni}_{1-x}\text{Pt}_x$ with $x=0.50$ at 10 kOe.

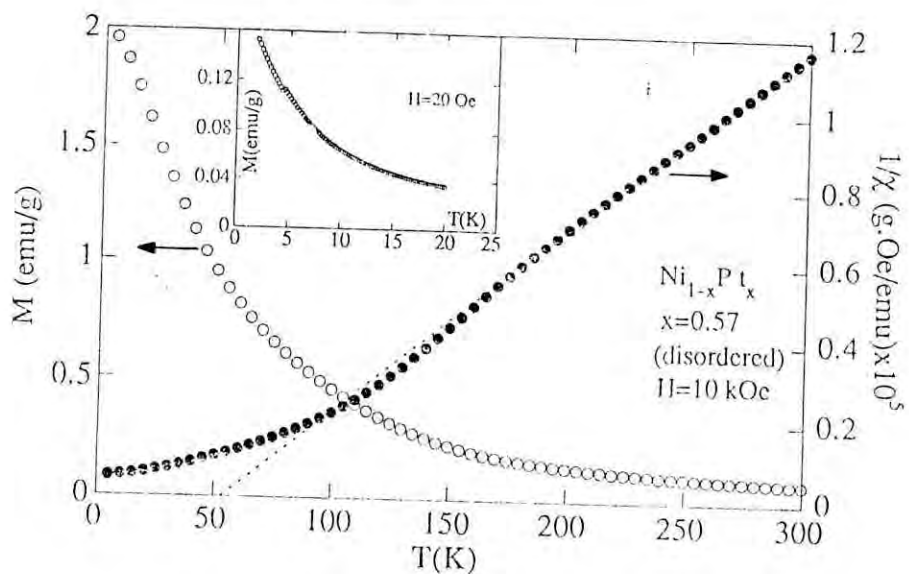


Fig.5.9. Temperature dependence of the magnetization and the reciprocal susceptibility of the disordered $\text{Ni}_{1-x}\text{Pt}_x$ with $x=0.57$ at 10 kOe; inset : M vs T curve at 20 Oe .

show any magnetic transition. A slight discontinuity at 4.6 K in the low field magnetization is due to sudden boiling of liquid helium which is a characteristic feature of the SQUID magnetometer used. The earlier reported inconsistent values of T_c , as mentioned before near the critical concentration may be due to the use of high field (in some cases greater than 20 kOe) for the determination of the transition temperature as mentioned by Ododo [36]. It has been suggested that very low field AC or DC measurements are satisfactory for the determination of the Curie temperatures of weakly ferromagnetic alloys [41].

The temperature dependence of the inverse mass susceptibilities of the sample $x = 0.50$ and 0.57 as shown in Fig 5.8 and 5.9 can be well fitted to a Curie-Weiss law, $\chi = C/T - \theta$ above 240 and 170 K with paramagnetic Curie temperature $\theta = 139$ and 53 K respectively. The molar Curie constants are 0.29 and 0.25 emuK/mole, leading to effective paramagnetic moments (P_{eff}) of $1.42\mu_B/f.u.$ and $1.52 \mu_B/f.u.$ respectively. Paramagnetic Curie temperature exceeds ferromagnetic Curie temperature by 75% for $x = 0.5$ sample implying the existence of large amount of short range ordering above T_c .

5.3.2 Ordered alloys

Magnetization as a function of internal magnetic field of $\text{Ni}_{1-x}\text{Pt}_x$ with $x=0.24$ and 0.30 measured at 4.2 and 293 K for the ordered and disordered phases are displayed for comparison in Fig.5.10a and 5.10b respectively. Magnetization of the ordered alloys are well saturated with an internal magnetic field of 3.5 kOe like those of disordered alloys at 4.2 K. But Arrott plots do not show any spontaneous magnetization at 293 K for the ordered and disordered phases of the sample $x=0.30$ indicating that they are paramagnetic at 293 K. Ordering decreases magnetization by about 13% at 4.2 K for both the samples. The Curie temperatures for the samples with $x=0.24$ and 0.30 have been determined by low field DC magnetization and AC susceptibility measurements and are depicted in Fig.5.11a and 5.11b respectively. The Curie temperature decrease from 367 and 292 K in the disordered state to 357 and 278 K in the ordered state for the samples with $x=0.24$ and 0.30 respectively. Table 5.2 shows the result of the ordered $\text{Ni}_{1-x}\text{Pt}_x$ alloys. Fig.5.12a and 5.12b show the magnetization versus internal magnetic field curves for $x=0.44$ and 0.50 respectively of $\text{Ni}_{1-x}\text{Pt}_x$ alloys in the ordered states and their Arrott plots are displayed in Fig.5.13a and 5.13b respectively. The magnetic isotherms at 5 K for $x=0.44$ and 0.50 samples show a very rapid initial rise and then slowly bends but continue to increase with no sign of saturation at the maximum magnetic field of 50 kOe giving magnetization per gram 3.72 and 0.95 emu/g. The magnetic isotherms at higher temperatures also display the same trend. This type of magnetization versus field behaviour at different temperatures have been observed for the disordered alloy with $x=0.57$ (see Fig. 5.3) as described before. These alloys are paramagnetic in the sense that no spontaneous magnetization (M_0) is observed at 5 K in their Arrott plots (Fig. 5.13a,b) and no transition temperature could be detected in the temperature dependence of magnetization with low fields. The rapid initial increase in magnetization at very low field is most likely due to the presence of some small amount of randomly oriented ferromagnetic

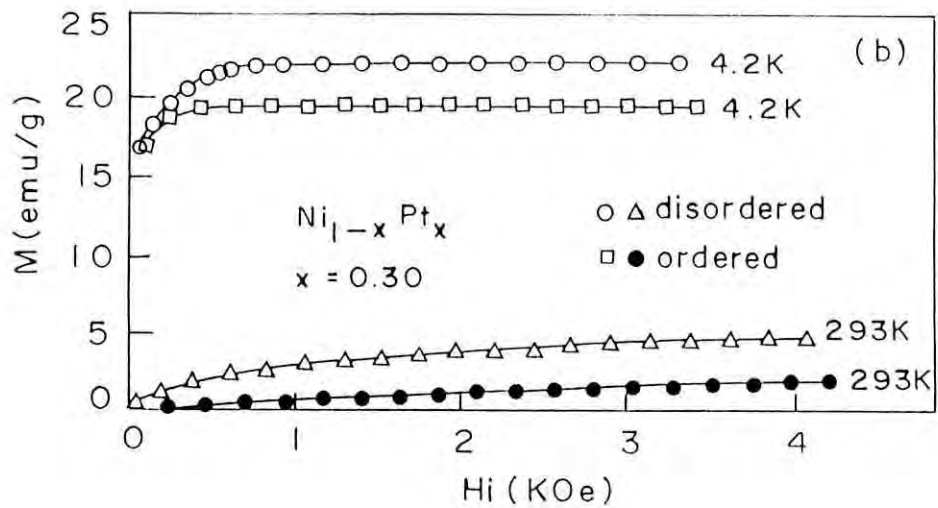
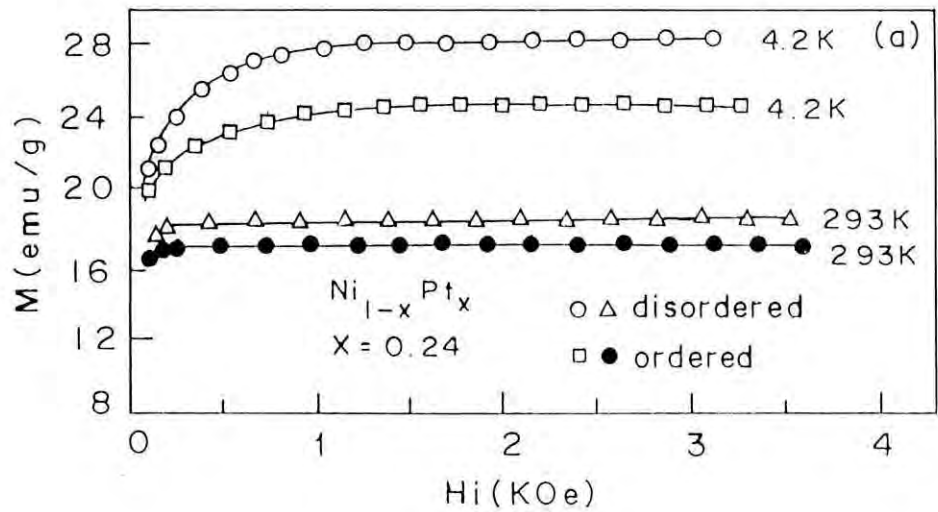


Fig. 5.10. Magnetization as a function of internal magnetic field of the $Ni_{1-x}Pt_x$ alloys with (a) $x=0.24$ and (b) $x=0.30$ at 4.2 and 293 K in the ordered and disordered states.

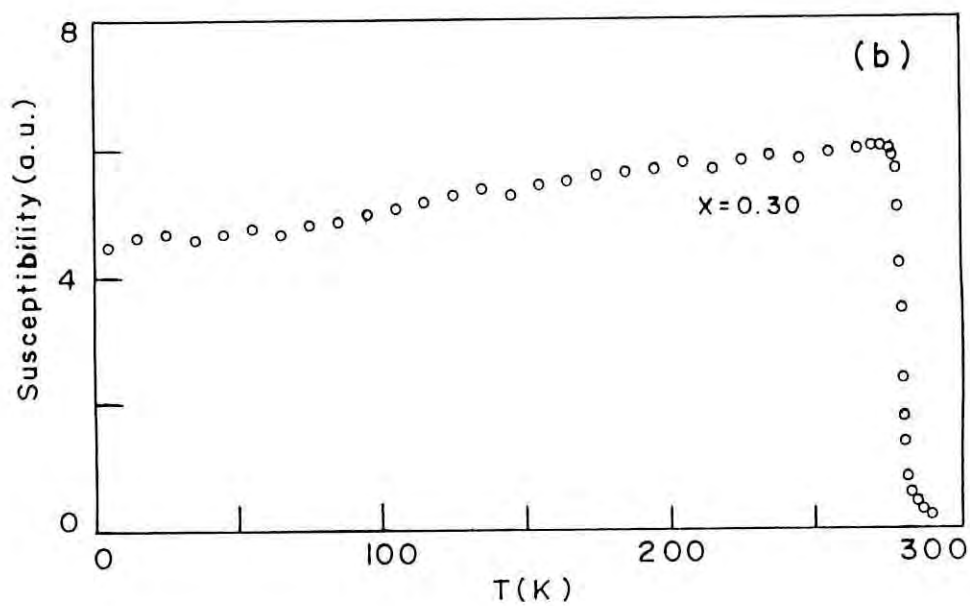
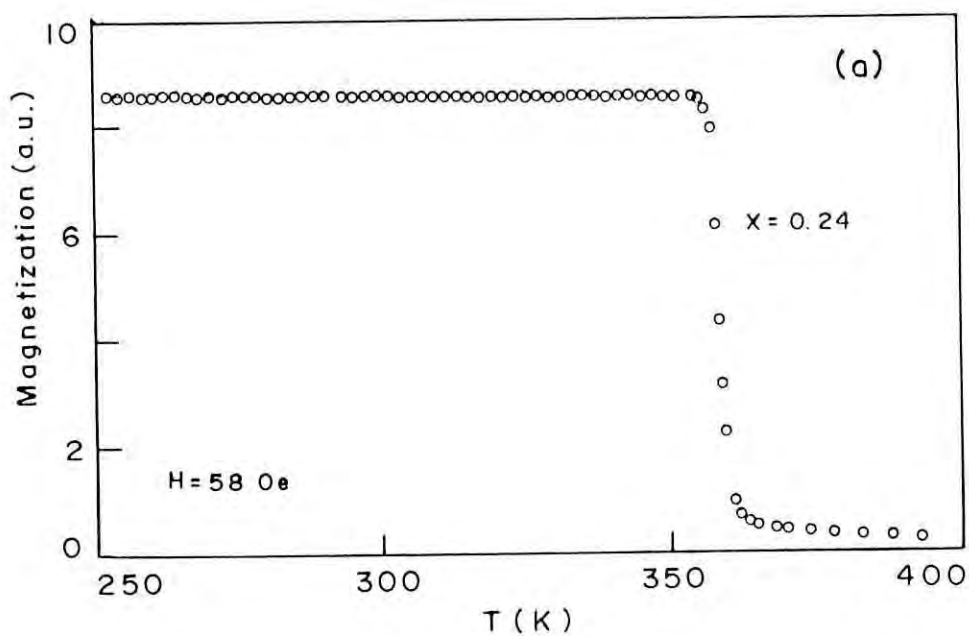


Fig. 5.11 Temperature dependence of (a) Low field DC magnetization with $x=0.24$ and (b) AC susceptibility with $x=0.30$ of the ordered $\text{Ni}_{1-x}\text{Pt}_x$ alloys.

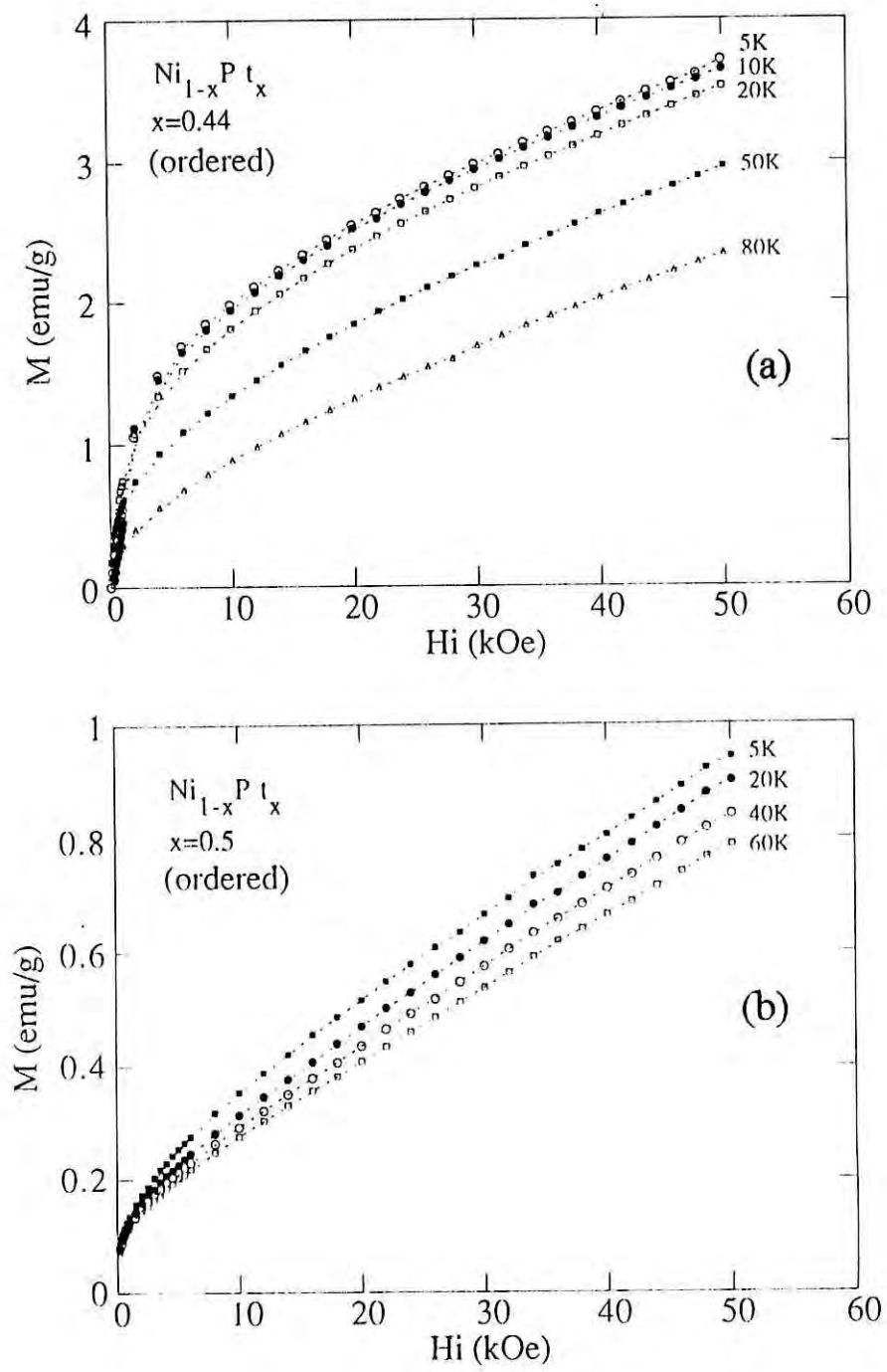


Fig 5.12. Magnetic isotherms of the ordered $\text{Ni}_{1-x}\text{Pt}_x$ with (a) $x=0.44$ and (b) $x=0.50$

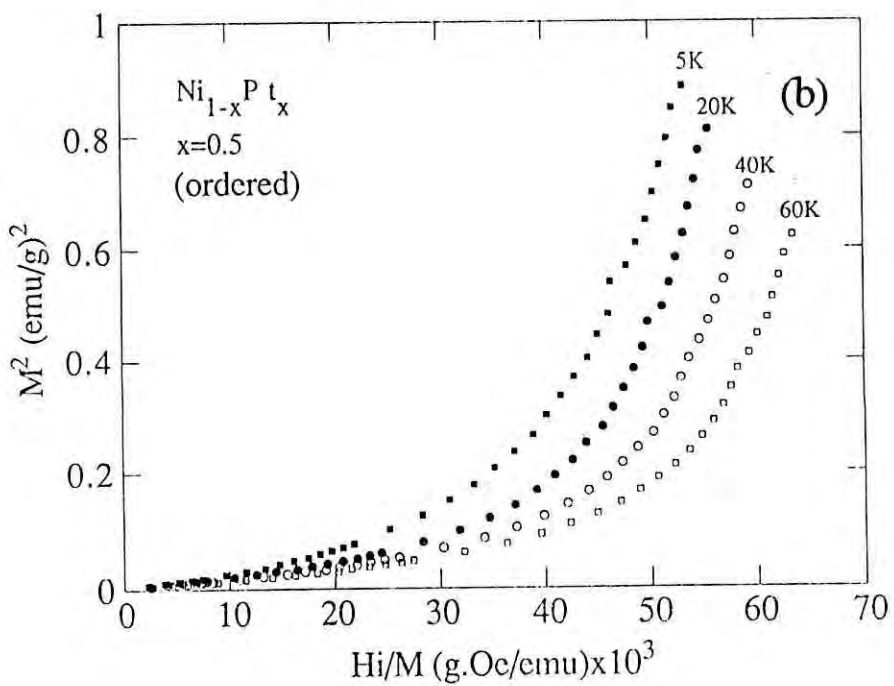
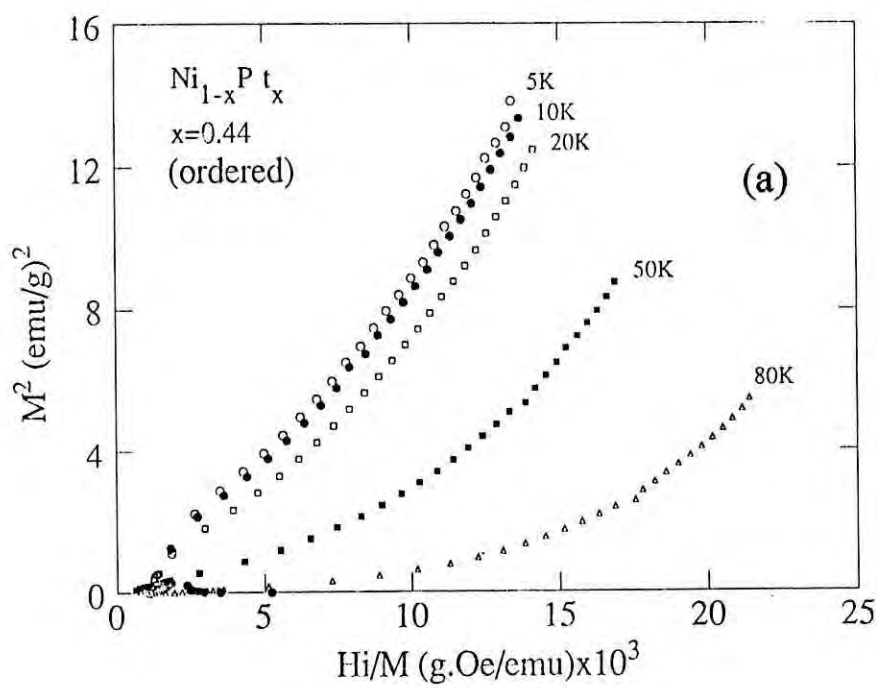


Fig.5.13. Arrott plots from the magnetic isotherms of (a) Fig. 5.12a and (b) Fig. 5.12b.

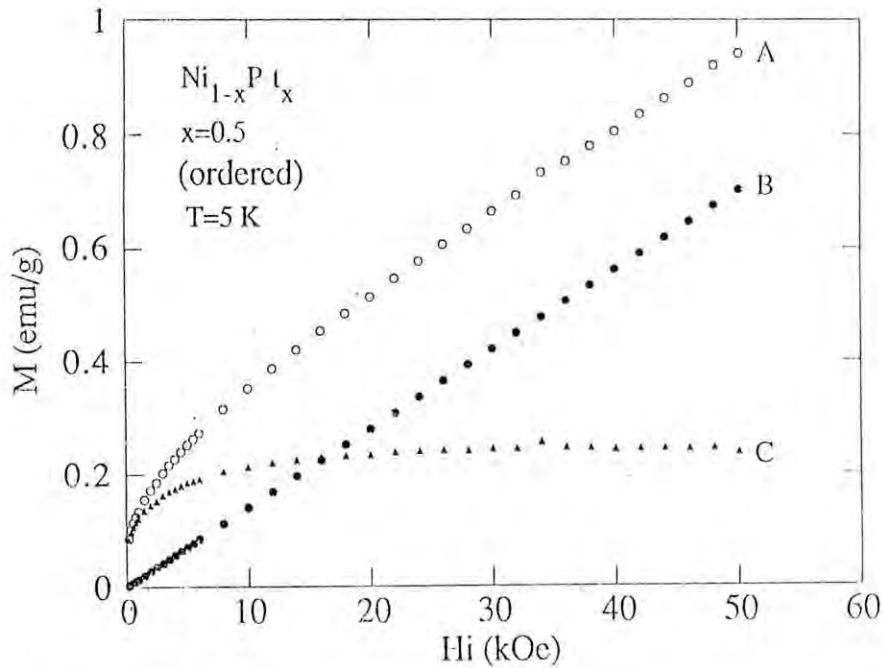


Fig. 5.14. Analysis of the magnetization curve of the ordered $\text{Ni}_{1-x}\text{Pt}_x$ alloy with $x=0.5$ at 5 K. Curve A is the sum of the curves B and C. Curve C represents the cluster magnetization as a function of field. B is the M vs H curve of the paramagnetic (noninteracting) NiPt phase

region rich in Ni atoms in the solid solution which align regularly with respect to each other with the application of magnetic field giving rise to magnetization. Fig.5.14 shows a simple analysis of this type of behaviour in which M vs H Curve (A) at 5 K for $x=0.5$ in the ordered state is used. The curve A is the sum of the curves B and C. C is the magnetization curve of the small amount of ferromagnetic phase or ferromagnetic clusters which is saturated at a field of less than 10 kOe. The curve B represents the field independent susceptibility of the sample which has the same slope as the straight line portion of the curve A. The magnetization curves of this nature can be expressed with the following equation [42],

$$M = \chi H + NJg\mu_B B_J \left(\frac{Jg\mu_B H}{kT} \right) \quad (5.3)$$

The first term of the above expression gives the magnetization from non-interacting atoms having a field independent susceptibility χ and the second term gives the average

magnetization from clusters containing small region rich in ferromagnetic atoms and coupled ferromagnetically with the application of field. Magnetic isothermals for the sample $x=0.57$ show field independent susceptibility as generally observed for the paramagnets.

The temperature dependence of magnetization of the ordered samples with $x=0.44, 0.50$ and 0.57 is shown in Fig.5.15-5.17. The sample with $x=0.57$ shows (Fig.5.17) the Curie-Weiss behaviour with $\theta = -134$ K indicating antiferromagnetic interaction. The molar Curie constant is 0.38 leading to effective paramagnetic moment of $1.74 \mu_B/\text{f.u.}$ Sample with $x=0.44$ and 0.50 does not follow Curie-Weiss law. Temperature dependence of magnetization for $x=0.5$ sample shows anomalous behaviour. From M vs T curve it is noticed that around 200 K there is a discontinuity of the curve. Upto 200 K magnetization of ferromagnetic clusters and average magnetization of the sample is observed. Little above 200 K ferromagnetic phase passes through ferromagnetic-paramagnetic transition (FM-PM), so magnetization decreases faster. Above 200 K magnetization originates mainly from non-interacting atoms term of the above equation and hence shows a temperature dependence typical for a paramagnet.

Therefore it is understood that ordered samples near the critical concentration are magnetically inhomogeneous. Some randomness and heterogeneity persists up to high temperature. Ferromagnetic clusters are there in the both the ordered and disordered alloys near the critical concentration. The results show that effect of atomic ordering on the magnetic properties of Ni-Pt system around the composition Ni_3Pt is small. Around equiatomic composition NiPt , atomic ordering changes the magnetic order, i.e. atomically disordered alloys are ferromagnetic, but ordered alloys are paramagnetic (magnetically disordered). It is interesting to notice that ferromagnetism disappears on the ordered samples throughout the composition range in which $L1_0(\text{fct})$ structure exists. So $L1_0$ structure might be responsible for the unusual magnetic behaviour of the alloys near the critical concentration. One of the

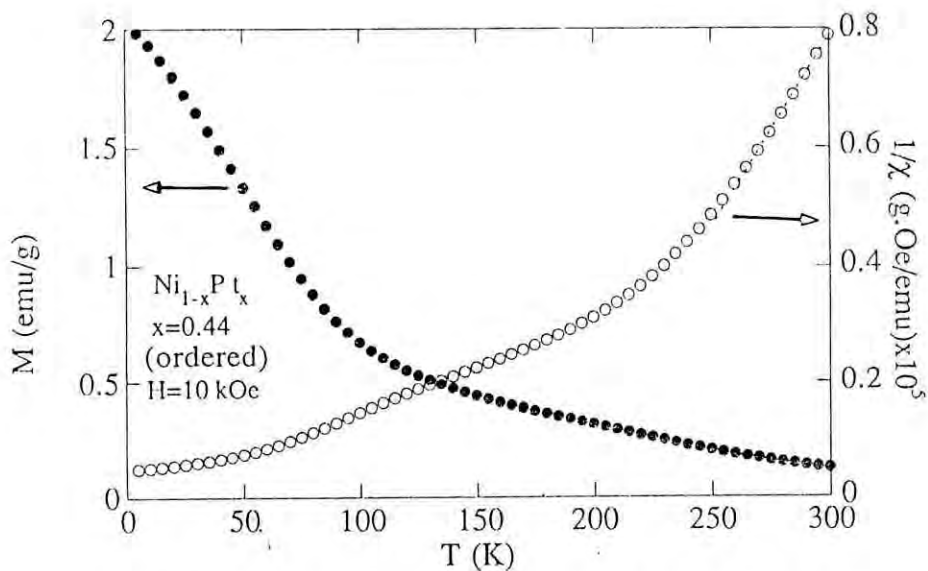


Fig. 5.15. Temperature dependence of the magnetization and the reciprocal susceptibility of the ordered $\text{Ni}_{1-x}\text{Pt}_x$ with $x=0.44$ at 10 kOe.

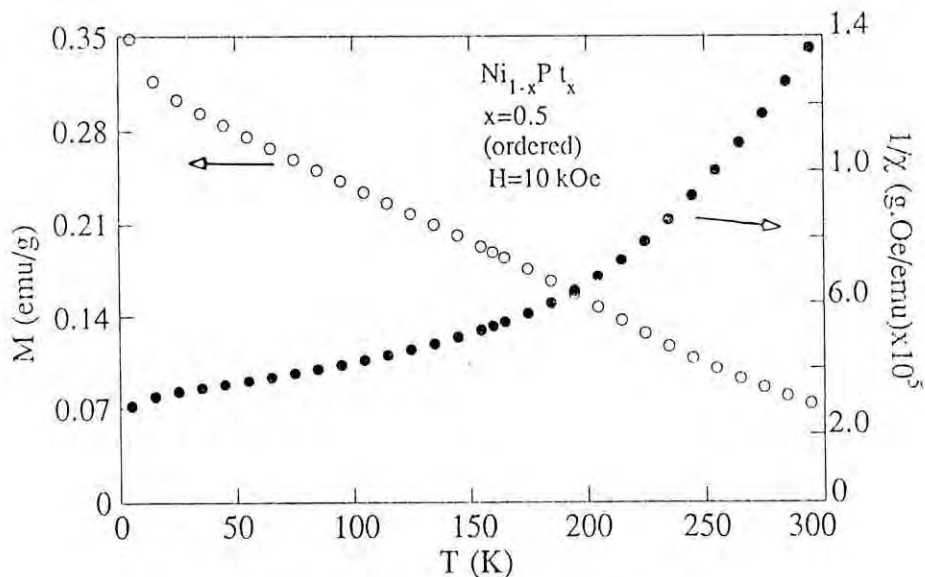


Fig. 5.16. Temperature dependence of the magnetization and the reciprocal susceptibility of the ordered $\text{Ni}_{1-x}\text{Pt}_x$ with $x=0.50$ at 10 kOe.

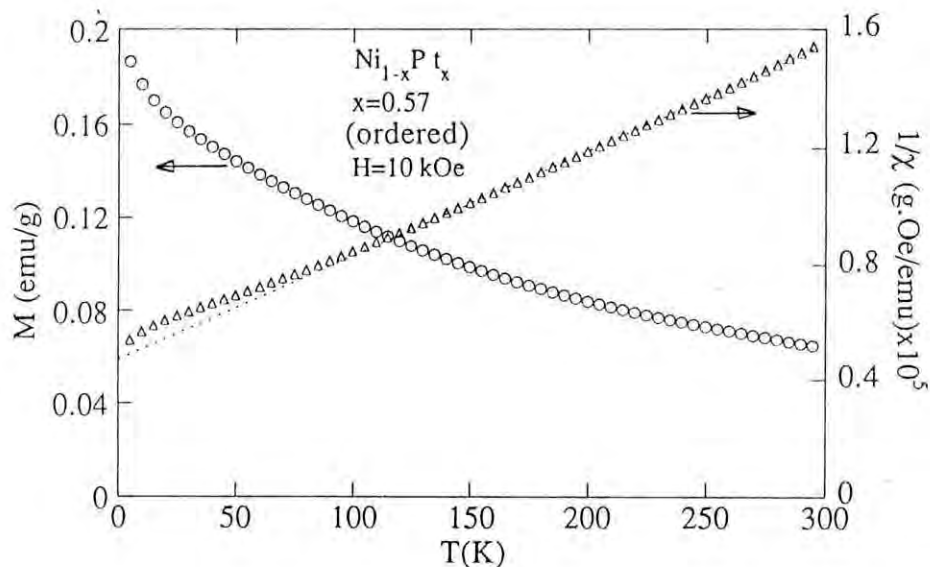


Fig.5.17. Temperature dependence of the magnetization and the reciprocal susceptibility of the ordered $Ni_{1-x}Pt_x$ with $x=0.57$ at 10 kOe.

possible interpretation of such peculiar magnetic behaviour might be related to the distortion of the crystal lattice $[Al(fcc) \rightarrow L1_0(fct)]$ which is obvious from present X-ray measurements. This lattice distortion is likely to change the exchange integral by its dependence on the interatomic distances of magnetic atoms. Our experimental data show that in the disordered fcc Ni-50at% Pt alloy has lattice parameter $a=3.751 \text{ \AA}$, while ordered fct state has $a=3.819 \text{ \AA}$ and $c=3.604 \text{ \AA}$. Ni atoms have a nearest neighbour distance of $a/\sqrt{2}$ in both the ordered and disordered states. It is rather difficult to explain that the increase of only 0.048 \AA in the nearest neighbour distance of a Ni atom in ordered state than from a disordered one is sufficient to decrease the exchange integral to such an extent that it results in paramagnetism. The most

likely interpretation of the observed magnetic properties could be given through local environment effects. The magnetic state of a transition metal atom is very sensitive to its local environment [43-45]. This has been shown by a large number of experimental data on dilute alloys, intermetallic compounds near stoichiometry, concentrated alloys near the composition at which the alloy becomes ferromagnetic, ferromagnetic alloys for different states of order. The moment on the Ni atom is dependent on the number of Ni nearest neighbours. In the ordered Ni-50%at Pt each Ni atom has four nearest neighbours, whereas in the disordered state it may have up to twelve but on average six. The average number of Ni nearest neighbours at the critical concentration ($x=0.57$) is approximately five in the disordered state. So the reason for the absence of ferromagnetism in the atomically ordered Ni-50%at Pt alloy with a Ni atom having four Ni nearest neighbours is clearly understood, i.e. a nearest neighbour number greater than four is necessary for the Ni-Pt alloys to be ferromagnetic at absolute zero. Again for the disordered fcc Ni-24%at Pt alloy, a Ni atom may have on average nine Ni nearest neighbours and in the ordered $L1_2$ cubic structure Ni has eight nearest neighbours. It is clear that in both the cases the number of Ni nearest neighbours in the atomically ordered alloy is less than in the disordered alloy. Therefore if it is assumed that nearest-neighbour Ni-Ni interactions are dominant then a reduced value of the molecular field coefficient is expected on ordering with a consequent reduction in T_c .

Table 5.2 Magnetic properties of ordered $\text{Ni}_{1-x}\text{Pt}_x$

Platinum content x	0.24	0.30	0.44	0.50	0.57
$M_0(H=0), T=4.2\text{K}$ (emu/g)	24.6	19.4			
4.2K M_S (emu/g)	24.80	19.63	3.72 ^a	0.95 ^a	0.78 ^a
293K M_S (emu/g)	17.17	1.96 ^b			
μ ($\mu\text{B}/\text{f.u.}$)	0.40	0.35			
T_C (K)	357	278			

^a Value corresponding to $H=50$ kOe

^b Value corresponding to $H=5$ kOe

Reference

1. Gauthier, Y, Y, Joly, R. Baudoing and J. Rundgren, 1985, Phys. Rev. B, 31, 6216
2. Baudoing, R, Y, Gauthier, M, Lundberg and J. Rundgren, 1986, J. Phys. C: Solid State Phys. 19, 2825
3. Massalski, T. B., H. Okamoto, and P. K. Subramanian, Binary Alloy Phase Diagram (ASM Int. Materials Park, 1990), vol. 2, page 1744
4. Dahmani, C. E., M. C. Cadeville, J. M. Sanchez and J. L. Moran-Lopez, Phys. Rev. Letters, (1985), 55, 1208
5. Hansen, M., Constitution of Binary alloys. McGraw Hill, NY, 2nd edition, 1958.
6. Cadeville, M. C., C. E. Dahmani and F. Kern. J. Mag. Mag. Mat., 1986, 54-57, 1055
7. Treglia, G. and F. Ducastelle, J. Phys. F. Met. Phys., 1987, 17, 1935
8. Dahmani, C. E., M. C. Cadeville and V. Pierron-Bohnes, Acta Metallurgica (1985). Vol. 33, P. 369-377
9. Beille, J., D. Bloch, and M. Besnus J. Phys. F: Metal Phys., 1974, 4, 1275
10. Alberts, H. L., J. Beille and D. Bloch, Phys. Rev., 1974, B9, 2233
11. Besnus, M. J. and A. Herr Phys. Lett., 1972, 39A, 83
12. Fischer, G. and M. J. Besnus, Solid State Comm., 1969, 7, 1527
13. Marian, V., Ann. Phys., 1937, 7, 459
14. Beille, J., D. Bloch and E. P. Wohlfarth, Phys. Lett., 1973, 43A, 207
15. Edwards, D. M. and E. P. Wohlfarth Proc. Roy. Soc., 1968, A303, 127.
16. Mathon, J., Proc. Roy. Soc., 1968, A306, 355.
17. Ododo, J. C. and W. Howarth, Solid State Comm. 1978, 26, 39
18. Ododo, J. C., Solid State Comm. 1978, 25, 25
19. Ododo, J. C. and B. R. Coles, J. Phys. F: Metal Phys., 1977, 7, 2393
20. Hicks, T. J., B. Rainford, J. S. Kouvel, and G. G. Low, Phys. Rev. Lett. 1969, 22, 531,
21. Medina, R. A. and J. W. Cable, Phys. Rev., 1977, B15, 1539.
22. Muellner, W. C. and J. S. Kouvel, Phys. Rev. 1975, B11, 4552.
23. Acker, F. and R. Huguenin, J. Mag. Mag. Mat., 1979, 12, 58.
24. Para, R. E., and J. W. Cable, Phys. Rev. B, 1980, 21, 5494.
25. Pataud, P., Ph.D Thesis (1976), University of Grenoble, France.
26. Gillespie, D. J., C. A. Macliet and A. I. Schindler, Amorphous Magnetism, 1973, Plenum Press, New York, P. 343
27. Bolling, G. F., Phys. Cond. Mater., 1968, 7, 162 Bolling, G. F., A. Arrott and R. H. Richman, 1968, Phys. Stat. Solid, 26, 743

28. Kortekaas, T.F.M. and J.J.M.Franse, *J.Phys.*, 1976, F6, 1161
29. Kortekaas, T.F.M., J.J.M.Franse and H.Holscher, *Phys.Lett.*, 1974, A50, 153
30. Gillespie, D.J and A.I.Schindler, *AIP Conf.Proc.* 1972, 5, 461
31. Neel, L, *Ann. Phys.(Paris)*, 1932, 18, 1
32. Wojtowicz, P.J. and M.Rayl, *Phys.Rev.Lett.*, 1968, 20, 1491, from which paper the current use of the term "kink point" method arises.
33. Fisher, G., A.Herr and A.J.P.Meyer, *J.Appl.Phys.*, 1968, 39, 545
34. Burger, J.P., *Ann. Phys.*, 1964, 9, 945,
35. Takahashi, T. and Shimizu, M., *J.Phys. Soc. Jpn.*, 1965, 20, 26
36. Ododo, J.C. *J. Phys. F: Metal Phys.* 1980, 10, 2515
37. Shimizu, M. and Katzuki, A. *J.Phys. Soc. Jpn.*, 1964, 19, 1135
38. Shimizu, M., Takahashi, T. and Katzuki, A. *J.Phys. Soc. Jpn.*, 1963, 18, 260
39. Beille, J., D. Bloch and R. Kuentzler, *Solid State Comm.* 1974, 14, 963
40. Moorish, A.H., *The Physical Principles of Magnetism* 1965 (Wiley & sons, New York)
41. Praddaude, H.C. and S.Foner, *Solid State Comm.*, 1976, 20, 1117
42. Nordblad, P., *Ph.D. Thesis*, 1980, Uppsala University
43. F. Brouers, F. Gautier and J. Van der Rest: *J. Phys. F; Metal Phys* 1975 Vol. 5. P 975-93
44. J. Van der Rest, F. Gautier and F. Brouers: *J. Phys. F; Metal Phys.* 1975 Vol.5. P995-1013
45. J. Van der Rest: *J.Phys. F; Metal Phys.* Vol. 7 No. 6, 1977, P 1051-68.

CHAPTER 6

Measurements on $\text{Ni}_{1-x}\text{Fe}_x\text{Pt}$ alloys

6.1 Introduction

The equiatomic binary alloy of nickel-platinum exhibits interesting magnetic properties. Atomic ordering in NiPt alloy destroys magnetic ordering i.e. the disordered alloy is ferromagnetic and the ordered one is paramagnetic. This suggests that the magnetic state of the equiatomic NiPt alloy depends sensitively on its local environment. The disordered ferromagnetic alloy has a Curie temperature of 79 ± 2 K and magnetic moment of $0.176 \mu_B/\text{f.u.}$ The susceptibility is greatly reduced on ordering from 15×10^{-5} emu/g Oe in the disordered state to 1.9×10^{-5} emu/g Oe in the ordered state.

Platinum is an exchange enhanced paramagnet and the enhancement factor for Pt ≈ 3 while that for Pd ≈ 10 [1]. This means that the platinum host will produce the giant moment polarization. Similarly Parra and Medina [2] determined the magnetic enhancement factor for pure platinum from neutron scattering data obtained with Ni-Pt alloys and found that Pt is a highly polarizable metal. This polarizability is responsible for the onset of giant moments by the presence of a ferromagnetic impurity such as iron. Dilute PtFe alloys have been considered as typical examples of giant moment ferromagnets and have been confirmed by magnetization and unpolarized neutron scattering measurements [3-5]. From magnetization measurement Crangle and Scott [3] calculated giant moments of $4.9-6.2 \mu_B$ per iron atom in PtFe alloys with Fe concentration 1-6 at.% indicating that each Fe atom significantly polarizes the surrounding Pt matrix. In order to see the effect of Fe in equiatomic NiPt alloy a range of pseudobinary $\text{Ni}_{1-x}\text{Fe}_x\text{Pt}$ ($0.02 \leq x \leq 0.2$) alloys have been chosen in which platinum is kept at 50at.% throughout and Ni is replaced by increasing amount of iron. The magnetic and crystallographic properties of pseudobinary $\text{Ni}_{1-x}\text{Fe}_x\text{Pt}$ ($0.2 \leq x \leq 1$) alloys have been studied only at room temperature [6] in the ordered and disordered states. An

increase of Curie temperature and magnetization with increasing amount of Fe is found and that these values are higher in the disordered phases than in the ordered ones. The disordered alloys show coercivity increasing with Fe content reaching a maximum value of 1.5 kOe at $x=1$ i.e. in FePt. Kawamiya et al [7] observed substantial increase of Curie temperatures with the addition of small amount of Fe.

The aim of this work is to study in detail the effect of atomic order-disorder on the crystallography, magnetization and magnetic phase transition of $\text{Ni}_{1-x}\text{Fe}_x\text{Pt}$ alloys. The role of an Fe atom in the inducement of giant moments is pursued in the ordered and disordered phases. Particular attention has been given to understand the mechanism of magnetization process by measuring the zero field cooled (ZFC) and field cooled (FC) magnetization. Field and temperature dependence of hysteresis loop measurements in the zero field cooled state are performed to fully understand the coercivity mechanism.

6.2 Experimental

The $\text{Ni}_{1-x}\text{Fe}_x\text{Pt}$ polycrystalline samples with $x=0.02, 0.05, 0.1$ and 0.2 have been prepared in an arc furnace under inert gas atmosphere. Ordered and disordered phases have been obtained by suitable heat treatment described in chapter 3.

X-ray diffraction studies reveal that disordered samples are single phase with fcc structures and ordered ones are fct structure with a small amount of second phase (composition unidentified) together with traces of disordered phases. Scanning electron microscopy in the back scattered electron mode has been utilized to detect surface defects of the sample with $x = 0.05$ in both the ordered and disordered phases. This study revealed some precipitated phases in the ordered alloy. A full account of X-ray investigation is given in chapter 3.

Magnetization measurements on $\text{Ni}_{1-x}\text{Fe}_x\text{Pt}$ alloys in the ordered and disordered states have been performed with a VSM in the temperature range 4.2-300 K and magnetic fields up to 5 kOe. Some measurements up to magnetic fields of 50 kOe have been performed at 4.2 K with a VSM in conjunction with a superconducting magnet. A SQUID magnetometer has extensively been used to measure field and temperature dependence of magnetization from 5-300 K and magnetic field 0-50 kOe. Magnetization measurements are carried out under zero field cooled (ZFC) and field cooled (FC) condition. Hysteresis loops have been measured at different temperatures for the ordered samples including the initial magnetization curves under zero field cooled condition from which temperature dependence of coercivity, $H_c(T)$, and critical field, $H_p(T)$, and remanence, $M_r(T)$ are estimated.

The magnetization versus temperature measurements of the samples have been done under the following conditions:

- a) The zero field cooled magnetization (ZFC) curves are obtained by cooling the samples from above the Curie temperature (T_c) in zero applied field down to 5 K. Then the magnetic field is applied and the measurements are recorded as the temperature is raised up to above T_c with the constant applied field. When zero field cooled magnetization curves for different applied magnetic fields are important, then each time the samples have to be thermally demagnetized by warming it up above T_c and then cooled down to cryogenic temperature without field and repeat the measurements with necessary applied magnetic field.
- b) In the following, the temperature is decreased to 5 K without changing the magnetic field and measurements are recorded. This gives the so called field cooled (FC) magnetization curves. Both ZFC and FC measurements are realized at the same rate.
- c) Thermoremanent magnetization (TRM) is obtained by cooling the sample in the constant chosen field to 5 K, switching off the field and taking the measurements with increasing temperature up to above T_c .
- d) Initial magnetization curves are obtained by cooling the sample in zero magnetic field from above T_c to the chosen cryogenic temperature and at this constant temperature magnetization

is measured as a function of magnetic field.

6.3. Results and discussion

6.3.1 Disordered alloys

Magnetization as a function of internal magnetic field measured with a VSM at 4.2 K for $\text{Ni}_{1-x}\text{Fe}_x\text{Pt}$ alloys are shown in Fig.6.1. Measurements have been taken as the field is slowly swept automatically from zero to 5 kOe and back to zero again with the same sweep rate in order to see any hysteresis effects. No noticeable hysteresis has been observed. Magnetization seems to be saturated with an internal magnetic field of 3 kOe. From these measurements magnetic moments μ in Bohr magneton have been calculated and are listed in Table 6.1 together with magnetization per gram at 4.2 K and other magnetic parameters.

Temperature dependence of magnetization and inverse susceptibility of the disordered $\text{Ni}_{1-x}\text{Fe}_x\text{Pt}$ with $x=0.05$ in the temperature range 5-300 K and in an applied magnetic field of 5 kOe is shown in Fig.6.2. In set of the figure shows the low field DC magnetization measured with a field of 20 Oe. From these measurements magnetization of 15 emu/g at 5 K or $0.341 \mu_B/\text{f.u.}$ and $T_C=189$ K from the kink of DC magnetization are obtained. A non-linear least-squares fitting shows that magnetizations has a T^2 dependence at least up to $0.75 T_C$. The inverse susceptibility is well described by Curie-Weiss law above 240K with a paramagnetic Curie temperature $\theta = 205$ K. The Curie constant is 0.43 emu K/mole which is compatible with a paramagnetic effective moment (P_{eff}) of $1.87 \mu_B/\text{f.u.}$

The Curie temperatures (T_C) of all the disordered samples have been determined by different methods and they are found to be in good agreement. Fig 6.3a and 6.3b demonstrate the low field(10^{-3} Oe), low frequency (37 Hz) AC susceptibility and low field (58 Oe) DC magnetization measurements of disordered $\text{Ni}_{1-x}\text{Fe}_x\text{Pt}$ alloys with different concentrations. Both the methods of measurements indicate well defined transition from

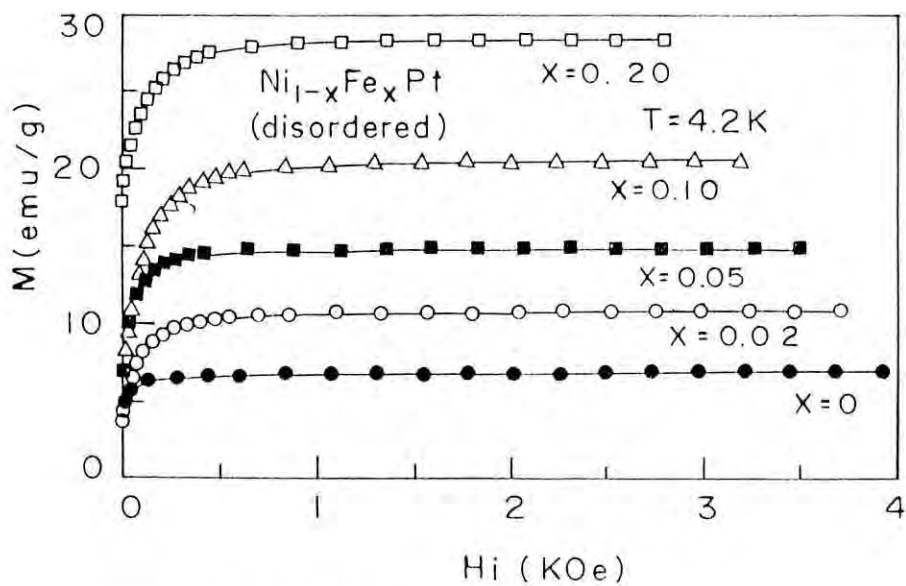


Fig.6.1. Magnetization versus internal magnetic field of the disordered $Ni_{1-x}Fe_xPt$ alloys at 4.2 K.

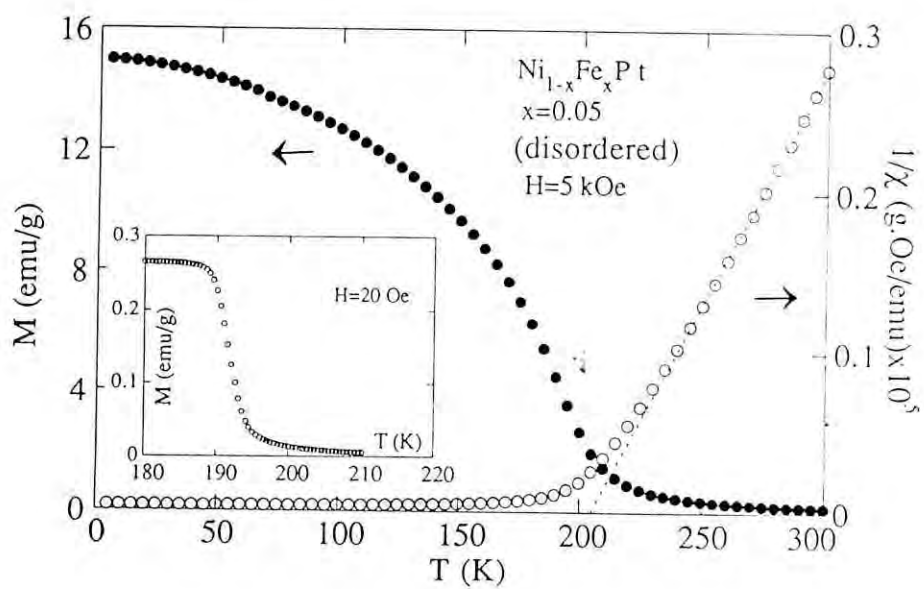


Fig.6.2. Temperature dependence of the magnetization and the reciprocal susceptibility of the disordered $Ni_{1-x}Fe_xPt$ at magnetic field of 5 kOe; inset: M vs T curve at $H = 20$ Oe.

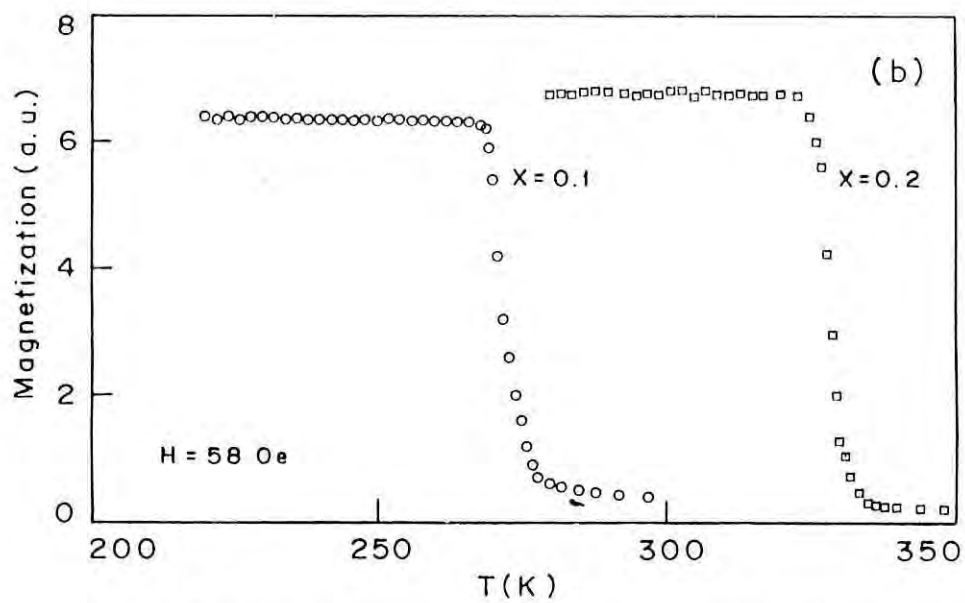
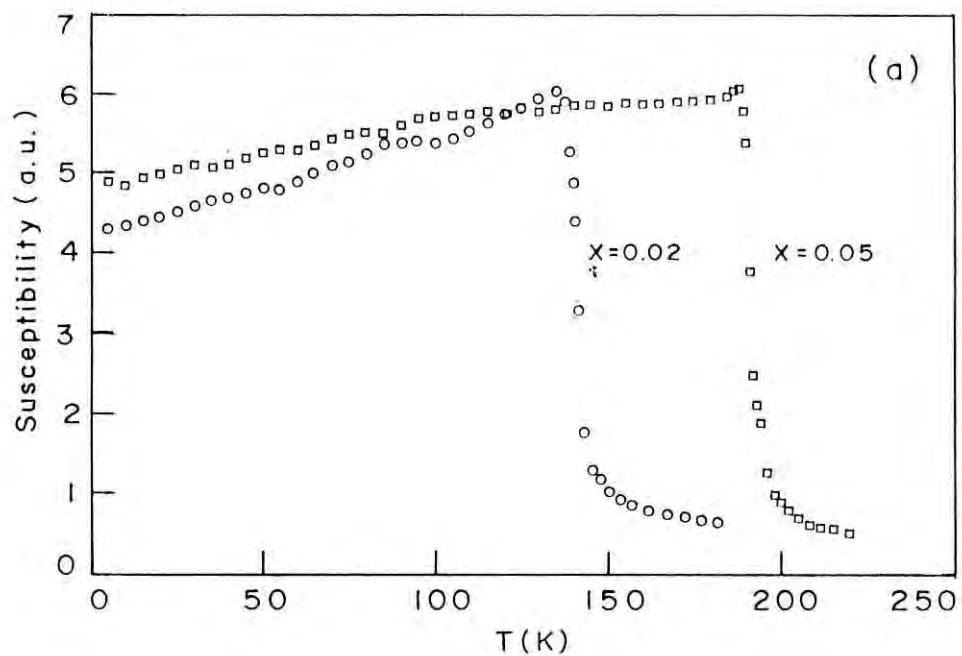


Fig.6.3. Temperature dependence of (a) AC susceptibility with $x=0.02$ and 0.05 and (b) DC magnetization with $x=0.1$ and 0.2 at magnetic field of 58 Oe of the disordered $\text{Ni}_{1-x}\text{Fe}_x\text{Pt}$ alloys.

ferromagnetic to paramagnetic state and the sharpness of the transitions confirms the metallurgical homogeneity of the alloys. Low field DC magnetization (Fig.6.3b) tends to the limiting value of H_a/D , where D is the shape-dependent demagnetizing factor of the specimen, just below the ferromagnetic Curie point. Whose magnitude is determined solely by the shape of the specimen. Accordingly the susceptibility shown in Fig.6.3b should diverge just below the T_c so that it is limited by $1/D$ to the lowest temperature. A gradual decrease in the AC susceptibility at temperatures below the ferromagnetic Curie point is perhaps not peculiar to $Ni_{1-x}Fe_xPt$ alloys. Similar observations have already been reported in the present work for Ni-Pt system and others for the PtCo [8] and PtFe [9] system. It is likely that the gradual decrease of AC susceptibility below T_c is a manifestation of the Hopkinson effect, according to which the initial susceptibility increases to a sharp maximum just below the T_c and then drops off to a small value [10] which is due to intrinsic magnetic anisotropy and domain wall mobility. AC measurements indicate a Curie temperature of 190 K for $x=0.05$ sample and compares well with 189 K and 188.5 K determined by kink point method and Arrott plots respectively. All the determined T_c values of $Ni_{1-x}Fe_xPt$ alloys are collected in Table 6.1.

Fig.6.4 shows the Arrott plots of the disordered sample with $x=0.05$ for the temperatures below and above T_c which have been constructed from a series of magnetic isotherms. Only some of the curves extracted from the magnetic isotherms are presented for the sake of clarity. The Arrott plots indicate a gradual transition between ferromagnetism and paramagnetism and it is observed that the transition temperature is between 188 and 189 K. It is noticed that the Arrott plots are non-linear at least up to little above T_c . Therefore parabolic extrapolation is employed instead of linear extrapolation from high field linear portion to the ordinate and the abscissa to obtain the values of M_0^2 and χ_0^{-1} . Even for the crystalline Fe, Co and Ni Arrott plots are non-linear at low fields [11-14]. When the Arrott plots are non-linear extrapolation overestimates the true value of T_c [11,12]. By contrast a parabolic extrapolation yields a T_c value that agrees remarkably well [12] with the values determined by other methods. Kaul [15] has given a theoretical justification for the parabolic extrapolation of the

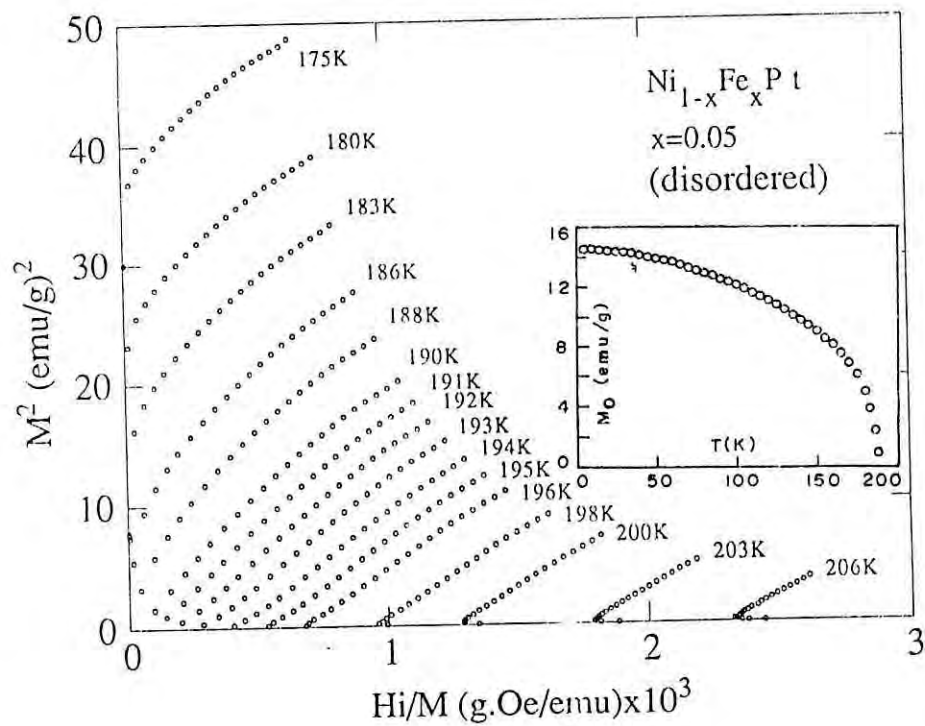


Fig.6.4. Arrott plots of the disordered $\text{Ni}_{1-x}\text{Fe}_x\text{Pt}$ alloys with $x=0.05$ near the Curie temperature; inset: variation of the spontaneous magnetization with temperature determined from the Arrott plots.

Arrott plots on the basis of molecular field theory. In set of Fig.6.4 shows the temperature dependence of the spontaneous magnetization, M_0 , which is determined by the parabolic extrapolation of Arrott plots of Fig.6.4. and the extrapolation of $M_0 = 0$ gives a $T_c = 188.5$ K. It has been mentioned before that this value of T_c is in excellent agreement with those determined from low field DC and AC measurements. The critical isotherms have been analyzed following the relation $M \propto H^{\frac{1}{\delta}}$ where $\delta = 3$ in the molecular field approximation and $\delta = 5$ in the Heisenberg model [15]. The isotherms at $T = 188$ and 189 K suggest a value of $\delta \approx 4.20$ from log-log plots of magnetization and field. This value is consistent with the value of 4.20 obtained for pure Ni [11].

It is observed that the magnetic moment and the Curie temperature both increase as Fe concentration increases (see fig. 6.27 & 6.28) and that the increase of both the parameters are larger with smaller concentration of Fe and gradually reduces i.e. the curves bend slowly downward. Enhancement of Curie temperature with the replacement of Ni with Fe is due to the increase of the average exchange interaction among the magnetic moments and this increases as Fe concentration increase. Substitution of Fe for Ni in ferromagnetic NiPt alloy produces a giant enhancement of magnetic moment. Fig. 6.29 shows that the moments per Fe atom are very large and their concentration dependence is significant. For example when $x = 0.02$ which is equivalent to 1 at.% Fe enhances magnetic moment from $0.176 \mu_B$ to $0.247 \mu_B$ per formula unit resulting a moment of $7.4 \mu_B$ per Fe atom. This large moment can not be due to Fe atom only. The large moments observed in these alloys are a consequence of the polarizability of the NiPt matrix. Further discussion on this will continue at the end of this chapter.

Table 6.1 Magnetic properties of disordered Ni_{1-x}Fe_xPt alloys

Iron Content x	x=0	x=0.02	x=0.05	x=0.1	x=0.2
M _S (emu/g)T=4.2K	7.72 ^a	10.89	15.00	20.75	28.40
μ(μ _B /f.u.)	0.176	0.247	0.341	0.47	0.643
T _c (K)	79	138	189	269	326
θ(K)	139		205		
C (emu/mole)	0.25		0.43		
P _{eff} (μ _B /f.u.)	1.42		1.87		
μ(μ _B /Fe)		7.4	6.9	6.16	4.95

^a value corresponding to 50 kOe magnetic field

6.3.2 Ordered alloys

Magnetization versus field curves for all the ordered

$\text{Ni}_{1-x}\text{Fe}_x\text{Pt}$ alloys at 4.2 K measured with a VSM under zero field cooled condition are demonstrated in Fig.6.5. A complex initial magnetization process is noticed. A relatively insignificant increase of magnetization occurs up to a certain critical field, (4 kOe for $x=0.02$ and 6 kOe for $x=0.05$ samples respectively) a rapid increase thereafter and approaches slowly to saturation in higher fields but even at field as high as 50 kOe the magnetization is not saturated. A strong hysteresis effect is observed with $M_r/M_s \approx 0.5$. This behaviour is in contrast with the disordered samples which are saturated only under an internal magnetic field of 3 kOe with no hysteresis. This slow approach to saturation up to the magnetic field of 50 kOe for the ordered samples is assumed to be associated with very high magnetic anisotropy of the samples and consequently narrow domain walls since the domain wall width is given by $\delta \propto \left(\frac{A}{K}\right)^{\frac{1}{2}}$, where A and K are the exchange and anisotropy constant respectively.

This behaviour may either be the result of metamagnetism or due to magnetic hardness arising from domain wall pinning effects. The latter is more likely since all the alloys are ferromagnetic with large remanences. This type of critical field behaviour in magnetization versus field have been observed in systems like Dy_3Al_2 [16], $\text{Tb}_{0.27}\text{Dy}_{0.73}\text{Fe}_2$ [17],

$\text{R}(\text{Fe}_{1-x}\text{Al}_x)_2$, $\text{R}=\text{Dy, Er, Tb}$ [18-20], $\text{R}_2(\text{Fe}_{1-x}\text{Mn}_x)_{14}\text{B}$, $\text{R}=\text{Nd, Pr, Y}$ [21] and

$\text{Co}_{3.5}\text{Fe}_{0.5}\text{CuCe}_{1.09}$ [22] and have been explained as domain wall pinning effects.

The magnetization of all the ordered samples are not saturated. So an estimate of the saturation magnetization, M_s , has been made by plotting M vs $1/H$ and extrapolating the data to infinite field. M_s values obtained in this way show that only 80% of the saturation magnetization is achieved at fields as high as 50 kOe. Due to the large difference in extrapolated M_s value and magnetization value at 50 kOe and considering the uncertainty in the extrapolation procedure to infinite field, experimental values of magnetization at 50 kOe for all the samples have been used to calculate the magnetic moments μ in Bohr magneton of the samples. Initial susceptibility has been calculated from the linear part of the initial

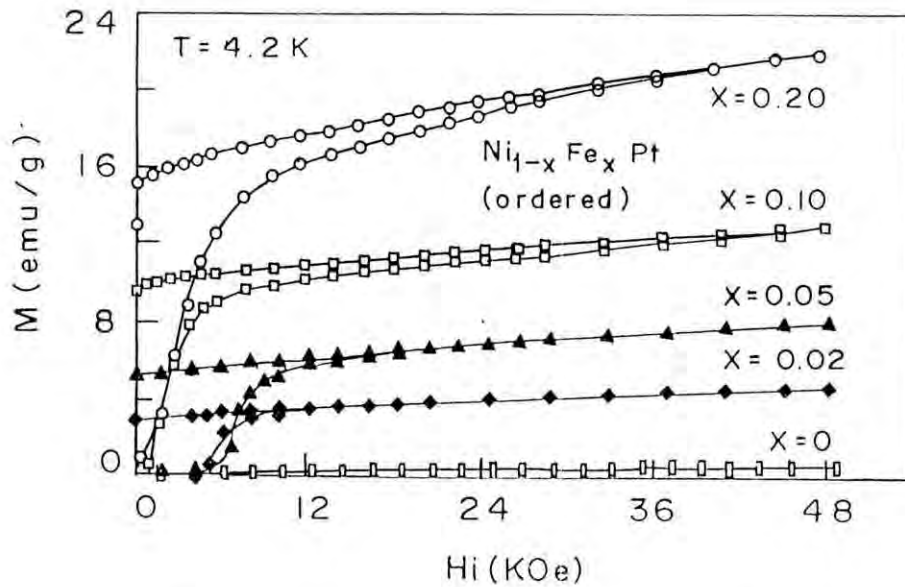


Fig.6.5. Magnetization versus internal magnetic field of the ordered $Ni_{1-x}Fe_xPt$ alloys at 4.2 K.

magnetization curve for $H < 200$ Oe. Magnetic moment μ , saturation magnetization, M_s , magnetization at 50 kOe, remanence, and other relevant magnetic parameters are summarized in Table 6.2.

The complete hysteresis loops including the initial magnetization curves are measured for all the samples with a SQUID magnetometer at different temperatures. Two representative curves of the samples with $x=0.05$ and 0.2 measured at 5 K are depicted in Figs. 6.6 and 6.7. From the hysteresis loop coercivity (H_c) and the Critical field (H_p) have been estimated. Coercivity is defined as the field value corresponding to null magnetization ignoring the slight magnetic relaxation effect with time and to overcome this effect hysteresis mode (faster mode) has been used in the measurements with SQUID magnetometer. Critical field (H_p) has been taken to be the field at which the differential magnetic susceptibility dM/dH attains its maximum value since this appears to be more precisely measurable than the field at which

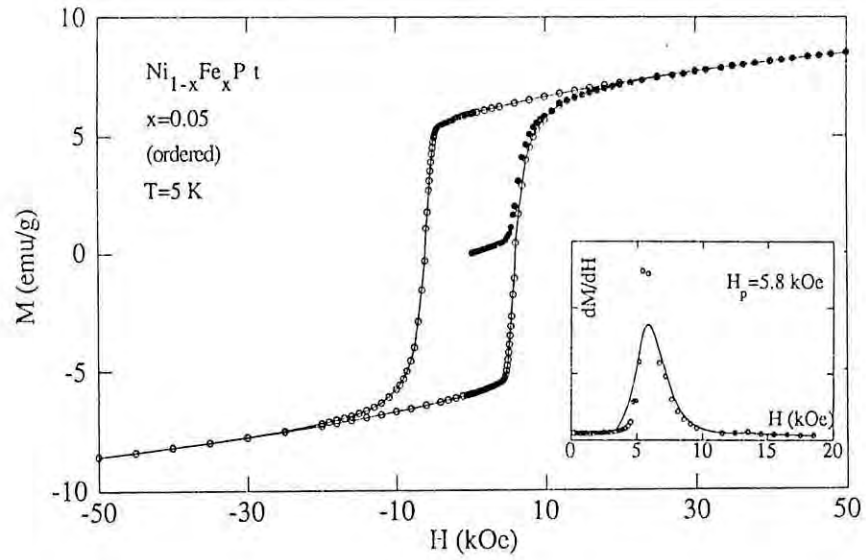


Fig.6.6. Zero field cooled hysteresis loop with initial magnetization curve of the ordered $\text{Ni}_{1-x}\text{Fe}_x\text{Pt}$ alloys with $x=0.05$ at 5 K; inset: the first derivative of the initial magnetization with respect to field.

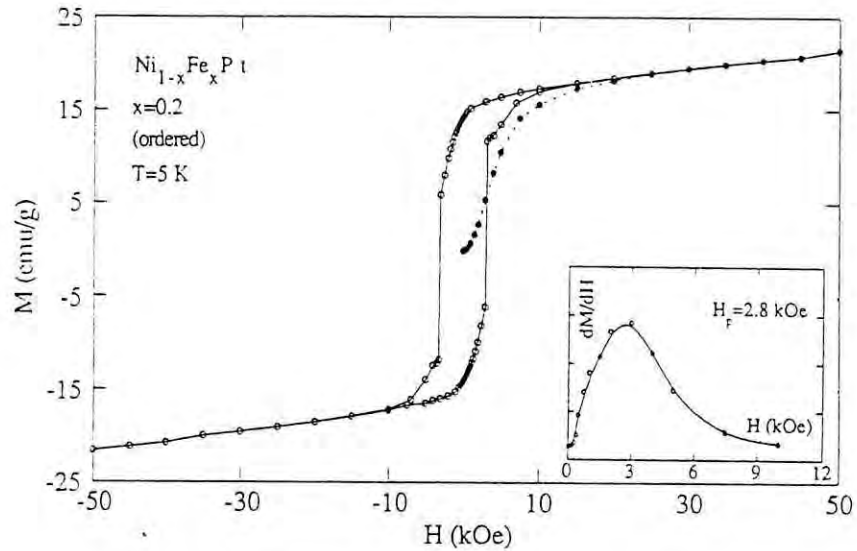


Fig.6.7. Zero field cooled hysteresis loop with initial magnetization curve of the ordered $\text{Ni}_{1-x}\text{Fe}_x\text{Pt}$ alloys with $x=0.2$ at 5 K; inset: dM/dH of the initial magnetization curve.

Table 6.2 Magnetic properties of ordered Ni_{1-x}Fe_xPt alloys

Iron Content x	0	0.02	0.05	0.1	0.2
M(emu/g) T=5 K H=50 kOe	0.95	4.53	8.60	13.56	21.53
M _S (emu/g) T=5 K		5.76	10.42	15.96	25.52
μ(μ _B /f.u.)		0.103	0.19	0.31	0.49
T _C (K)		38	100	179	261
θ(K)		37	105	218	343
C(emu/mole)		0.30	0.37	0.33	0.31
P _{eff} (μ _B /f.u.)		1.54	1.72	1.61	1.57
M _T (emu/g) T=5 K		2.59	5.97	9.64	14.24
H _C (kOe) T=5 K		4.238	6.050	2.218	3.165
H _p (kOe) T=5 K		4.000	5.800	2.000	2.800
χ ₀ (emu/gOe)X10 ⁻⁴		0.83	1.05	1.2	2.43
μ(μ _B /Fe)		10.3	7.6	6.2	4.9

departure from linear dependence is evident. In set of Figs. 6.6 and 6.7 display dM/dH curves for $x=0.05$ and 0.2 samples respectively. As can be seen from the Table 6.2 that H_p is nearly equal to H_c at 5 K for the samples studied.

It is evident that the hysteresis behaviour of the sample with $x=0.2$ differs from that of the sample with $x=0.05$. The initial magnetization curve rises slowly, crosses the cyclic loop at a field, $H=3.6$ kOe, slightly greater than H_c , extends outside and again coincides with the cyclic hysteresis loop at $H>20$ kOe. This behaviour persists for all hysteresis loops measured up to the temperature of $0.65 T_c$. As the temperature is raised the initial magnetization curve crosses and coincides the cyclic hysteresis loop at lower magnetic fields. A hysteresis loop including initial magnetization curve for $x=0.2$ measured at 170 K is shown in Fig. 6.8. Similar situation has been observed for the sample $x=0.1$. This type of behaviour have been found in re-entrant spin glass magnets [23-26]. But the initial magnetization curves for the samples $x=0.05$ (Fig.6.6) and 0.02 are situated well inside the hysteresis loop. The hysteresis loops at different temperatures for $x=0.05$ are shown in Fig.6.9. This means that there are two different mechanisms governing the initial magnetization processes of this system.

Initial magnetization curves as a function of magnetic field at different temperatures between 5 K and 101 K are presented in Fig. 6.10. All curves are not shown for clarity. These curves are part of complete hysteresis loops measured at different temperatures with magnetic field up to 50 kOe. At each temperature the sample is thermally demagnetized prior to the measurement by heating it above the Curie temperature (T_c) and cooled in zero field ($H=0$) to the measurement temperature and then hysteresis loop measurement performed. In this way the critical field (H_p) and the coercive field (H_c) are determined as a function of temperature. In the initial magnetization curves (particularly at low temperatures) magnetization remains close to zero until H reaches a limit H_p beyond which rapid increase in magnetization is observed. H_p and H_c increase with decreasing temperatures. At all temperatures it is necessary for the applied field to reach the value of the coercive force to change the magnetization substantially. As a result of these measurements it appears that the

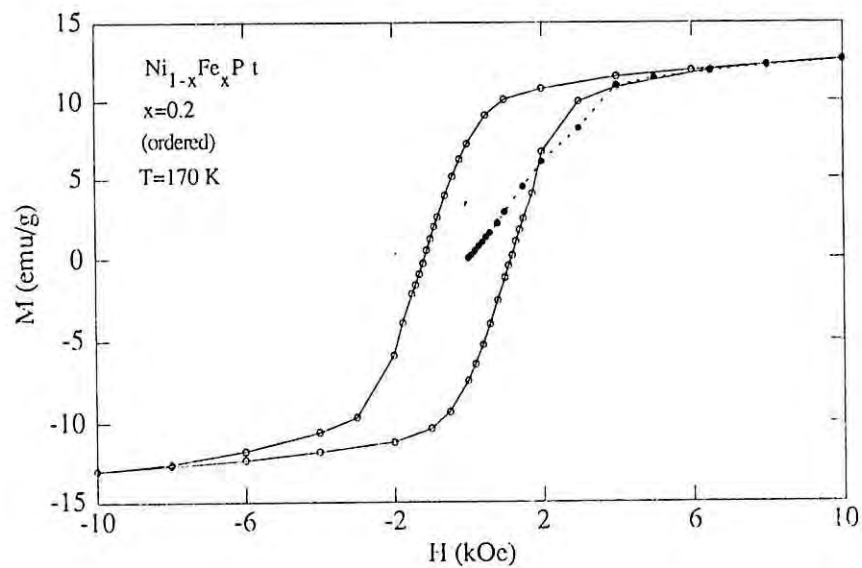


Fig.6.8. Hysteresis loop of the ordered $\text{Ni}_{1-x}\text{Fe}_x\text{Pt}$ with $x=0.2$ including initial magnetization curve at 170 K.

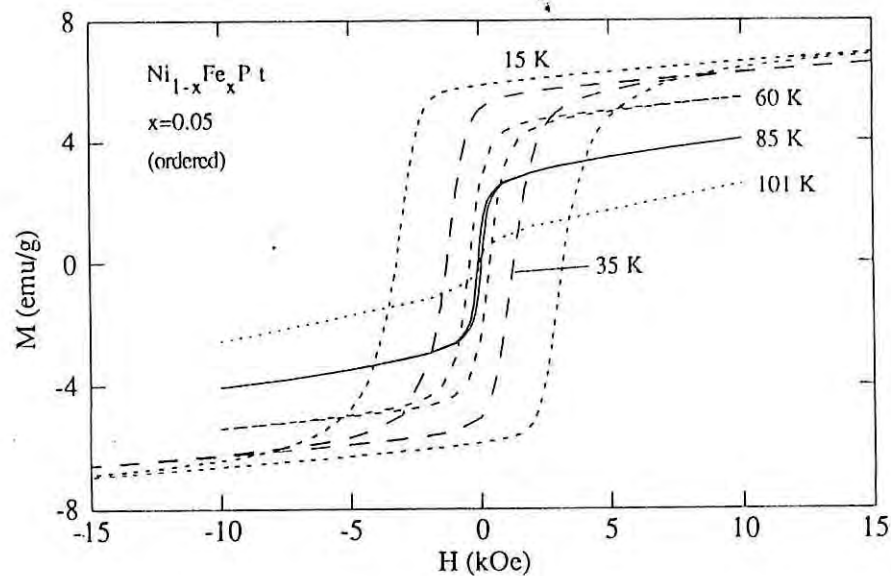


Fig.6.9. Hysteresis loop of the ordered $\text{Ni}_{1-x}\text{Fe}_x\text{Pt}$ with $x=0.05$ at different temperatures.

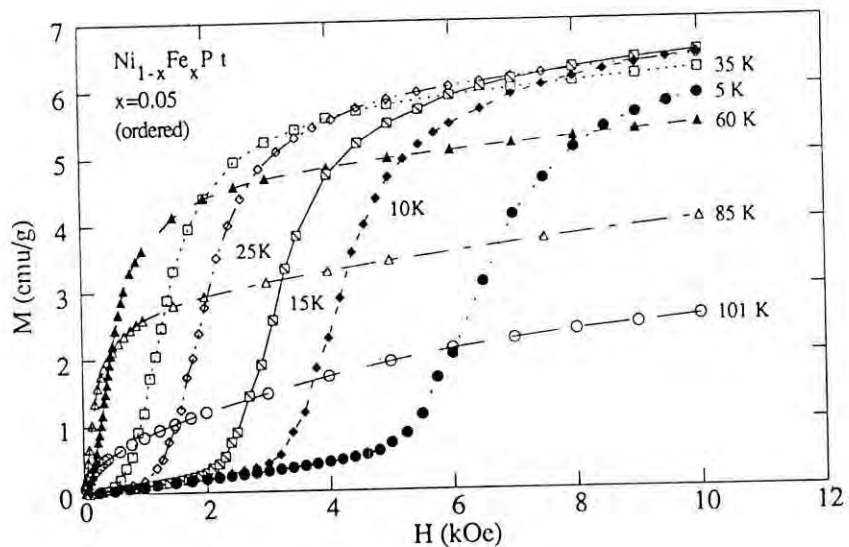


Fig.6.10. Initial magnetization curves in the zero field cooled condition of the ordered $\text{Ni}_{1-x}\text{Fe}_x\text{Pt}$ with $x=0.05$ at different temperatures.

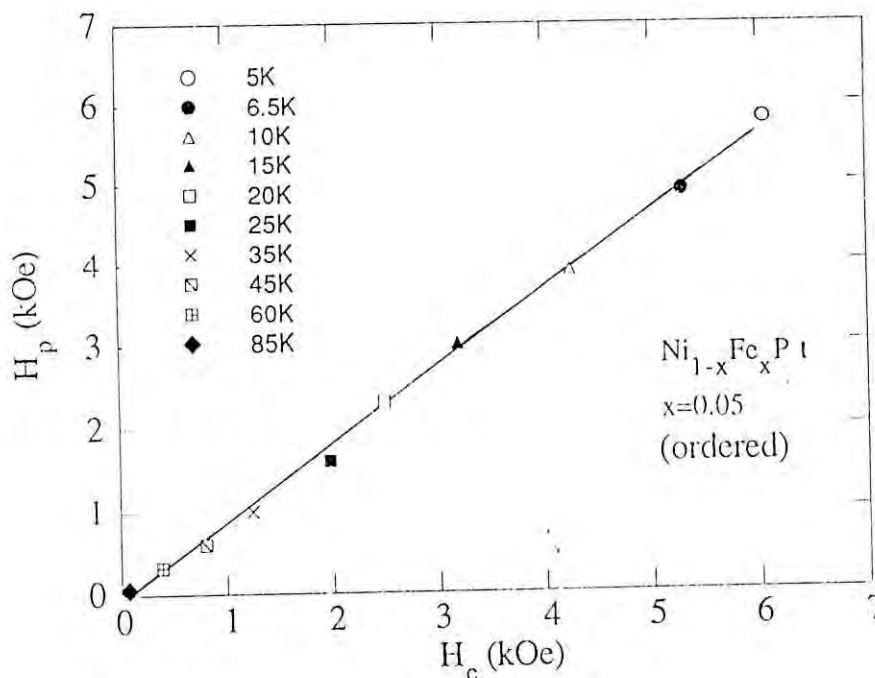


Fig.6.11. Variation of the critical field, H_p , with coercive field, H_c , of the ordered $\text{Ni}_{1-x}\text{Fe}_x\text{Pt}$ with $x=0.05$ at different temperatures.

magnetization process is governed by domain wall pinning. Domain wall motion is inhibited until the field reaches the critical field H_p , the field required to free (unpin) the domain wall from the pinning centres. Thus increase in H_c at low temperatures implies that the effectiveness of the pinning centres impeding the domain wall motion increases as the temperature decreases to 5 K. With this model it is predicted that $H_c \propto H_p$.

The values of H_p and H_c at different temperatures are collected in Fig. 6.11. A linear least squares fitting with the experimental data shows that $H_c = 1.05 H_p$. Folks et al [17] found the similar results from their analysis of the zero field cooled hysteresis loops for Terfenol-D at low temperatures. The magnetization process in this material appeared to be governed by domain wall pinning.

The domain wall pinning mechanism of magnetic hardening can be deduced from the morphology and /or the behaviour of initial magnetization curves and/or applied field dependence of coercivity [27,28]. A study of field dependence of coercivity (H_c) and remanence (M_r) measured at 5 K for all the ZFC ordered alloys of $Ni_{1-x}Fe_xPt$, obtained from a series of hysteresis loops by successively increasing applied field, are demonstrated in Figs.6.12 and 6.13. H_c and M_r remain very small below a certain critical field indicating that only reversible magnetization process occur in this field range. Beyond this field magnetization is irreversible where M_r and H_c rises sharply with magnetic field (H) and then levels off at a magnetic field slightly greater than H_c . The field at which dM_r/dH and dH_c/dH have maximum value appears to be almost equal to the critical field (H_p) of the initial magnetization curve at 5 K. There is no significant change in the value of H_c and M_r when magnetic field is increased up to 50 kOe i.e. H_c and M_r are saturated. This indicates that the domain nucleation is not the governing factor of the magnetization process in the ordered $Ni_{1-x}Fe_xPt$ system. From Fig. 6.12 it is seen that for the sample with $x=0.1$ and 0.2 , H_c increase beyond the value corresponding to maximum field (H_{max}) and then decrease and level off. This phenomena is understood from the fact that initial magnetization curve of the sample $x=0.2$ crosses the cyclic hysteresis loop at $H=3.6$ kOe and again merges at $H>20$ kOe (see Fig.6.7). Similar

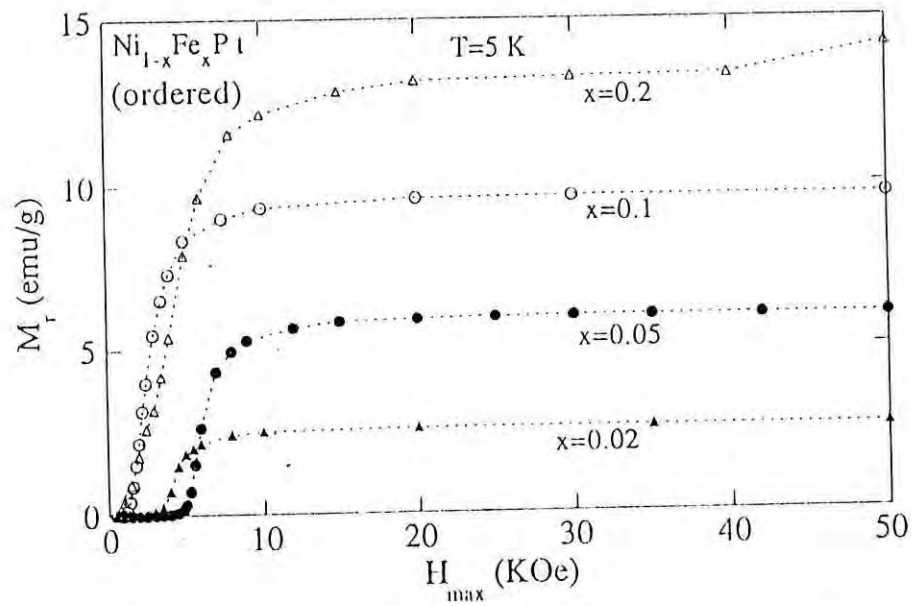


Fig.6.12. Remanent magnetization, M_r , as a function of the maximum magnetic field, H_{max} , at 5 K of the ordered $Ni_{1-x}Fe_xPt$ alloys.

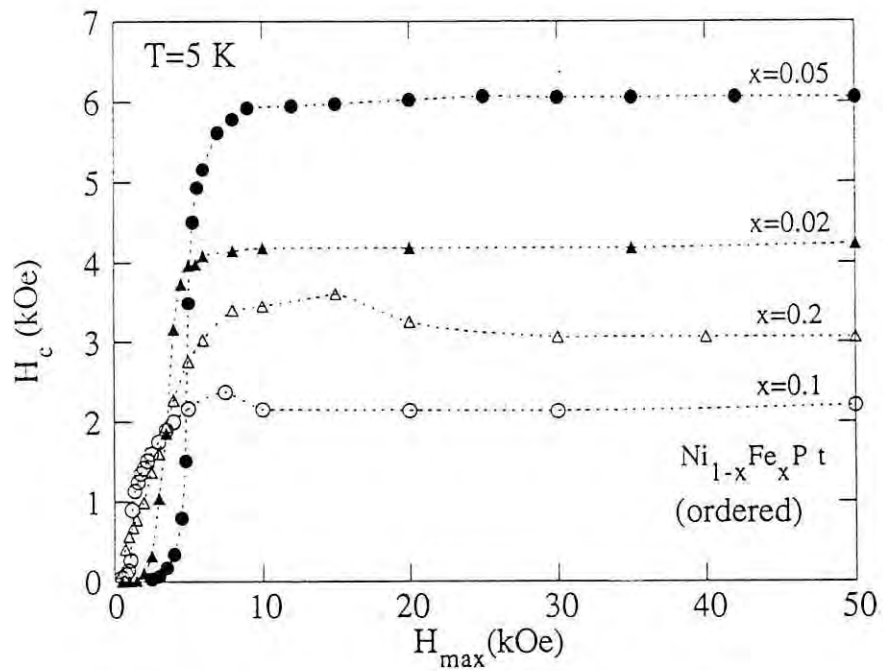


Fig.6.13. Coercive field, H_c , as a function of the maximum magnetic field, H_{max} , at 5 K of the ordered $Ni_{1-x}Fe_xPt$ alloys.

situation prevails for the sample $x=0.1$ where the initial magnetization curve intersects the cyclic hysteresis loop at $H=6$ kOe and again coincides at $H>10$ kOe. Such type of dependence of H_C and M_T on magnetic fields have been observed by Chin et al [28] and Ding et al [29] in hard magnetic materials where the coercivity is thought to be controlled by domain wall pinning.

From the study of initial magnetization processes and field dependence of M_T and H_C , it is understood that domain wall pinning type of magnetic hardening occurs in these alloys. Now let the phenomena observed in the present system be understood in terms of coercivity mechanism. In real crystals, the magnetization reversal takes place through nucleation of reverse domains, followed by displacement of domain walls. Therefore, one of the two mechanisms, either hard nucleation of reverse domains or pinning of domain walls, has to account for the coercivity. In the case of nucleation-controlled coercive force, initial magnetization increases steeply with magnetizing field, indicating the existence of easily movable domain walls. Coercive force is developed, depending on the maximum applied magnetizing field, showing that once reverse domains are eliminated in a grain, nucleation of reverse domains can not occur easily. In the case of a pinning-controlled coercive force, the magnetization remains nearly zero up to a value H_p , the pinning field, before increasing steeply to saturation. The coercive force is independent of the applied magnetizing field greater than critical field (H_p) [30].

To understand the magnetic behaviour of the ordered $Ni_{1-x}Fe_xPt$ system more closely temperature dependence of magnetization have been measured in detail. Fig.6.14 shows M vs T curves for the $Ni_{1-x}Fe_xPt$ alloys at constant applied magnetic field $H=500$ Oe in ZFC and FC condition. The behaviour of the M vs T curves for all the samples depends on whether a sample is cooled with or without an applied field. The ZFC curves are irreversible, in contrast with the FC curves which are reversible. A big thermal hysteresis is observed between FC and ZFC magnetization curves. For the zero field cooled samples magnetization increase with decreasing temperature and after passing through a broad maxima magnetization decrease

with decreasing temperature. For $x=0.02$ and 0.05 magnetization decrease very quickly and become almost zero at still lower temperature in contrast with $x=0.1$ and 0.2 samples in which magnetization decrease very slowly down to 5 K. From the curves in Fig. 6.14 it seems that the decrease in magnetization at higher temperatures after the maxima correspond to the ferromagnetic-paramagnetic transition temperatures because they are comparable with the values of the Curie temperatures determined by AC susceptibility measurement. The low temperature decrease of magnetization may be due to increasing magnetic hardness with decreasing temperature. To clarify this effect of decreasing magnetization at cryogenic temperature M vs T curves at different applied fields have been measured. Figs. 6.15 and 6.17 show the temperature dependence of magnetization at various applied fields in ZFC and FC condition for $x=0.02$ and 0.05 . The maxima in the ZFC curves depend strongly on the applied magnetic fields which become broader and shift to lower temperatures as the applied magnetic field increases and finally disappear in stronger magnetic fields when ZFC and FC magnetization are identical. Fig. 6.16 presents a ZFC magnetization curve with applied magnetic field of 50 kOe which does not show any maxima and identical with FC magnetization curve. But it should be noted that the field in which the maxima disappears is larger than the coercivity of the alloys investigated.

The ZFC magnetization versus temperature curves show that with small applied fields in the order of few oersted up to few hundred oersted magnetization below certain temperature down to 5 K is nearly zero and remains constant before rising quickly and passing through a maximum. The range of temperature in which magnetization is almost constant again decreases as the applied magnetic field increases. This is because the domain wall can not move with such small applied fields to give rise to magnetization due to wall pinning. The magnetization values increase only when the wall energy is high enough to detach the domain wall from pinning due to thermal energy. For the magnetization versus field curve a similar effect occurs, but in this case the energy is provided through the external magnetic field and moments interaction. It appears that the decrease in magnetization in ZFC condition at low

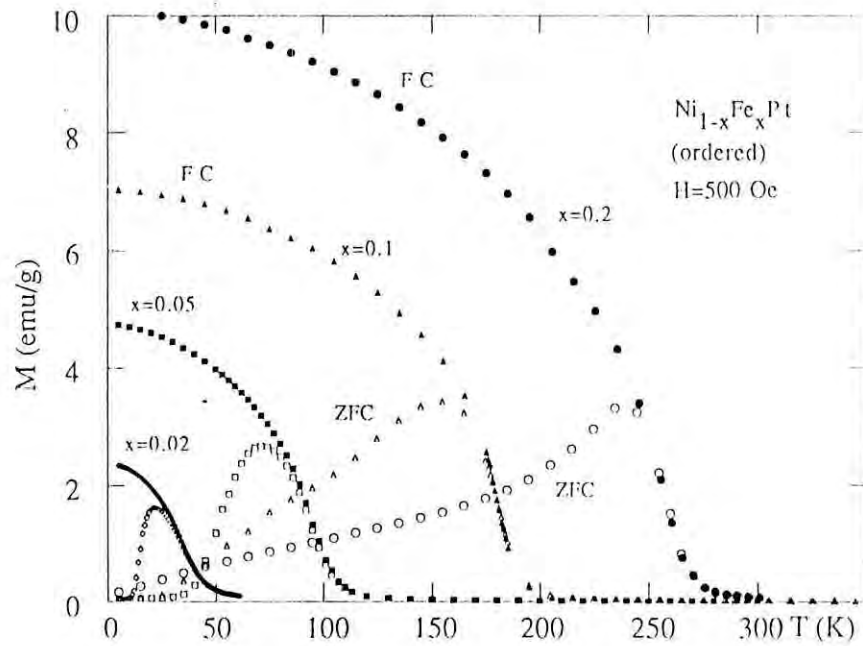


Fig.6.14. Zero field cooled and field cooled magnetization as a function of temperature of the ordered $\text{Ni}_{1-x}\text{Fe}_x\text{Pt}$ alloys at constant magnetic field $H=500$ Oe.

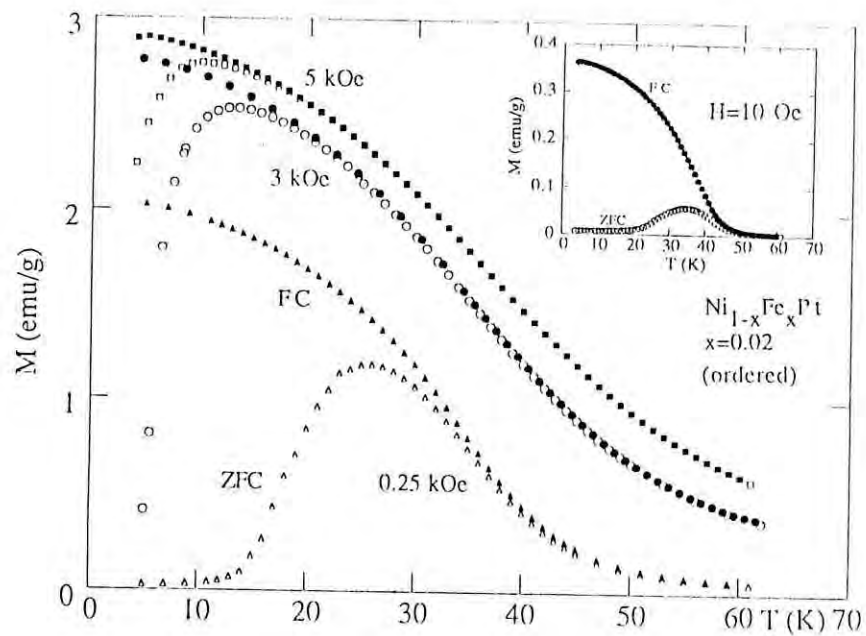


Fig.6.15. Temperature dependence of the ZFC and FC magnetization of the ordered $\text{Ni}_{1-x}\text{Fe}_x\text{Pt}$ with $x=0.02$ at different magnetic fields; inset: ZFC and FC magnetization of this alloy at $H=10$ Oe.

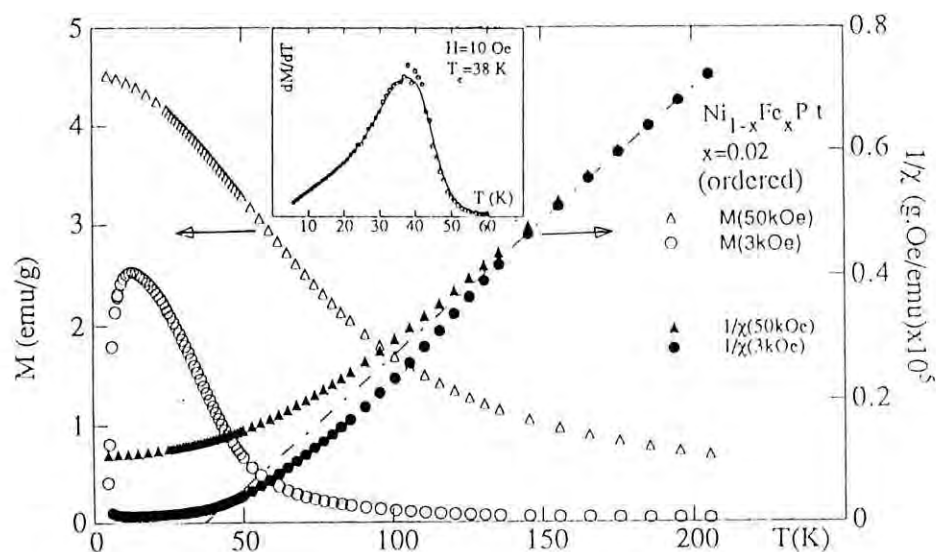


Fig.6.16. Temperature dependence of the ZFC magnetization and the reciprocal susceptibility of the ordered $\text{Ni}_{1-x}\text{Fe}_x\text{Pt}$ with $x=0.02$ at $H=3$ kOe and 50 kOe; inset: the first derivative of the magnetization with respect to temperature at $H=10$ Oe

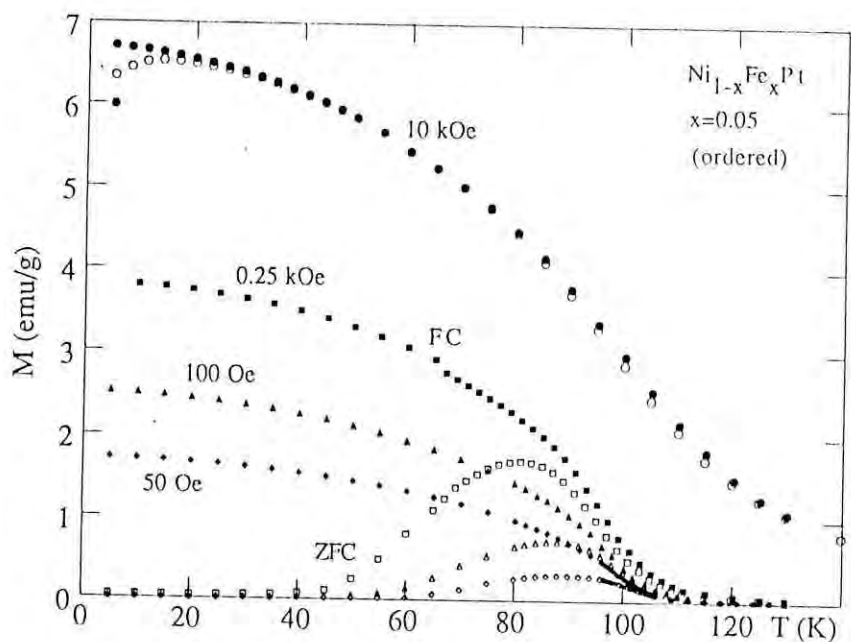


Fig.6.17. Zero field cooled and field cooled magnetization as a function of temperature of the ordered $\text{Ni}_{1-x}\text{Fe}_x\text{Pt}$ with $x=0.05$ at various applied magnetic fields.

temperature may well be a magnetic hardness effect suggesting an increase in coercive force at low temperature. The origin of the thermomagnetic history effects in the temperature dependence of the magnetization in the ordered samples is the thermally activated magnetization process which gives rise to a strong temperature dependence of the coercive force. The applied field corresponds to the coercive field at that temperature where dM/dT attains its maximum value in the low temperature side, i.e. below the maximum.

In the M vs T measurements, no correction has been made for demagnetizing effect. So writing

$$M = \chi(H_a - DM)$$

where M is the magnetization, H_a the applied field, χ the susceptibility and D is the demagnetizing factor, it can be written

$$M = \frac{\chi H_a}{(1 + \chi D)}$$

which for high permeability materials, tends to the value,

$$M_{max} = H_a/D$$

unless D is very small. Thus the value of M will remain approximately constant in any given applied field when ever the condition $\chi D \gg 1$ applies. The fall off in M from the constant value, which occurs at high and low temperatures, thus indicate a decrease in susceptibility, such that the condition $\chi D \gg 1$ is no longer fulfilled. This effect is to be expected on approaching the Curie temperature, but not at low temperatures. Therefore, a drop in χ requires a rapid increase in magnetic hardness. The ZFC magnetization and inverse susceptibility as a function of temperature are presented in Fig.6.16 and 6.18 in a wider temperature range for $x=0.02$ and 0.05 . The susceptibility follows the Curie-Weiss law above 245 and 145 K with paramagnetic Curie temperatures $\theta = 37$ and 105 K for $x=0.02$ and 0.05 respectively. The Curie constants are compatible with average effective paramagnetic moment, $P_{eff} = 1.54$ and $1.72 \mu_B$ /f.u. respectively.

In $Ni_{1-x}Fe_xPt$ ordered system ferromagnetic-paramagnetic transition is rather broad. Therefore it is difficult to determine T_C accurately. In set of Fig.6.16 shows the dM/dT of the

field cooled M vs T ($H=10$ Oe) curve depicted in the inset of Fig. 6.15 for the sample $x=0.02$. T_c is found to be $T_c = 38$ K comparable with the value of 37.3 K determined from Arrott plots (Fig.6.19) and 39K from AC susceptibility measurements. T_c determined by dM/dT of the ZFC magnetization vs temperature for $x=0.05$ with an applied of 50 Oe is $T_c=100$ K, while $T_c=101$ K found by AC susceptibility measurements.

Thermoremanent magnetization (TRM) for all the samples have been measured from 5 K up to above T_c to observe how TRM decays with temperature and to have idea about the transition temperature. TRM should vanish maximum at T_c . Thermoremanent magnetization for $Ni_{1-x}Fe_xPt$ alloys are presented in Fig 6.20-6.22. Measurements are taken by switching off the fields of the FC magnetization with different applied magnetic fields at 5K and increase the temperature up to above T_c and simultaneously recording the magnetization data. From these curves it is noticed that TRM decays with temperature and vanishes little above T_c for small applied fields and have still finite value further away from T_c for higher applied fields. This is easily understood from the fact that the superconducting magnet with the SQUID magnetometer retain little remanent field when the applied field is switched off. This remanent field of the magnet is higher when switched off from higher magnetic fields. So the small finite TRM observed even at T_c and above is clearly understood and it reflects the temperature dependence of magnetization with the small remanent field of the superconducting magnet. However from these measurements transition temperatures (T_c) are well estimated. From these measurements it is learnt that the ordered $Ni_{1-x}Fe_xPt$ alloys display strong hysteresis behaviour which persists up to the ferromagnetic Curie temperatures.

The pinning of domain walls by, in principle, all kinds of defects (internal stresses, grain boundaries, inhomogeneities and precipitates, phase boundaries, dislocations, etc.) contribute to the coercive field. A powerful method to ascertain the origin of the coercive field is to study its dependence with temperature. Temperature dependence of coercive field of $Ni_{1-x}Fe_xPt$ alloys are presented in Figs.6.23-26. The thermal variation of the coercive field of all the samples in the present system are not similar. For the sample with $x = 0.02$ and 0.05 a

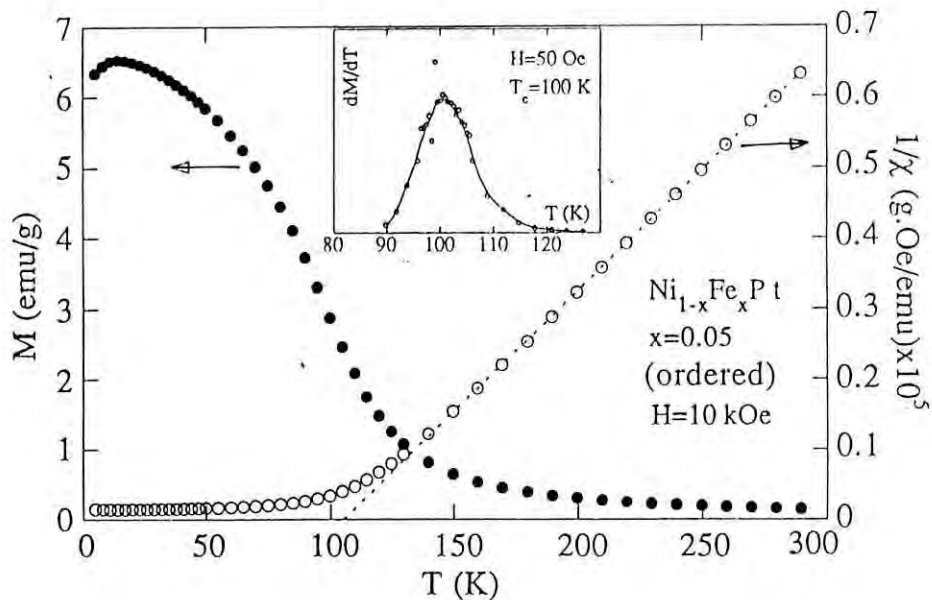


Fig.6.18. Temperature dependence of the ZFC magnetization and the reciprocal susceptibility of the ordered $\text{Ni}_{1-x}\text{Fe}_x\text{Pt}$ with $x=0.05$ at $H=10$ kOe; inset: dM/dT for this alloy at $H=50$ Oe.

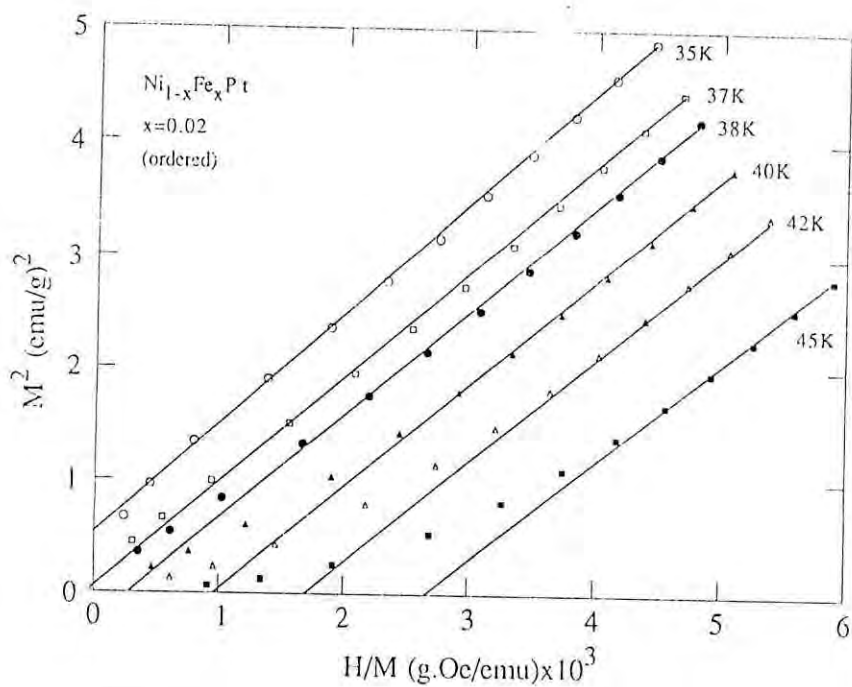


Fig.6.19. Arrott plots of the ordered $\text{Ni}_{1-x}\text{Fe}_x\text{Pt}$ with $x=0.02$ at different temperatures.

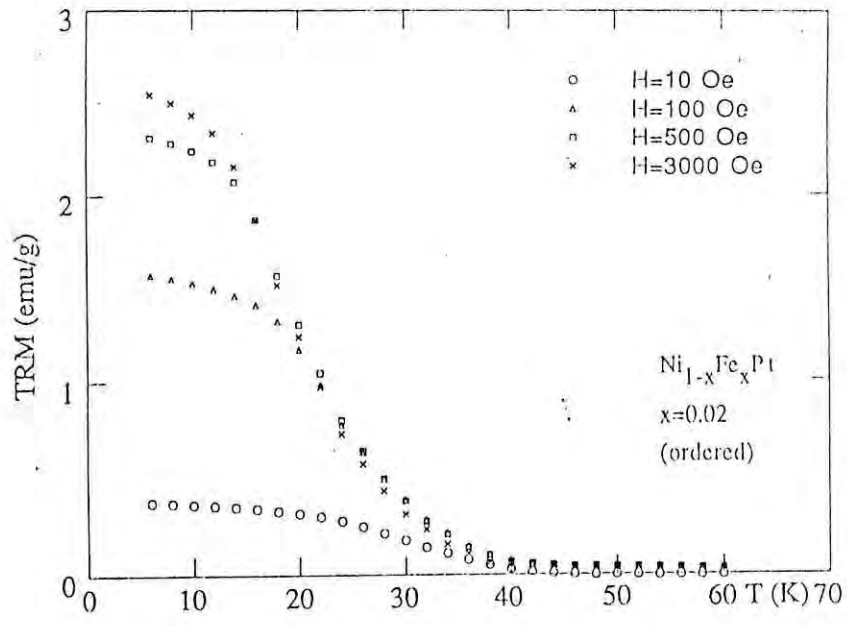


Fig.6.20. Thermoremanent magnetization of the ordered $\text{Ni}_{1-x}\text{Fe}_x\text{Pt}$ with $x=0.02$ at different applied fields during cooling as shown against each symbol.

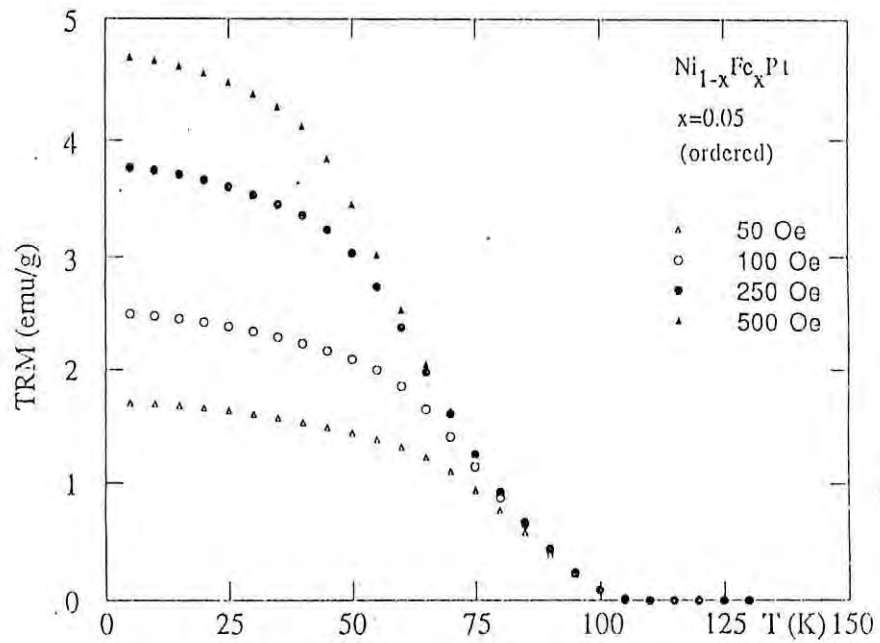


Fig.6.21. Thermoremanent magnetization of the ordered $\text{Ni}_{1-x}\text{Fe}_x\text{Pt}$ with $x=0.05$ at different applied fields during cooling as shown against each symbol.

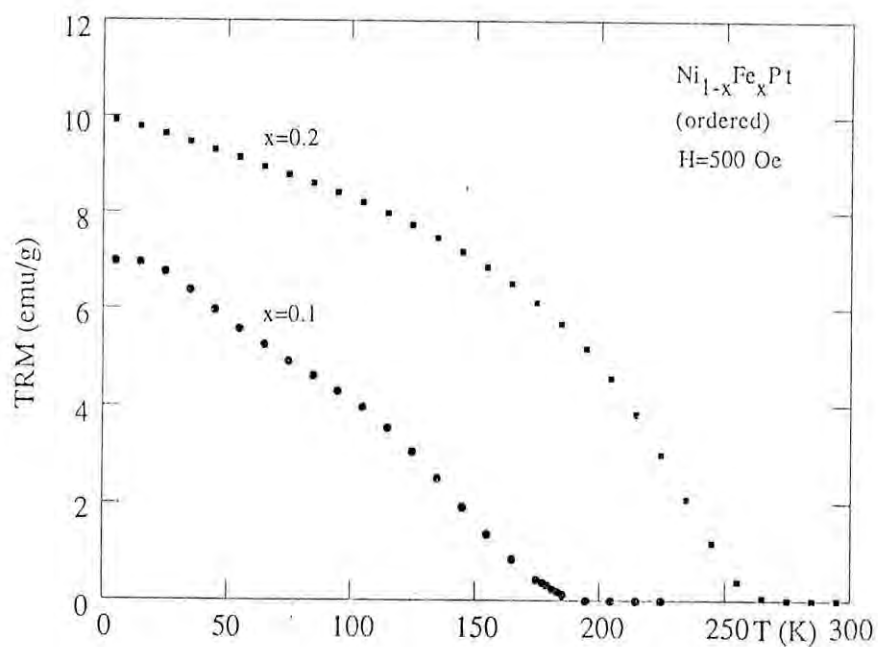


Fig.6.22. Thermoremanent magnetization of the ordered $\text{Ni}_{1-x}\text{Fe}_x\text{Pt}$ with $x=0.1$ and 0.2 with an applied field of 500 Oe during cooling.

strong dependence of the coercive field with temperature is observed which can be fitted by an exponential. The rapid decrease in H_c with increasing temperature is assumed to be related to the strong thermally activated process of domain wall unpinning. The coercive force corresponding to a particular temperature is obtained from the M vs T curves using different constant fields. The field for which the low temperature inflection occurs in these curves at a particular temperature gives the coercive field at that temperature. The coercive fields determined in this way are shown Fig.6.23 as open circles. These results are in excellent agreement with the coercive fields measured from hysteresis loops at different temperatures. From the exponential fitting coercive field at zero kelvin are determined and found to be 8.34 and 7.59 kOe for $x = 0.02$ and 0.05 compared with 4.24 kOe at 4.2 K and 6.05 kOe at 5 K respectively. Temperature dependence of coercive force for $x = 0.1$ and 0.2 are much slower

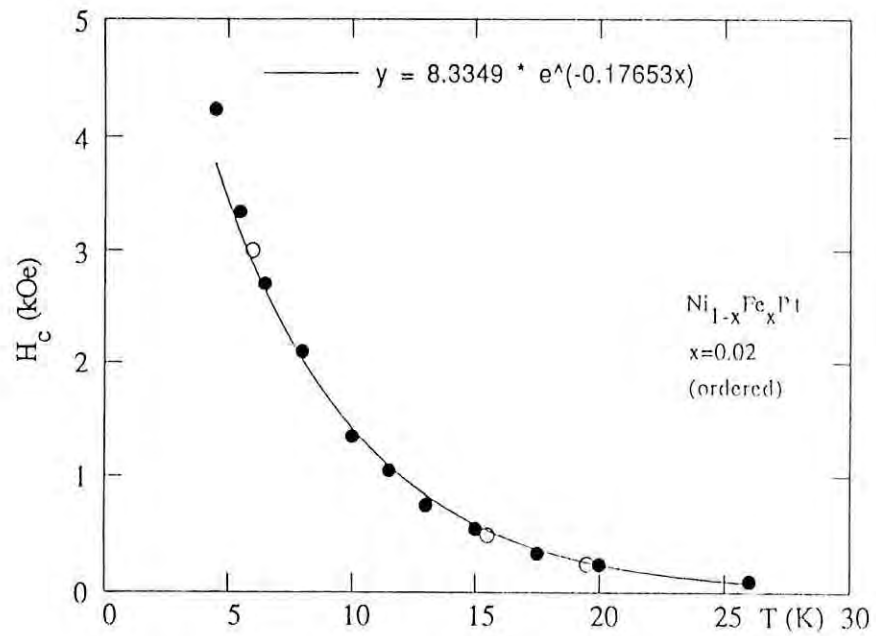


Fig.6.23. Temperature dependence of the coercivity of the ordered $Ni_{1-x}Fe_xPt$ with $x=0.02$ fitted with an exponential.

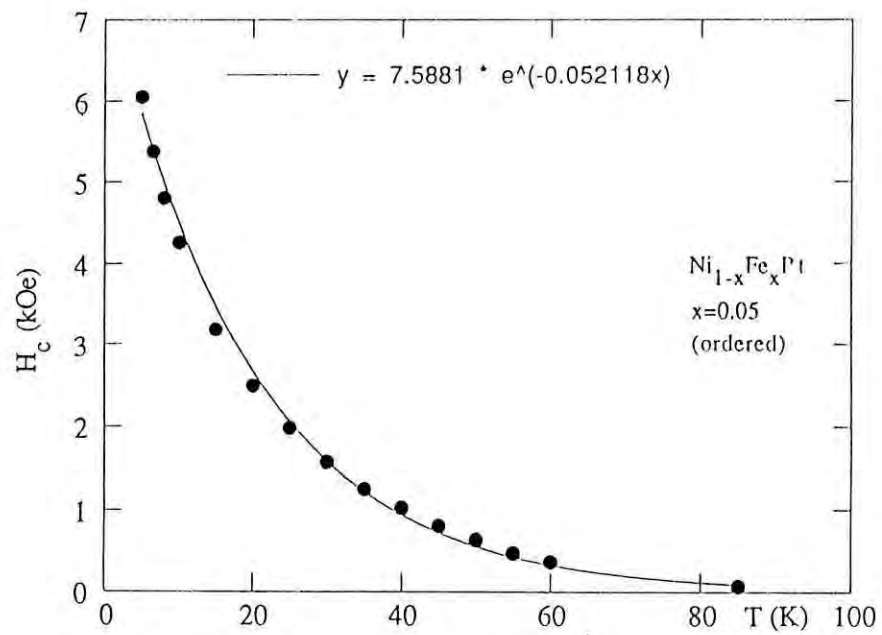


Fig.6.24. Temperature dependence of the coercivity for the ordered $Ni_{1-x}Fe_xPt$ with $x=0.05$ fitted with an exponential.

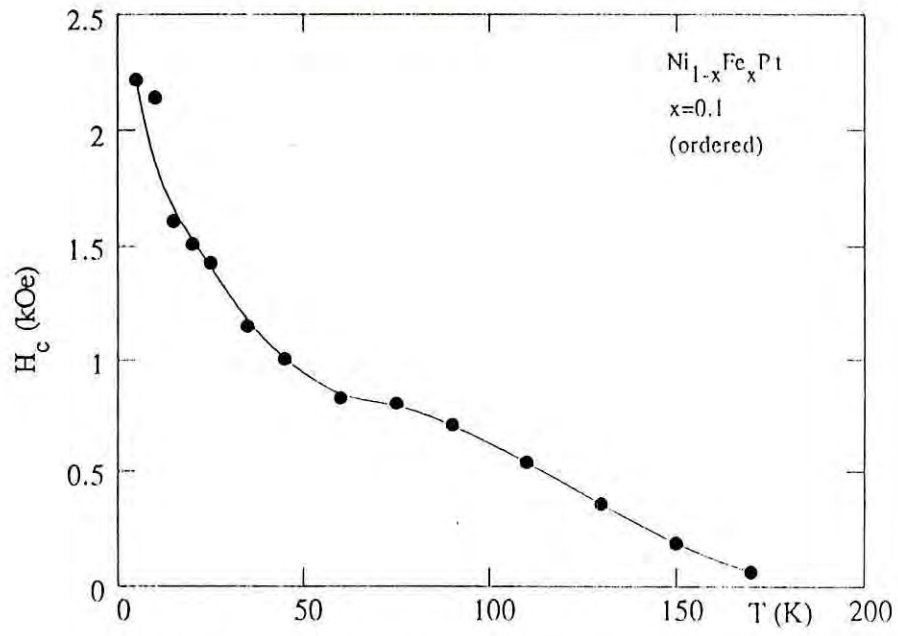


Fig.6.25. Temperature dependence of the coercivity of the ordered $\text{Ni}_{1-x}\text{Fe}_x\text{Pt}$ with $x=0.1$

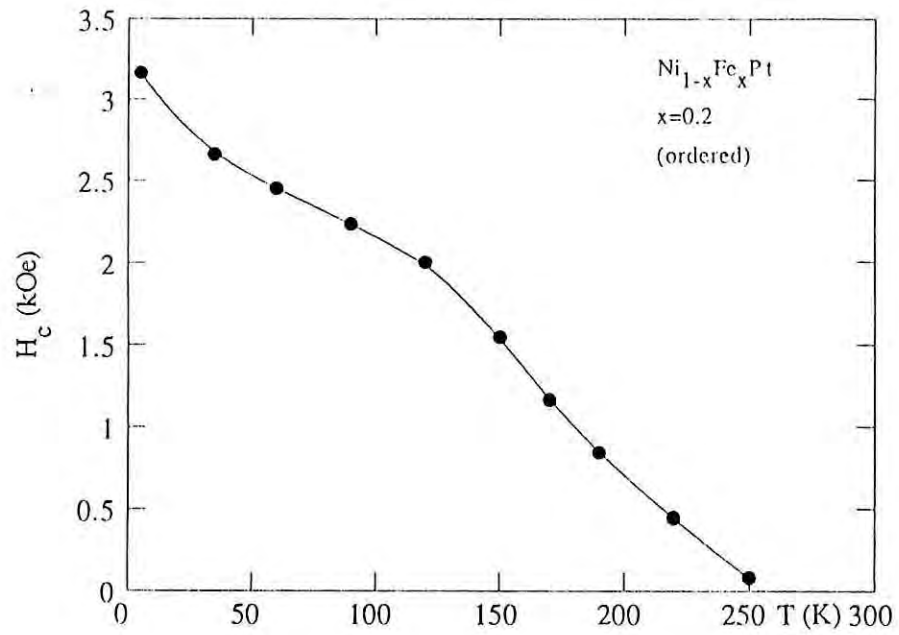


Fig.6.26. Temperature dependence of the coercivity of the ordered $\text{Ni}_{1-x}\text{Fe}_x\text{Pt}$ with $x=0.2$

where the contribution of thermal activation of the domain wall unpinning is much weaker. It is observed that for the sample $x=0.1$, the coercive field increases rapidly like those of $x=0.02$ and 0.05 at very low temperatures and then slows down. If the coercivity at zero kelvin is considered then it is found that the coercivity decreases with increasing Fe concentrations.

An analysis of the origin of the coercive field requires some knowledge about the defects present in the samples. The defects observed through X-ray analysis and SEM study are assumed to be the possible sources of domain wall pinning and hence of coercive field in this system. These defects which lead to the creation of energetic barriers for the magnetization process at low temperatures are responsible for low temperature magnetic hardness. The coercive field found in this system can be understood by Kersten's [31,32] theory of critical bowing and irreversible displacement of the domain walls pinned by the defects. In this model the domain wall, pinned by lines of defects, bows until a critical radius, from where it moves irreversibly under a critical field equal to the coercive field.

Concentration dependence of magnetic moment, μ , and Curie temperature, T_c , are shown in Figs. 6.27 and 6.28. It is noticed that magnetic moment and Curie temperature both increase with increasing Fe concentration x , but this increase of μ and T_c with x is faster at low concentration than for the higher concentrations. Giant moments have been found to be associated with an Fe atom when a small amount of Fe is substituted for Ni in the Ferromagnetic and paramagnetic NiPt alloys. Fig. 6.29 shows the magnetic moment per Fe atom as a function of Fe concentration x in both the ordered and disordered phases. The values of the giant moments for the ordered phase are found to be very large compared to the disordered phase at low iron concentrations. The giant moment per Fe atom for both the phases depend sensitively on the Fe concentrations and have higher values for lower concentrations. This can be explained according to the work of Kim and Schwartz[33] who examined the spin polarization around a localized moment in a magnetized band. They concluded that the polarizability decreases with increasing polarization. This effect has experimentally been observed in Pd and Pt based alloys with Fe by a decrease of average

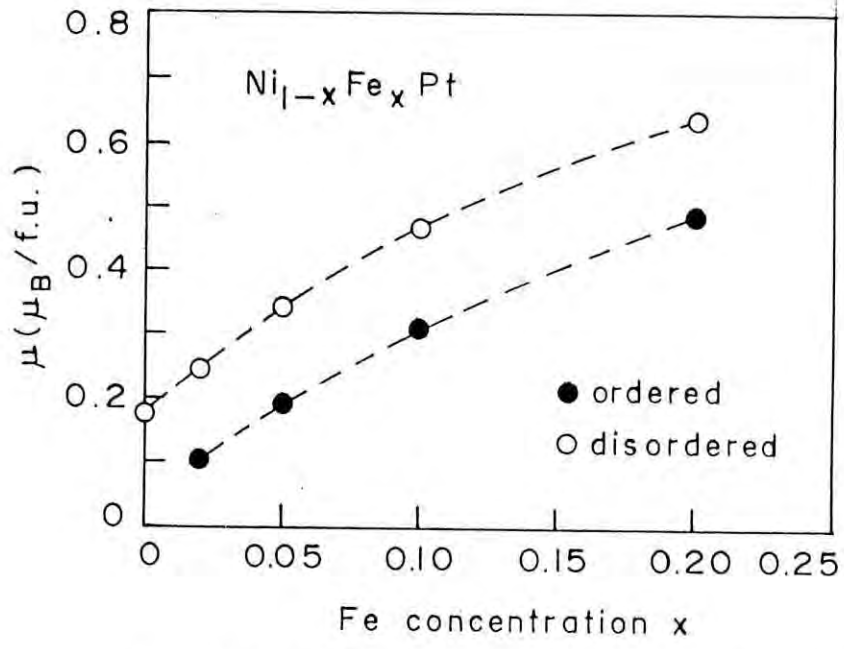


Fig.6.27. Magnetic moment per formula unit of the ordered and disordered $Ni_{1-x}Fe_xPt$ alloys as a function of Fe concentration x .

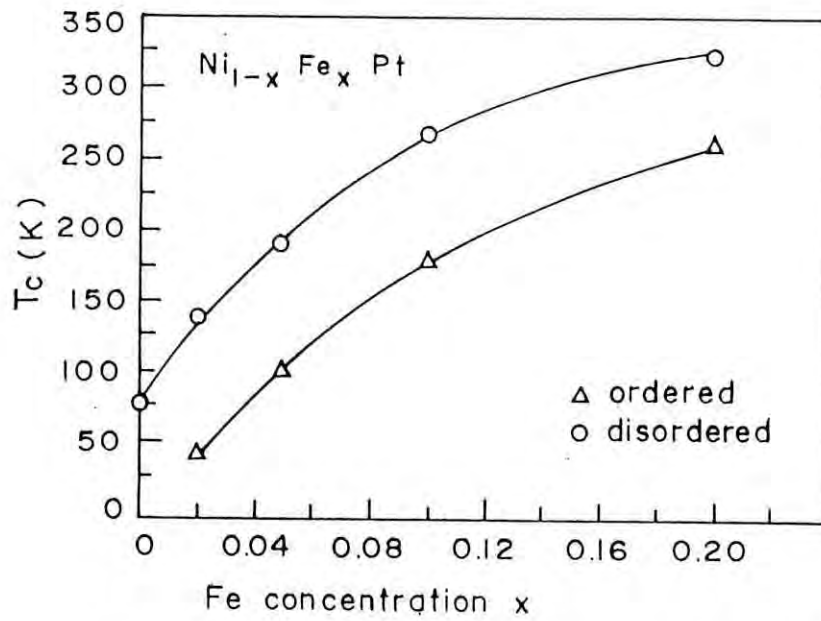


Fig.6.28. Dependence of the Curie temperature of the ordered and disordered $Ni_{1-x}Fe_xPt$ alloys against Fe concentration x .

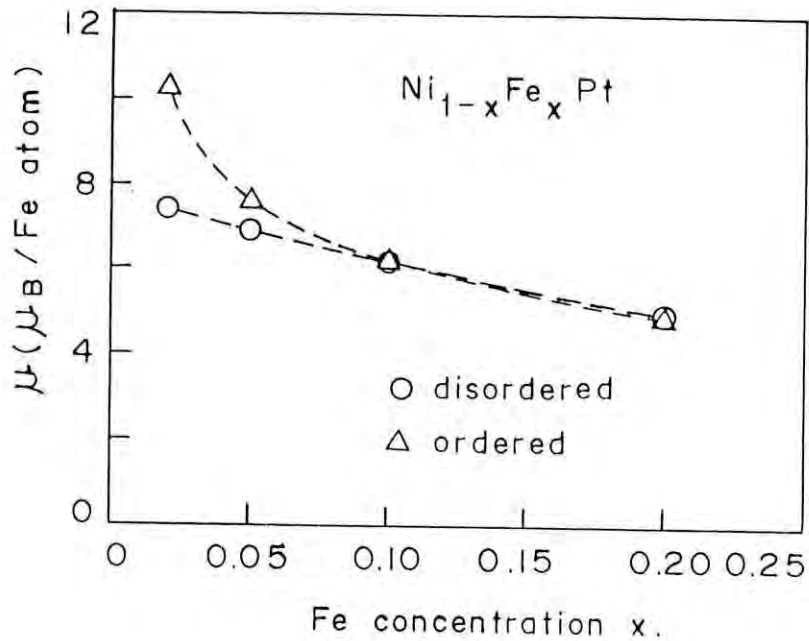


Fig.6.29. Magnetic moment, μ , per Fe atom of the ordered and disordered $\text{Ni}_{1-x}\text{Fe}_x\text{Pt}$ alloys as a function of Fe concentration x .

magnetic moment per 3d atom with increasing concentrations of 3d elements [1,34]. The giant moment per Fe atom in the iron doped alloys is calculated from the increase in magnetic moment due to the replacement of Ni atoms by Fe atoms and by attributing net increased moment to the Fe atoms taking into account the moment of Ni atoms which are replaced.

In this connection it may be mentioned that small amount of Fe dissolved both in ferromagnetic and in paramagnetic alloys in the Ni_3Al and Ni_3Ga phases lead to giant moment inducement[35,36]. The composition of these two alloys are close to the critical concentration and their exchange enhancement factors are of the order of 35. Supergiant moments of $80\mu_B$ have been observed in these alloys with small amount of Fe dissolved in the matrix. The evidence for these is obtained by magnetization, neutron and Mossbauer

measurements[37-40]. The effect of dissolving Co in these alloys is weaker.

The giant moment varies from 10.3 μ_B per Fe atom for $x=0.02$ to 4.9 μ_B per Fe atom for $x=0.2$ for the ordered phases compared to that of 7.4 μ_B and 4.95 μ_B per Fe atom for the disordered phases with $x=0.02$ and 0.2 respectively. Obviously this large moment can not possibly be only associated with the Fe atoms, because the maximum moment arising from 3d electrons can not exceed 5 μ_B . Therefore, part of the observed moment must be due to polarization of the matrix parallel to the moment of the Fe atom rigidly coupled to the Fe moment. The polarized moment is thought to be fairly localized at the Fe sites. So the total effective moment is the sum of the localized moment on the Fe atom and induced moment in the host matrix. This moment has been considered as one magnetic moment and attributed to Fe atom which is then called a "giant" moment. When the concentration of Fe atoms is increased the polarization clouds begin to overlap affecting a decrease of the total moment per Fe atom because two overlapping polarization clouds contribute less to the magnetization than two separate clouds.

Reference

1. Mydosh, J.A. and G.J. Nieuwenhuys, in Ferromagnetic Materials, edited by E.P.Wohlfarth, Vol. 1, (North Holland Pub.Co.),1980, 82
2. Para,R.E. and R. Medina, Phys. Rev. 1980, B22, 5460
3. Crangle, J. and W.R.Scott, J. Appl. Phys. 1965, 38, 921
4. Bacon, G.E. and J. Crangle, Proc. Roy. Soc. London, 1963, A272, 387
5. Ododo, J.C. J. Phys.1982, F12, 1821
6. Martin,D.C., J.Phys.,1975, F5, 1031
7. Kawamiya,N.,and K.Adachi,1975, Trans.Japan.Inst.Met. 16,327
8. Rao,K.V.,O.Rapp,C.Johannesson,J.A.Budnick,T.J.Burch and V.Cannela, Magnetism and Magnetic Materials, Philadelphia, 1975,AIP Conf.Proc.no.29,346
9. Ododo, J.C., J. Phys.F: Metal Phys. 1979 Vol.9,1441
10. Chikazumi,S.,1964,Physics of Magnetism (Wiley: Newyork),273
11. Kouvel,J.S.and M.F.Fisher, Phys.Rev.,1964,136,A1626
12. Rucker,W. and R.Kohlhaas,Z. Angew. Phys., 1967,23,146
13. Noakes,J.E. and A.arrott, J.Appl.Phys., 1967,38,973
14. Arrott,A. and J.E.Noakes, Phys.Rev.Lett.,1967,19,786
15. Kaul,S.N., J.Magn.Mag.Mat.,1985,53,5
16. Barbara,B., C.Becle,R.Lemaire and D.Paccard, J.De Phys.(Paris),1971,32,C1-299
17. Folks,L.,C.D.Milham and R.Street, Proc.7th Int.Symposium on Magnetic Anisotropy & Coercivity in RE-TM alloys,1992, Canberra,Australia,274
18. Zhong,W.D.,J.Lan and G.Z.Li,J.Magn.Magn.Mat.,1988,74,39
19. Sima,V.,R.Grossinger,V.Sechovsky and H.Sassik, J.Phys. F14,1984,981
20. Oesterreicher,H.,J.Appl.Phys.,1971,42,5137 and 1973,34
21. Yang,Y.C. and Zhang,X.D.,J.Appl.Phys.,1990,67,4765
22. Nesbitt,E.A.,G.Y.Chin,G.W.Hull,R.C.Sherwood,M.L.Green and J.H.Wernick,Proc.1972,Conf.on Magn.Magn.Mat.,AIP Conf.Proc.1973

23. Senoussi, S., Phys. Rev. Lett., 1983, 51, 2218
24. Senoussi, S., J. de Phys. (Paris), 1984, 45, 315
25. Felner, I. and I. Nowik, J. Magn. Magn. 315 Mat., 1986, 58, 169
26. Zeleny, M., J. Magn. Magn. Mat., 1991, 94, 85
27. Pinkerton, P.E. and D.J. Van Wingerder, J. Appl. Phys. 1986, 60, 3685
28. Chin, T.S., J.M. Yau, Cheng-Hao Lin and T.Y. Chu, Proc. Int. Symp. on magnetic anisotropy & coercivity in RE-TM alloys, 1992, Canberra, Australia, P. 85
29. Ding, J., R. Street and P.G. McCormick, Proc. 7th Int. Symp. on magnetic Anisotropy & Coercivity in RE-TM alloys 1992, Canberra, Australia, 130
30. Concise Encyclopedia of Magnetic & Superconducting Materials, edited by Jan Evetts (Pergamon press), 1992, 70
31. Kersten, M., Z. Angew. Phys., 1956, 7, 313
32. Kersten, M., Z. Angew. Phys., 1956, 8, 382
33. Kim, D.J. and B. Schwartz, Phys., Rev, Lett., 1968, 20, 201
34. Boerstael, B.M., J.E. Van dam and G.J. Nieuwenhuys, in Magnetism edited by Simon Foner, Gordon and Breach, Science Pub. Inc., New York, 1976, 210
35. De Boer, F.R., C.J. Schinkel, J. Biesterbos and S. Proost, J. Appl. Phys., 1969, 40, 1049
36. Schinkel, C.J., F.R. DeBoer, J. Biesterbos, Phys. Rev. Lett., 1968, 26A, 50
37. Schalkwijk, M.S., P.E. Brommer, G.J. Cock and C.J. Schinkel, J. Physique (Paris), 1971, 32, C1, 997
38. Cable, J.W. and H.R. Child, AIP conf. Proc., 1973, 10, 1623
39. Ling, P.C. and T.J. Hicks, J. Phys., 1973, F3, 697
40. Liddel, P.R. and R. Street, J. Phys., 1973, F3, 1648

CHAPTER 7

Measurements on $\text{Ni}_{1-x}\text{Co}_x\text{Pt}$ alloys

7.1 Introduction

Pseudobinary $\text{Ni}_{1-x}\text{Fe}_x\text{Pt}$ alloys based on equiatomic NiPt display interesting magnetic properties in terms of magnetization process, coercivity mechanism and giant moment inducement by substituting small amount of Fe for Ni in both the ordered and disordered phases and have extensively been studied in the previous chapter. Similar studies have now been performed on the pseudobinary $\text{Ni}_{1-x}\text{Co}_x\text{Pt}$ with $0.01 \leq x \leq 0.10$ to see the effect of Co in the equiatomic NiPt in the ordered and disordered phases.

It is also well known that Pt is an exchange enhanced paramagnet and capable of producing giant moment polarization in the presence of 3d transition metals like Fe or Co. Concentration as low as 0.76 at.%Co makes the PtCo alloys ferromagnetic at absolute zero [1] and the same concentration of Fe is also required for the onset of ferromagnetism in PtFe alloy. Dilute ferromagnetic alloys of PtCo are giant moment ferromagnets and giant moments of $\approx 4\mu\text{B}$ have been found by a number of investigators [2-4]. Giant moments of approximately $6\mu\text{B}$ have been reported in dilute PtCo alloys by Swallow et al [5] and Tsiovkin et al [6] with Co concentration little less than the critical concentration.

Rudman [7] measured the magnetic properties of pseudobinary $\text{Co}_{1-x}\text{Ni}_x\text{Pt}$ alloys based on equiatomic CoPt with $0 \leq x \leq 0.2$ at room temperature with a view to observe the effect of composition changes outside the range of the binary constituents on the magnetic hardness of the simple binary alloy. Substitution of Co by Ni adversely affect the magnetic hardness of the binary CoPt alloy. There are no reports available on the effect of Co in NiPt in particular with very small concentrations of Co in the ordered and disordered phases.

The purpose of the present work is to investigate thoroughly the changes in magnetic moments and Curie temperatures in the ordered and disordered phases of $\text{Ni}_{1-x}\text{Co}_x\text{Pt}$ with increasing x. From ZFC and FC magnetization measurements magnetization process would be ascertained. The giant moment which is expected due to polarization of the

host matrix by Co atoms would be calculated and compared with the related magnetic system.

7.2 Experimental

The $\text{Ni}_{1-x}\text{Co}_x\text{Pt}$ polycrystalline samples with $x = 0.01, 0.02, 0.05, 0.07$ and 0.1 have been prepared by arc melting in an argon atmosphere. Disordered samples were obtained by rapid quenching from 1000°C and ordered ones by long annealing at temperature below order-disorder transition temperature details of which are given in chapter 3.

X-ray diffraction studies show that the disordered alloys are fcc and single phase while the ordered ones are fct with little amount of precipitate second phase (composition not identified) together with disordered phase.

Scanning Electron Microscope (SEM) in the back scattered electron mode has been used to detect any precipitate or defects in the ordered sample with $x=0.05$, since X-ray investigations indicate the presence of second phase in the ordered samples. SEM study distinctly shows precipitated phase black in colour randomly distributed in the matrix of the ordered phase while no such evidence could be detected in the disordered phase. This finding will become relevant for the analysis of the hysteresis behaviour and coercivity mechanism of the alloys concerned.

Magnetization in the ZFC and FC condition have been measured with the SQUID magnetometer in the temperature range $5\text{-}350\text{ K}$ and magnetic fields $0\text{-}50\text{ kOe}$. Hysteresis loops have been measured including the initial magnetization under ZFC condition at different temperatures from which the temperature dependence of coercivity, $H_c(T)$, and critical field, $H_p(T)$, are estimated.

The temperature dependence of the real component (χ') and the imaginary component (χ'') of the AC susceptibility are measured by Lake Shore AC susceptometer,

Model 7225 in order to determine the onset temperatures of the magnetic phase transitions. These measurements allow an unambiguous determination of the magnetic phase transition temperature. For highly anisotropic and multiphased materials like ordered $\text{Ni}_{1-x}\text{Co}_x\text{Pt}$ alloys, the value of χ' is mainly determined by the magnetic anisotropy energy and the domain wall energy. The value of χ'' reflects the energy absorption by the sample, which mainly arises from the domain wall movement. In the present investigation a field of 1 Oe and frequency 125 Hz are used. The onset temperature for the magnetic phase transition is identified to be the temperature where $d\chi'/dT$ achieves a maximum.

From the detailed experimental study the following characteristic magnetic parameters have been determined, (a) saturation magnetization, M_S , (b) magnetic moment, μ , in Bohr magneton, (c) ferromagnetic Curie temperature, T_C , (d) paramagnetic Curie temperature, θ , (e) Curie constant per mole, C , (f) effective paramagnetic moment, P_{eff} (g) Remanence, M_R , (h) Coercivity, H_C , (i) Critical field, H_P , (j) giant moment per Co atom.

7.3 Results and discussions

7.3.1 Disordered alloys

Magnetization curves measured at 5 K with a SQUID magnetometer as a function of magnetic field for the disordered $\text{Ni}_{1-x}\text{Co}_x\text{Pt}$ samples are presented in Fig.7.1. Magnetization show a good saturation with magnetic field of 10 kOe. No noticeable increase in magnetization occur with magnetic field up to 50 kOe. In order to check whether any hysteresis effects are there in the magnetization, measurements have been taken during increasing and decreasing of magnetic fields. Magnetization is found to be reversible with no hysteresis for the samples studied. Magnetic moments, μ , are calculated with these saturation values at 5 K.

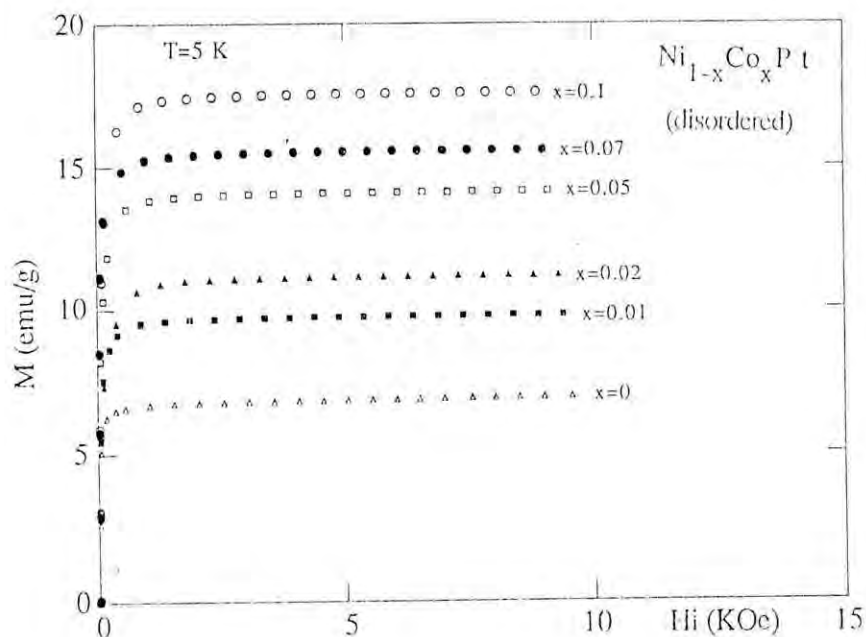


Fig. 7.1. Magnetization as a function of internal magnetic field of the disordered $\text{Ni}_{1-x}\text{Co}_x\text{Pt}$ alloys at 5 K.

Ferromagnetic Curie temperatures for the samples have been mainly determined from low field DC magnetization with the SQUID magnetometer using the kink point method. Figs. 7.2a,b show the ZFC magnetization of the samples with magnetic field as low as 20 Oe. The samples exhibit clear kink point at T_C reaching there the demagnetizing field limited magnetization. No decrease in magnetization of the ZFC (low field) curves below T_C also indicate that the alloys are magnetically soft. Ferromagnetic-paramagnetic transitions look quite sharp showing that the disordered phases are metallurgically homogeneous. Saturation magnetization M_S , magnetic moment μ and Curie temperature T_C together with other relevant magnetic parameters are summarized in Table 7.1.

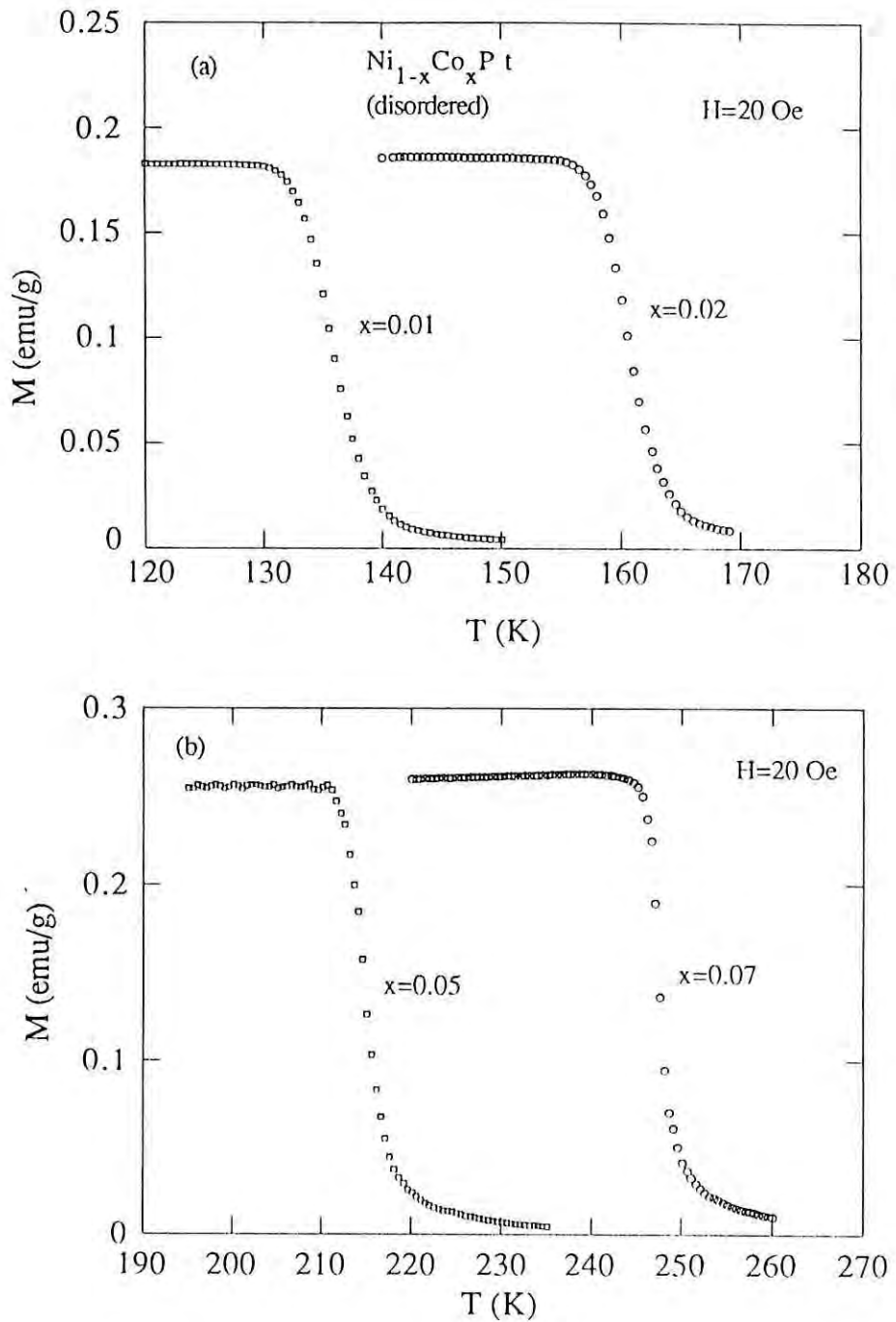


Fig.7.2. Low field DC magnetization as a function of temperature of the disordered $\text{Ni}_{1-x}\text{Co}_x\text{Pt}$ alloys with (a) $x=0.01$ and 0.02 and (b) $x=0.05$ and 0.07 at magnetic field of 20 Oe.

Temperature dependence of the saturation magnetization measured with applied fields of 5 and 10 kOe are demonstrated in Fig.7.3. A nonlinear least squares fitting show that magnetization follow T^2 dependence up to $0.8T_C$. As can be observed from Fig.7.3, increase of the Co content results in strengthening the interactions among the magnetic moments with the net outcome the appearance of the ferromagnetic phase being effected at higher temperatures.

The high field and high temperature susceptibility of the disordered samples are presented in Fig. 7.4. The data show excellent fit to the Curie-Weiss law using a least squares fitting routine from which the paramagnetic Curic temperatures, Curie constants and effective paramagnetic moments are deduced. The results are demonstrated in Table7.1. The Curie-Weiss behaviour occur from temperature little above T_C until 350 K for the samples. It is noticed that the values of the θ and P_{eff} increase with increasing x again showing that the exchange interaction increase with increase of Co concentration. The difference between θ and T_C is quite small which means that the short range ordering above T_C for the samples is not so strong.

A large number of magnetic isotherms from 5 K to far above T_C have been measured from 0-5 kOe magnetic field for the sample $x= 0.05$. Fig. 7.5 demonstrates the Arrott plots for some of the the isotherms close to T_C . From these plots spontaneous magnetization, M_0 , initial susceptibility, χ_0 and T_C (isotherm that passes through the origin) are determined. It is evident that the Arrott Plots are nonlinear from low temperature until little above T_C . Therefore parabolic extrapolation procedure has been adopted to determine the relevant magnetic quantities. Theoretical justification for the parabolic extrapolation is mentioned in previous chapter. From the Arrott Plots T_C is found to be 158 ± 0.5 K in good agreement with the values determined by kink point method $T_C = 157$ K. In set of Fig. 7.5 shows the temperature dependence of spontaneous magnetization determined from Fig 7.5. The critical isotherm at $T = 157$ K is analyzed with the relation $M = H^{1/\delta}$ with a log-log plot which gives a value of $\delta= 4.9$ compatible with the Heisenberg model ($\delta= 5$) but incompatible

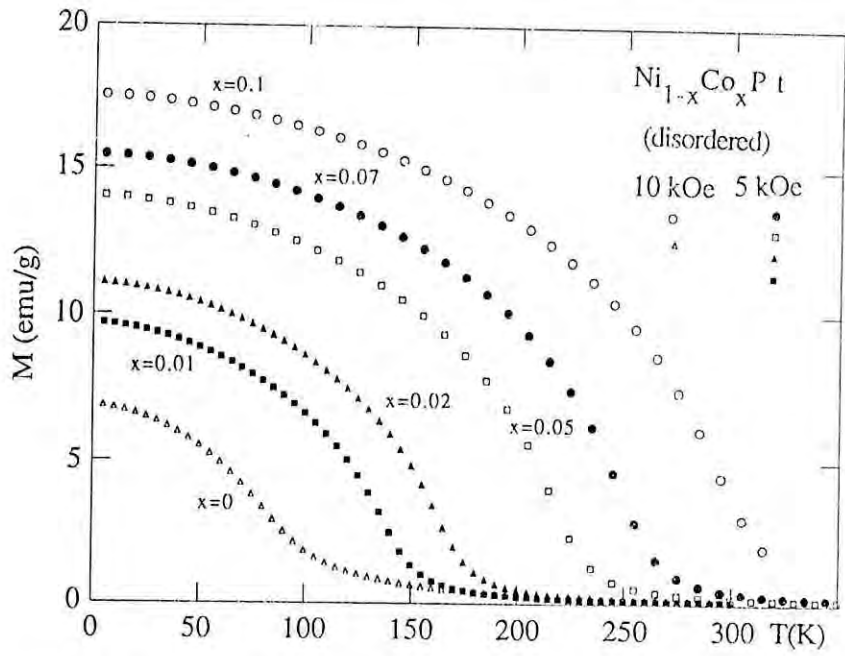


Fig.7.3. Variation of the saturation magnetization with temperature of $Ni_{1-x}Co_xPt$ alloys at magnetic field of 5 kOe with $x=0.01, 0.02, 0.05$ and 0.07 and at 10 kOe with $x=0.0$ and 0.1

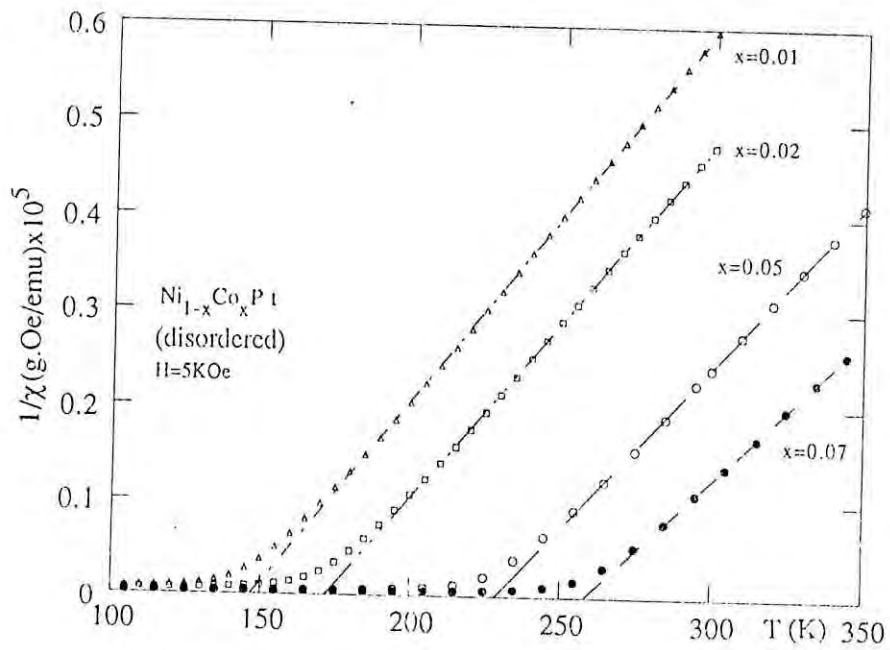


Fig.7.4. Temperature dependence of the inverse susceptibility of the $Ni_{1-x}Co_xPt$ alloys with different concentrations x .

Table 7.1 Magnetic properties of disordered Ni_{1-x}Co_xPt

Cobalt content x	0	0.01	0.02	0.05	0.07	0.1
M _S (emu/g) T=5K	7.72 ^a	9.69	11.07	14.02	15.46	17.55
μ (μ _B /f.u.)	0.176	0.221	0.252	0.319	0.352	0.40
T _C (K)	79	132	157	212	245	285
θ (K)	139	147	172	228	258	305
C (emuK/mole)	0.25	0.327	0.343	0.373	0.425	0.45
P _{eff} (μ _B /f.u.)	1.42	1.60	1.66	1.73	1.84	1.9
μ(μ _B /Co)		9.28	7.88	6.04	5.31	4.76

^a Value corresponding to H=50 kOe

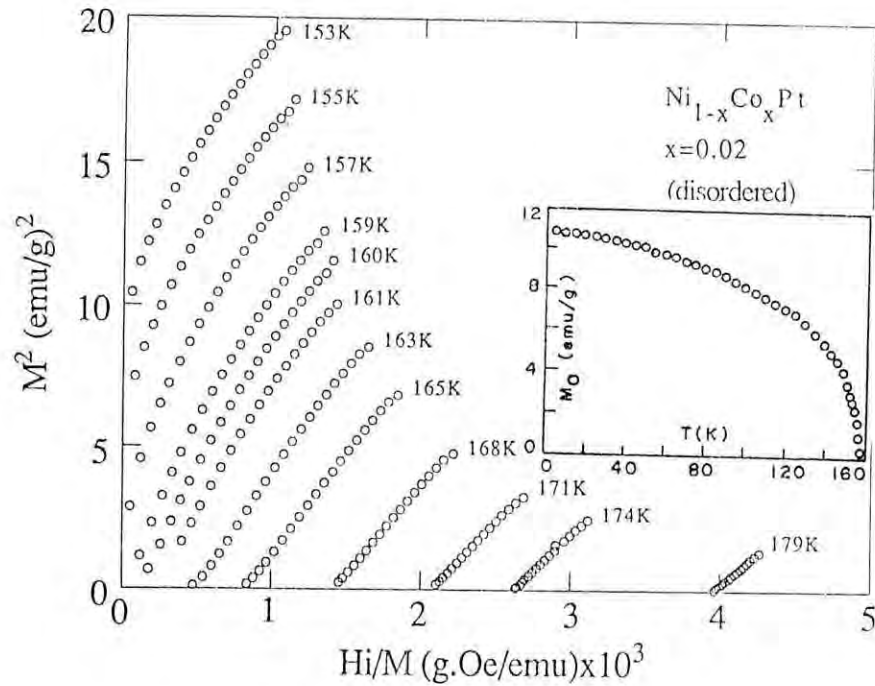


Fig.7.5. Arrott plots of the disordered $\text{Ni}_{1-x}\text{Co}_x\text{Pt}$ alloys with $x=0.05$ at different temperatures; inset: temperature dependence of the spontaneous magnetization determined from these plots.

with the molecular field model where $\delta = 3$.

It turns out from these measurements that the substitution of Co for Ni in the disordered NiPt results in substantial increase of magnetic moments and ferromagnetic transition temperatures. Increase of Curie temperature and magnetic moment is stronger for the low concentration of Co and gradually decrease with x . It is observed from the dependence of μ and T_C with x which initially increases with greater slopes but bend slowly downward with decreasing slopes. It should be mentioned that with increasing x , increase of T_C and μ is less rapid than proportional to x because then the polarization is becoming saturated and the magnitude of the moment per atom decreases. In fact it is understood that the substantial increase of T_C and μ in $\text{Ni}_{1-x}\text{Co}_x\text{Pt}$ with raising Co content are related to the

enhanced exchange interaction and polarization of the host matrix through the overlapping of the 3d electronic wave functions and the polarization clouds. If the total increased magnetic moment is attributed to the Co atom alone then a giant moment of $9.28\mu_B/\text{Co}$ atom for $x = 0.01$ is obtained which decrease with x and finally a moment of $4.76\mu_B/\text{Co}$ atom for $x = 0.1$ is attained. These values are much larger than the bare magnetic moment of the Co atom. Therefore the occurrence of this giant moment is understood by assuming that the bare magnetic moment of the Co atom polarizes the NiPt host matrix. This polarization gives rise to a net magnetic moment whose magnitude is much greater than the bare moment of the Co atom. This giant moment is considered as the sum of the Co moment and the induced moment of the matrix which has been attributed to the Co atom. Similar effect has been observed in $\text{Ni}_{1-x}\text{Fe}_x\text{Pt}$ alloys in the present study and in many other systems described in Chapter 6.

7.2.3 Ordered alloys

Ordered $\text{Ni}_{1-x}\text{Co}_x\text{Pt}$ alloys show unusual magnetic behaviour like that of $\text{Ni}_{1-x}\text{Fe}_x\text{Pt}$ alloys with attendant peculiarity of pronounced stepping behaviour in the initial magnetization process. This behaviour is in sharp contrast with that of the disordered alloys discussed so far. Hysteresis loops have been measured with a SQUID magnetometer at 5 K including the initial magnetization for all the samples with the maximum available magnetic field of 50 kOe. Figs. 7.6-7.9 display such measurements for $x = 0.01, 0.05, 0.07$ and 0.1 . For $x = 0.05, 0.1$ and 0.02 show peculiar multi stepping behaviour. For $x = 0.07$ the hysteresis behaviour is similar to that of Fe doped system. Here the initial magnetization curve reside inside the cyclic hysteresis loop. Hysteresis loop for the sample $x = 0.01$ is a typical for normal ferromagnetic material with a small coercive field. A coercive field as high as 13.44 kOe is observed at 5 K for $x = 0.07$ with a corresponding critical field of $H_p = 13$ kOe. The samples with $x = 0.05$ and 0.1 show high critical fields but very low coercive field.

The most striking feature of the demagnetization process in the sample $x = 0.05$

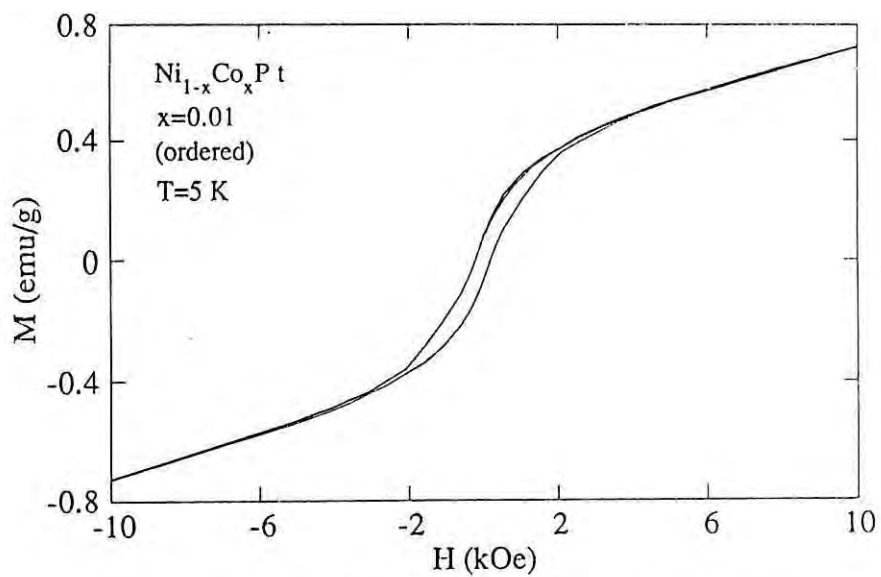


Fig. 7.6. Zero field cooled hysteresis loop of the ordered $\text{Ni}_{1-x}\text{Co}_x\text{Pt}$ with $x=0.01$ at 5 K.

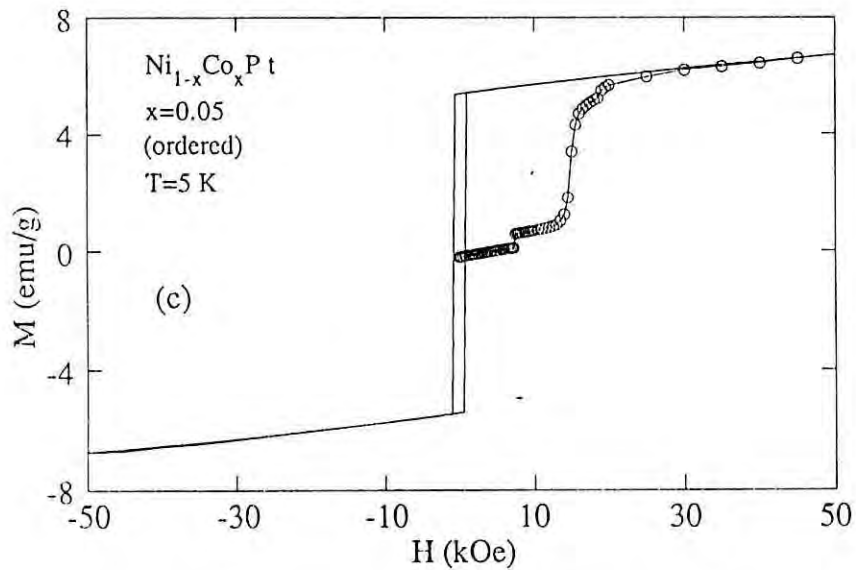


Fig. 7.7. Hysteresis loop with the initial magnetization curve of the ordered $\text{Ni}_{1-x}\text{Co}_x\text{Pt}$ with $x=0.05$ at 5 K.

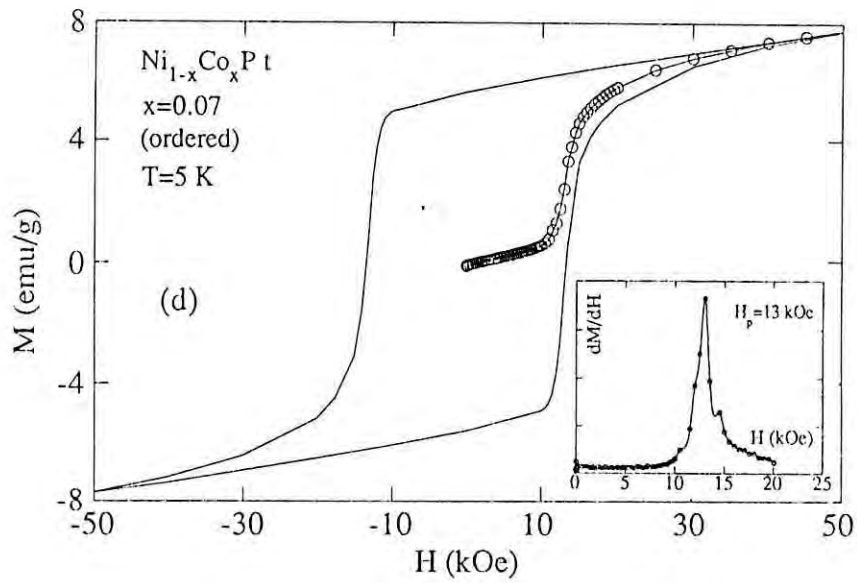


Fig.7.8. Hysteresis loop with the initial magnetization curve of the ordered $\text{Ni}_{1-x}\text{Co}_x\text{Pt}$ with $x=0.07$ at 5 K.

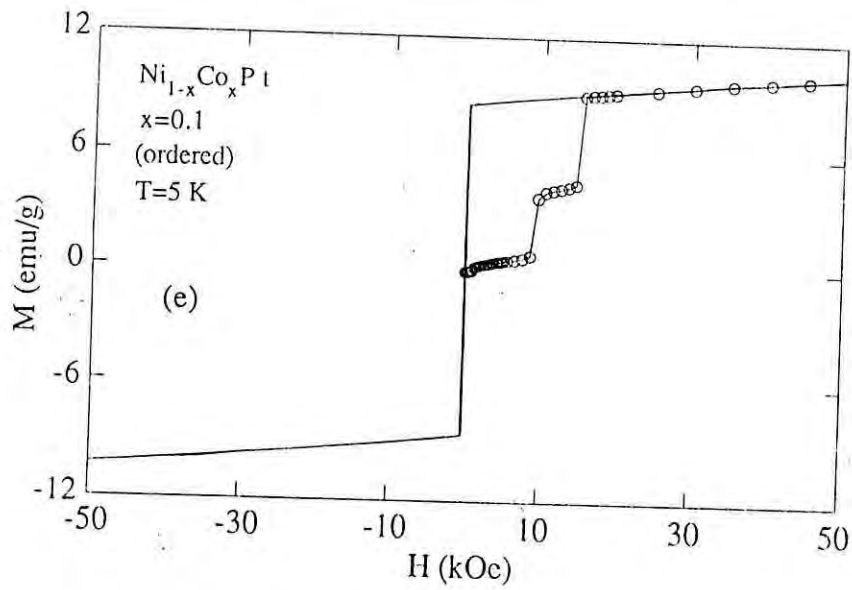


Fig.7.9. Hysteresis loop with the initial magnetization curve of the ordered $\text{Ni}_{1-x}\text{Co}_x\text{Pt}$ with $x=0.1$ at 5 K.

and 0.1 is the large instability of magnetization when the magnetizing field is reduced from the maximum value. This is characterized by sharp reversal of magnetization and can be regarded as a large single Barkhausen jump associated with the maximum volume of the crystal occurring at a field equal to the coercive field. It may be assumed, for the purposes of discussion, that the instability in the magnetization curve corresponds to the passage of domain wall from one position of stable equilibrium to another. It appears that there are two energy minima positions corresponding to two angular positions of the magnetic domains. The domains may be unstable under the influence of external magnetic field with a consequent reversal of magnetization vector from its previous direction to new angular position. It is not possible to say exactly what rearrangement of domains correspond to this large Barkhausen jump. But the size of the jump makes it clear that large domain with a substantial volume of the sample is involved in this magnetization reversal process. Stewart [8] and Williams et al. [9] observed such type of Barkhausen jump in the rectangular hysteresis loops of Fe-Si and Fe-Ni-Co soft magnetic alloys with uniaxial anisotropy.

Three critical fields for the sample $x = 0.05$ have been observed. First jump takes place at 7.3 kOe followed by 14.6 kOe and 18.6 kOe and finally merges with the cyclic loop at around 40 kOe. But for $x=0.1$, two prominent jumps are observed at 8.6 kOe and 14.5 kOe and finally coincides with the cyclic loop at 15.5 kOe. There is another small jump at around 2 kOe. It should be mentioned that the stepwise increase of magnetization with field are completely repeatable if the samples are thermally demagnetized by heating them up above the Curie temperature and cooled without a field. There is no traces of this peculiarity left if the sample is investigated a second time without thermally demagnetizing it or in the field cooled condition. This seems to exclude crystal-field effect as a source for this stepwise increase. The stepwise increase in magnetization could be in principle, connected with a multiphase material which has indeed been confirmed by x-ray and SEM investigations. Each critical field is assumed to correspond to a particular phase which is necessary to overcome the energy barrier to give rise to magnetization. The magnitude of the critical field depends on the

height of the energy barrier up to which the domain wall is pinned. None of these samples could be saturated with magnetic field up to 50 kOe indicating that the samples have high anisotropy at low temperature. Magnetization after showing first sign of saturation still increases slightly at higher fields in an almost linear fashion. This manifests in some curvature in the plots of M vs $1/H$. Therefore the saturation value should be taken with caution and has not been used in the calculation of magnetic moment, μ , in Bohr magneton. High remanences (M_r) with $M_r/M_s = 0.1 - 0.83$ with increasing x have been observed for the samples studied. From all these observations it is believed that the domain wall pinning effect, anisotropy and heterogeneity (multiphase) of the samples are responsible for the stepwise increase of magnetization with field, high remanence and almost linear increase of magnetization in very high magnetic fields. From these peculiar magnetization process, it is felt encouraging to investigate the temperature dependence of magnetization more closely.

Initial magnetization curves at different temperatures have been measured with magnetic fields up to 50 kOe for all the samples in the ZFC condition. Figs. 7.10 - 7.12 present initial magnetization curves for the samples $x = 0.01, 0.05$ and 0.07 . For $x = 0.01$ show a normal magnetization behaviour with no critical fields. In Figs. 7.11 and 7.12 it is observed that the stepwise increase in magnetization is relaxed with little rise in temperature and the critical field at which magnetization rises very sharply shifts to lower fields with increasing temperature. For $x = 0.05$, three step increase in magnetization reduced to one step at 15 K and finally stepping behaviour disappears above 35 K. For $x = 0.07$ the critical fields decrease with increasing temperature and comparable with the trend found in $Ni_{1-x}Fe_xPt$ with $x=0.05$ and 0.02 and many other system described in Chapter 6. Critical field (H_p) and coercive field (H_c) show strong dependence with temperature. These phenomena are interpreted as due to thermal activation processes. It is possible that at finite temperature T the wall can be unpinned in a field H less than the critical field H_p for a temperature lower than T if the balance of the energy barrier and magnetic energy from H is available from thermal energy kT .

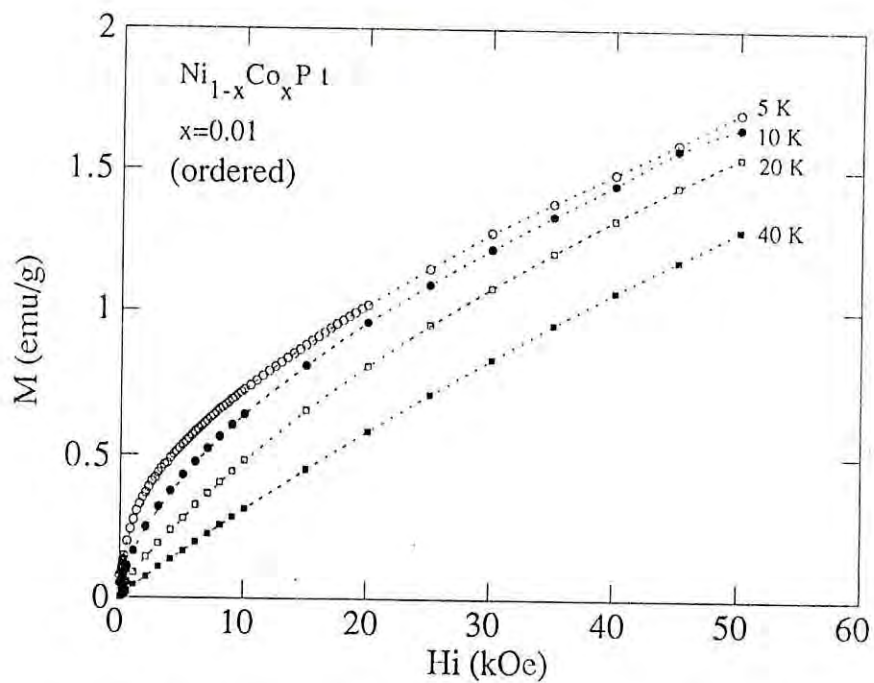


Fig. 7.10. Initial magnetization curves of the ordered $\text{Ni}_{1-x}\text{Co}_x\text{Pt}$ with $x=0.01$ at various temperatures.

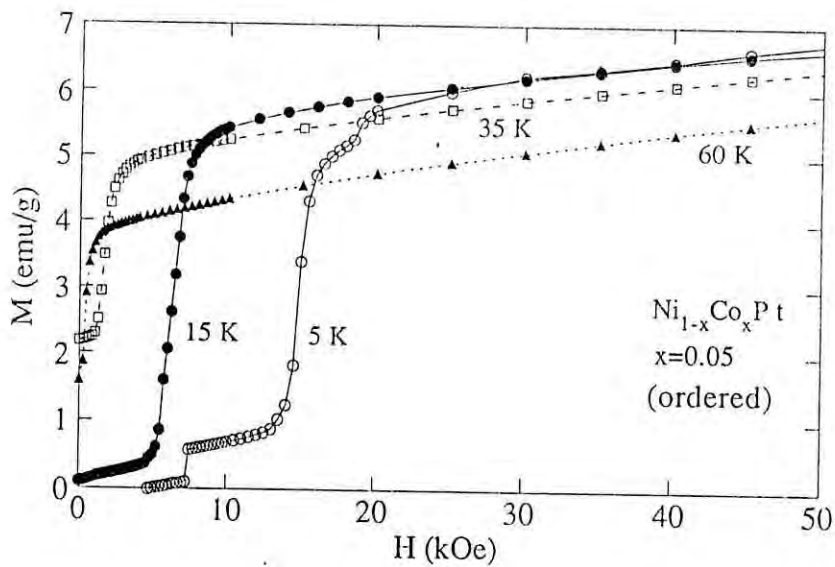


Fig. 7.11. Initial magnetization curves of the ordered $\text{Ni}_{1-x}\text{Co}_x\text{Pt}$ with $x=0.05$ at different temperatures.

A series of ZFC hysteresis loops for the sample $x=0.07$ have been measured at different temperatures and from these measurements $H_C(T)$ and $H_p(T)$ are determined. H_C and H_p increase as the temperature decrease. At all temperatures it is observed that applied magnetic field must reach the value close to H_p to free the domain wall from pinning to give sharp rise to magnetization. These measurements permit to conclude that domain wall pinning controls the magnetization process in this system. $H_C(T)$ is plotted against $H_p(T)$ in Fig. 7.13. A least squares fitting with the experimental data show that $H_C = H_p$ implying that the domain wall is pinned upto the energy associated with the critical field H_p

Temperature dependence of coercive field is given in Fig. 7.14 for the sample $x=0.07$. A strong temperature dependence is observed which is fitted by an exponential. Such type of dependence has been found in $Ni_{1-x}Fe_xPt$ with $x = 0.02$ and 0.05 and can be interpreted as due to strong dependence of the critical field H_p with temperature connected to the thermally activated process. Magnetic moments μ have been calculated using magnetization data at 5 K. Table 7.2 summarizes all the determined magnetic parameters.

Magnetization have been measured as a function of temperature with low applied DC field in order to find magnetic phase transition temperature. Figs. 7.15-7.16 display FC and ZFC magnetization curves for $x = 0.01$ and 0.02 , while Fig. 7.17 shows only ZFC curve for $x = 0.05$. M vs T curve for $x = 0.01$ (Fig. 7.15a,b) shows that it is a disordered ferromagnet where competing interactions between ferromagnetic and antiferromagnetic phases co-exist. It seems from FC and ZFC curves that ferromagnetic phase undergo a phase transition at temperature around 20 K. In set of the Figure shows dM/dT of the ZFC magnetization data and defines a Curie temperature of $T_C = 20 \pm 1$ K. It is seen from the Fig. 7.15a that the ferromagnetic state is dominant with small applied field. At this low field antiferromagnetic interaction does not play an important role, but as the applied field is increased antiferromagnetic interaction becomes prominent and dominates the ferromagnetic interaction.(See Fig.7.15b). Inset of Fig 7.15b shows magnetization as a function of temperature at $H=5kOe$ where the ZFC and FC magnetization curves are identical. The curves

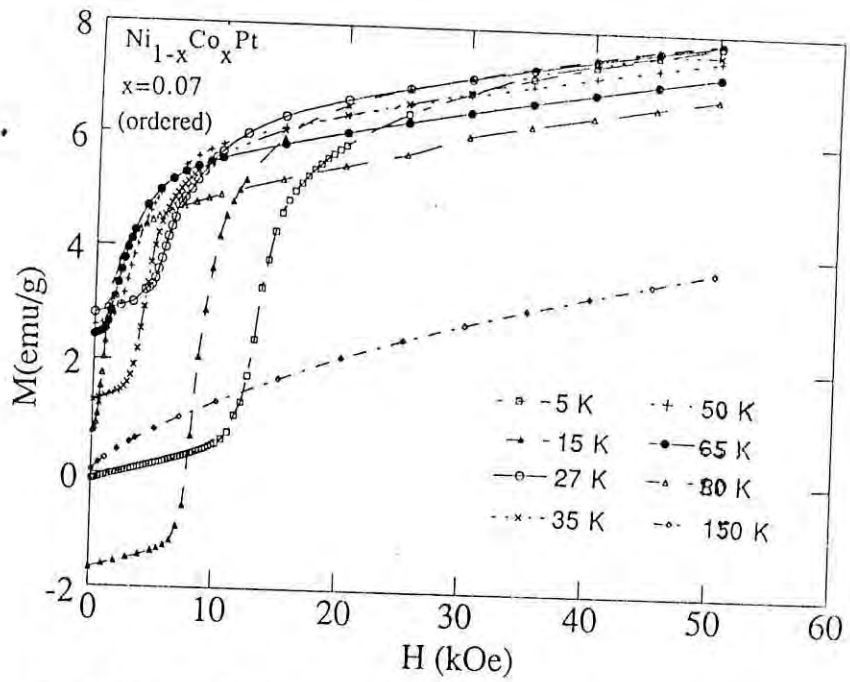


Fig. 7.12. Initial magnetization curves of the ordered $\text{Ni}_{1-x}\text{Co}_x\text{Pt}$ with $x=0.07$ at different temperatures.

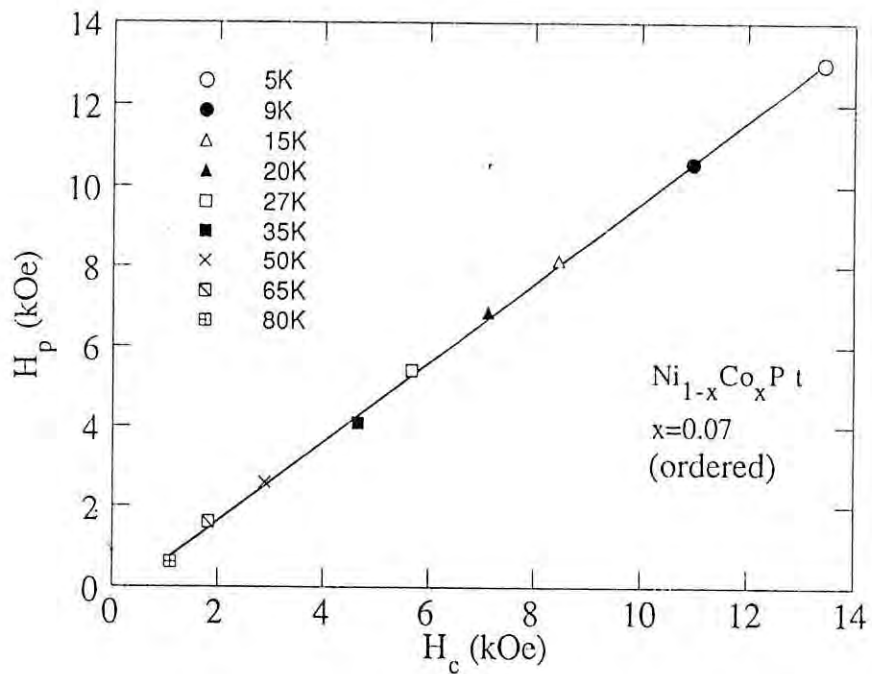


Fig. 7.13. Variation of critical field H_p with coercive field H_c at different temperatures in the ordered $\text{Ni}_{1-x}\text{Co}_x\text{Pt}$ with $x=0.07$.

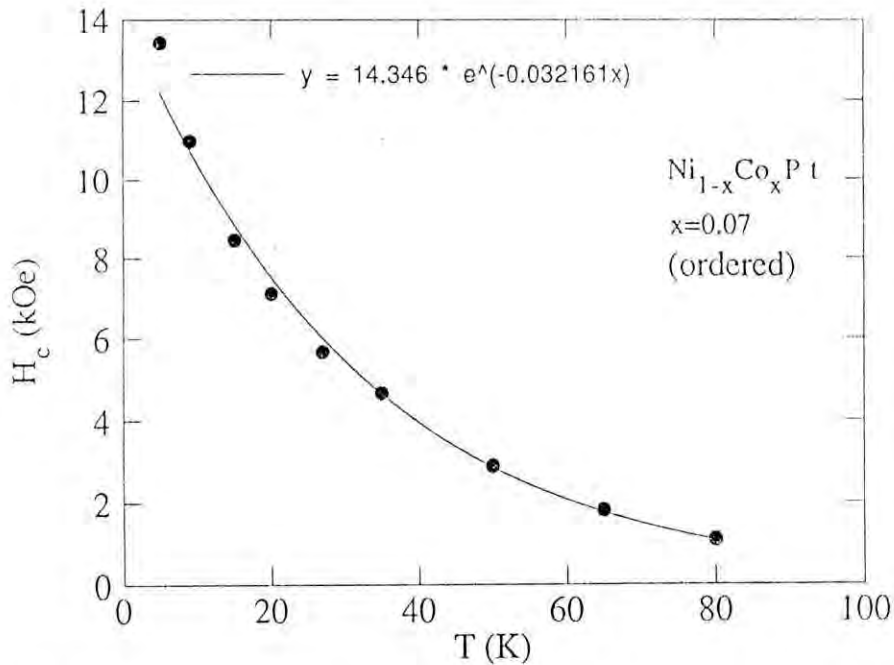


Fig.7.14. Variation of coercive field with temperature of the ordered $Ni_{1-x}Co_xPt$ with $x=0.07$ which is fitted by an exponential.

do not show any sign of ferromagnetic transition indicating that the antiferromagnetic interactions have overcome the ferromagnetic ones. From Figs. 7.16 and 7.17 it is evident that the samples are multiphase and both the phases are ferromagnetic with two different T_C . This supports the results of x-ray and SEM. It is quite difficult to determine precise value of T_C from these measurements. Curie temperatures of the two phases can be estimated from these curves. It appears that the Curie temperatures determined for the two different phases of the sample with $x=0.02$ are 20 and 50 K while 85 K and 105 K for $x = 0.05$. Thermoremanent magnetization also demonstrate that the samples are multiphase with two different Curie temperatures for the samples $x = 0.02$ and 0.05 , but for the sample $x = 0.1$, TRM measurement shows a single Curie point and x-ray analysis could not detect second phase in

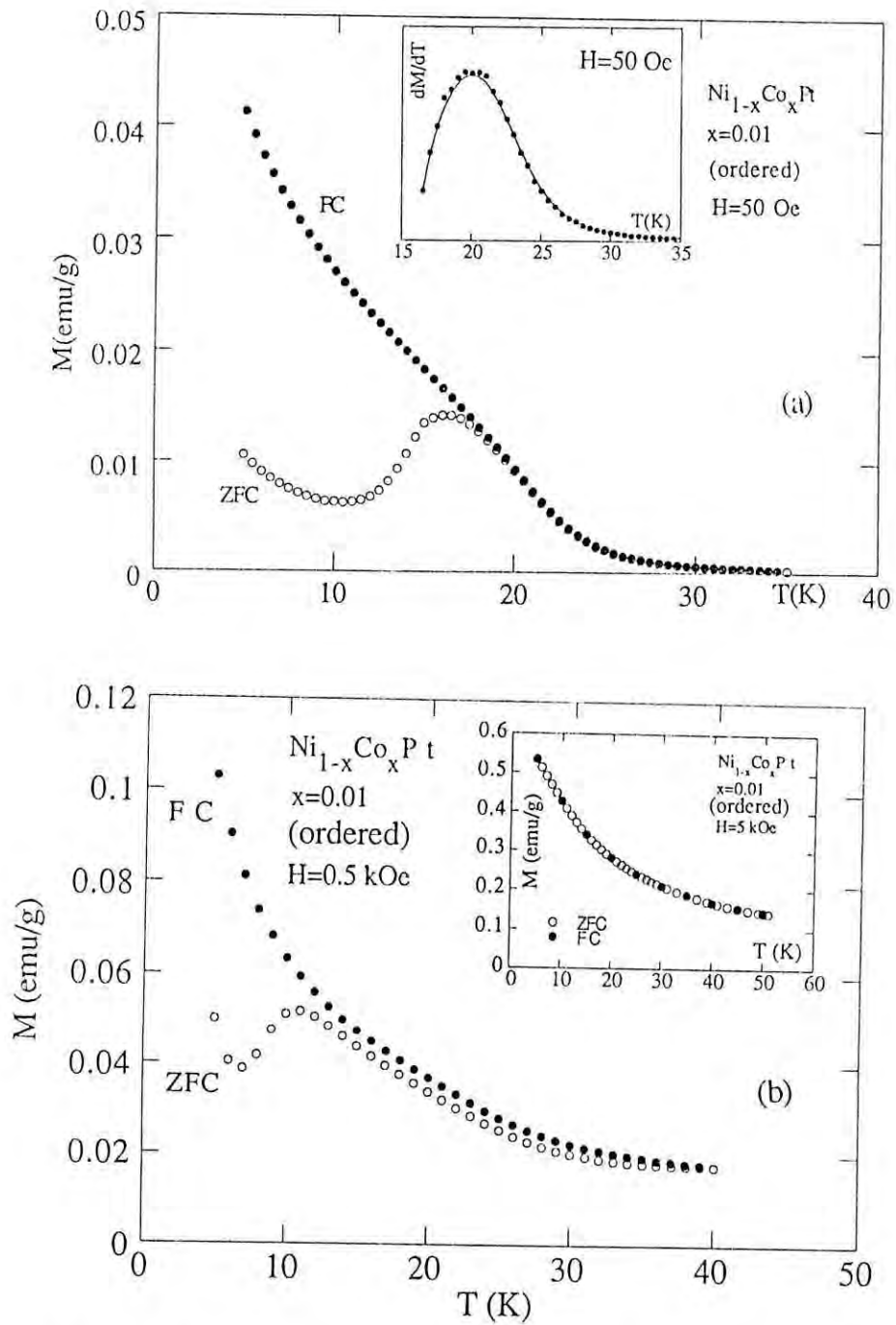


Fig.7.15. Temperature dependence of the zero field cooled and field cooled magnetization of the ordered $\text{Ni}_{1-x}\text{Co}_x\text{Pt}$ with $x=0.01$ at magnetic field of (a) 50 Oe (b) 0.5 kOe; inset: ZFC and FC magnetization at $H=5$ kOe.

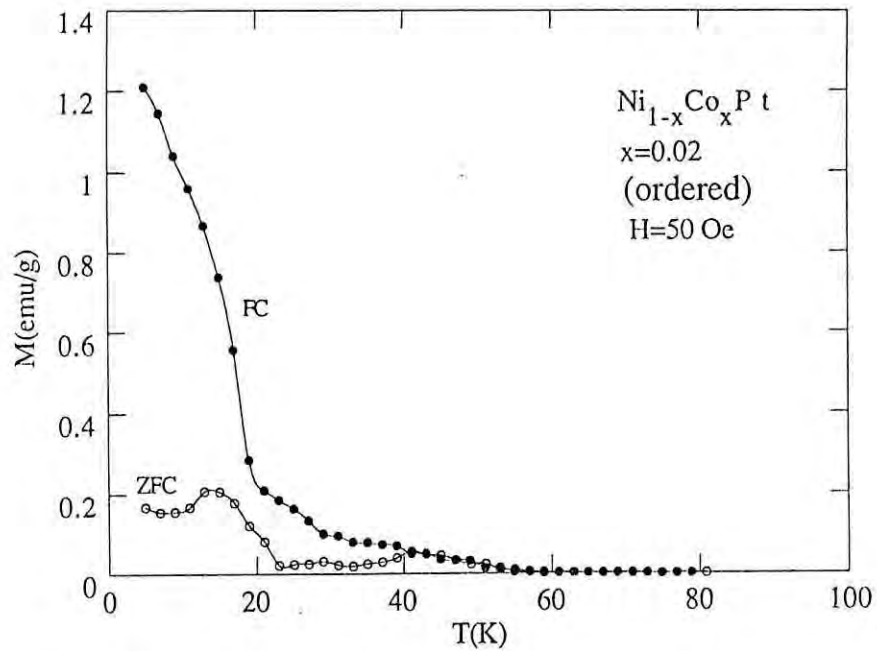


Fig. 7.16. Dependence of ZFC and FC magnetization of the ordered $\text{Ni}_{1-x}\text{Co}_x\text{Pt}$ with $x=0.02$ with magnetic field of 50 Oe.

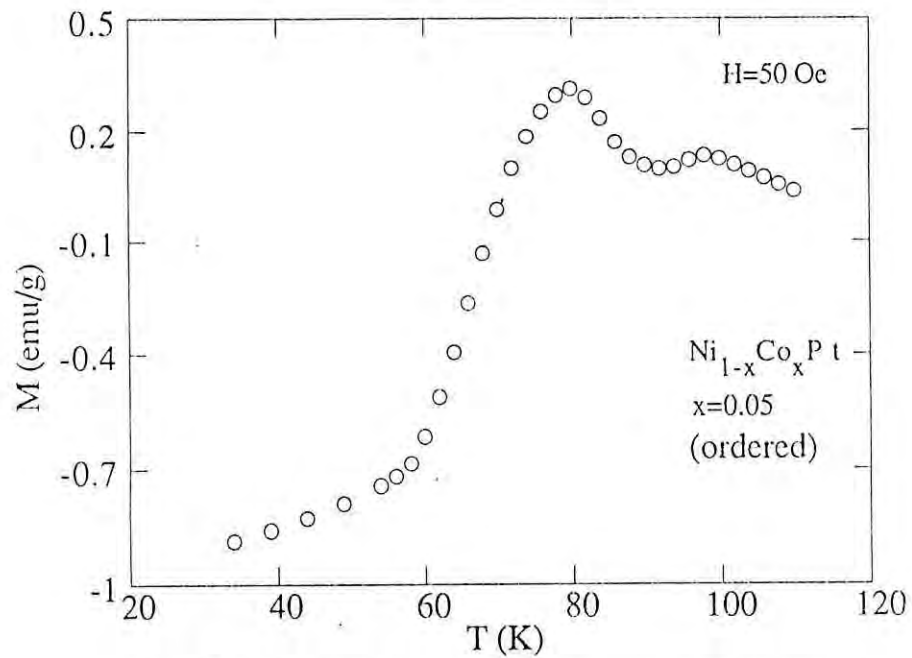


Fig. 7.17. Zero field cooled magnetization as a function of temperature of the ordered $\text{Ni}_{1-x}\text{Co}_x\text{Pt}$ with $x=0.05$ with magnetizing field of 50 Oe.

this composition. Estimation of the T_C from TRM seems quite agreeable with those of the low field DC magnetization measurements. Fig. 7.18 and 7.19 present TRM curves for the samples $x = 0.05$ and 0.1 .

High field magnetization vs temperature curves are shown in Figs. 7.20 - 7.22 for $x = 0.01, 0.07$ and 0.1 respectively. Fig. 7.20 shows that susceptibility does not follow Curie-Weiss law for a larger temperature range. It is only above 220 K that the Curie-Weiss law is obeyed. Below 220 K the alloy show progressive deviations from high temperature Curie-Weiss behaviour. A linear extrapolation of the linear part of the $\frac{1}{\chi}$ vs T gives $\theta = -89$ K and $P_{\text{eff}} = 1.70 \mu_B$. The negative value of θ implies antiferromagnetic interactions. This confirms the result of the magnetization vs temperature at $H = 5$ kOe where antiferromagnetic interactions are considered to be dominant.

The temperature dependence of magnetization for $x = 0.07$ and 0.1 show normal ferromagnetic behaviour observed in ferromagnetic materials showing a transition from ferromagnetic to paramagnetic state. The Curie temperatures for these samples are determined from dM/dT of their respective M vs T curves and are presented in the inset of Figs. 7.21 and 7.22. Due to the scattering of the data broad maxima are observed from which T_C may be determined within an accuracy of ± 5 K. The temperature dependence of the inverse susceptibility of the samples $x = 0.05, 0.07$ and 0.1 are shown in Fig. 7.23 and can be described well by Curie-Weiss law. The magnetic parameters extracted from the linear fitting are collected in Table 7.2.

AC susceptibility have been measured for the samples $x=0.01, 0.02,$ and 0.05 with a lake shore AC susceptometer with AC field of 1 Oe and frequency 125 Hz, in order to determine magnetic phase transition temperatures more accurately and to have a better idea about the domain wall effect of these materials. The real χ' and the imaginary χ'' components of the AC susceptibility of the $\text{Ni}_{1-x}\text{Co}_x\text{Pt}$ alloys with $x=0.01, 0.02$ and 0.05 as a function of temperature are shown in Figs. 7.24-7.26. From these curves magnetic phase transition

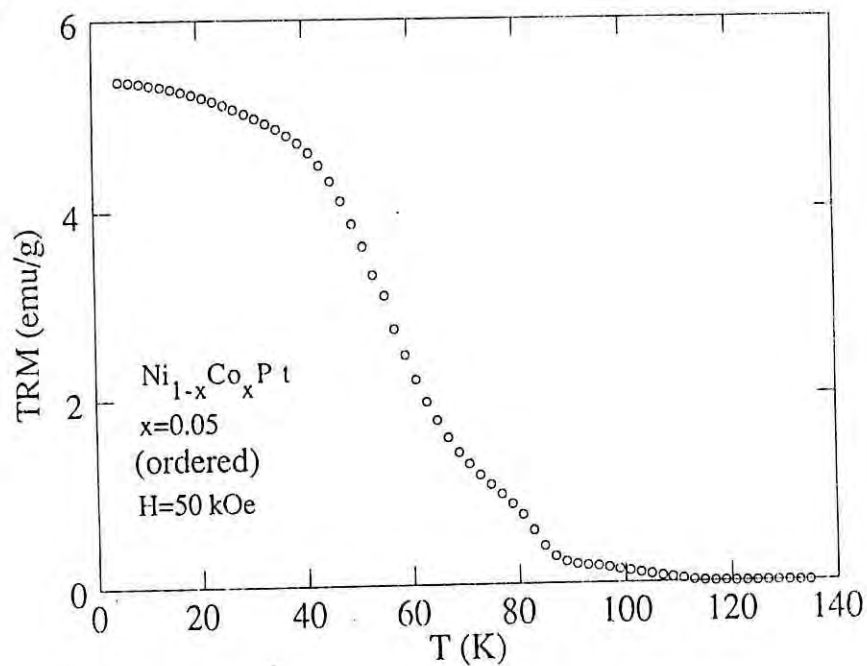


Fig. 7.18. Thermoramanant magnetization of the ordered $\text{Ni}_{1-x}\text{Co}_x\text{Pt}$ with $x=0.05$ cooled with $H=50 \text{ kOe}$.

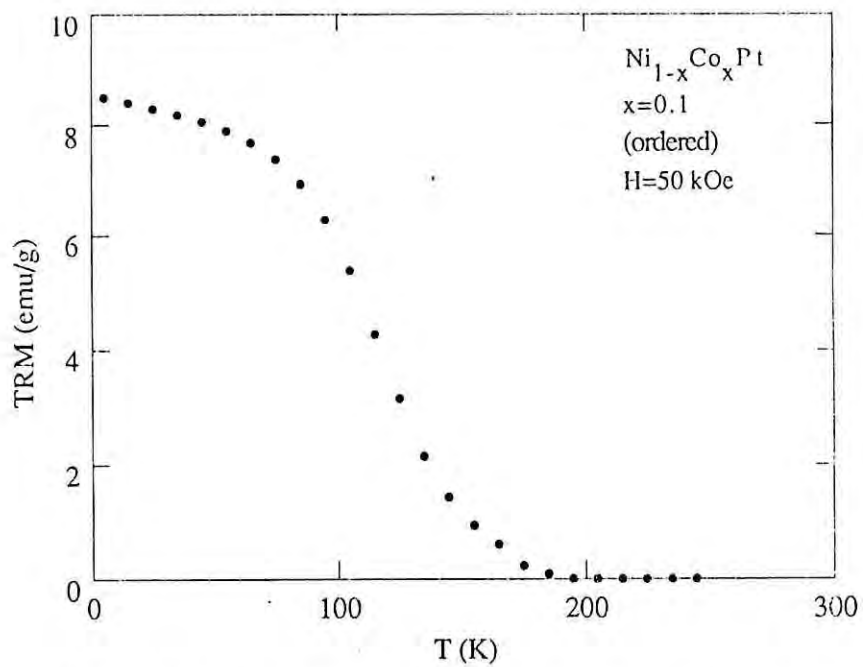


Fig. 7.19. Thermoramanant magnetization of the ordered $\text{Ni}_{1-x}\text{Co}_x\text{Pt}$ with $x=0.1$ cooled with $H=50 \text{ kOe}$.

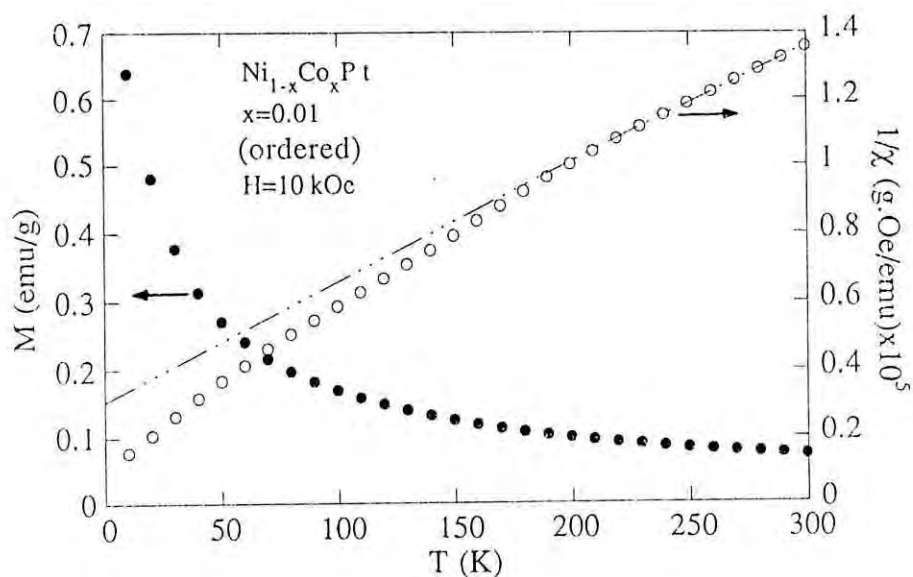


Fig.7.20. Variation of magnetization and reciprocal susceptibility with temperature of the ordered $\text{Ni}_{1-x}\text{Co}_x\text{Pt}$ with $x=0.01$ with applied field $H=10 \text{ kOe}$.

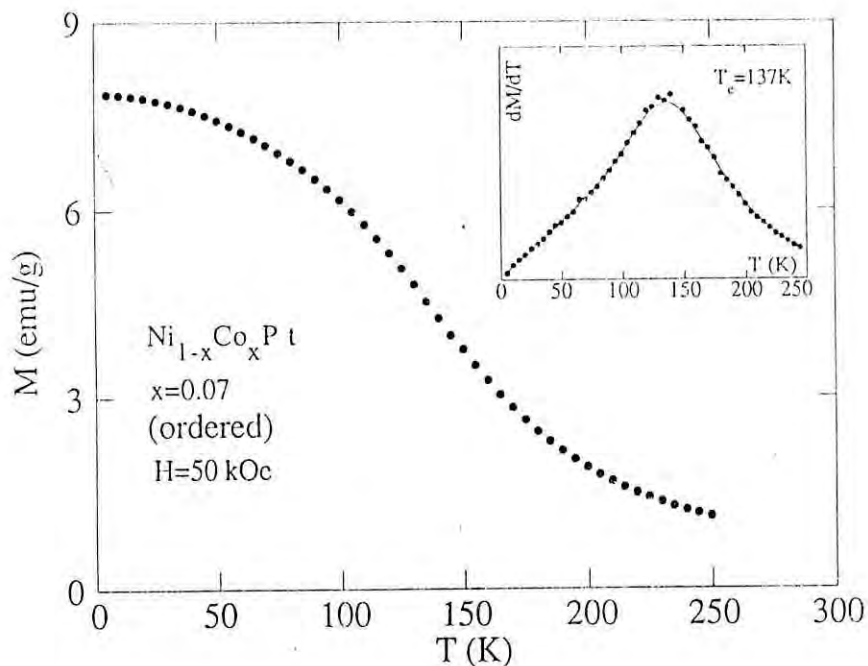


Fig.7.21. Temperature dependence of magnetization of the ordered $\text{Ni}_{1-x}\text{Co}_x\text{Pt}$ with $x=0.07$ with applied field $H=50 \text{ kOe}$; inset: the first derivative of the magnetization with respect to temperature.

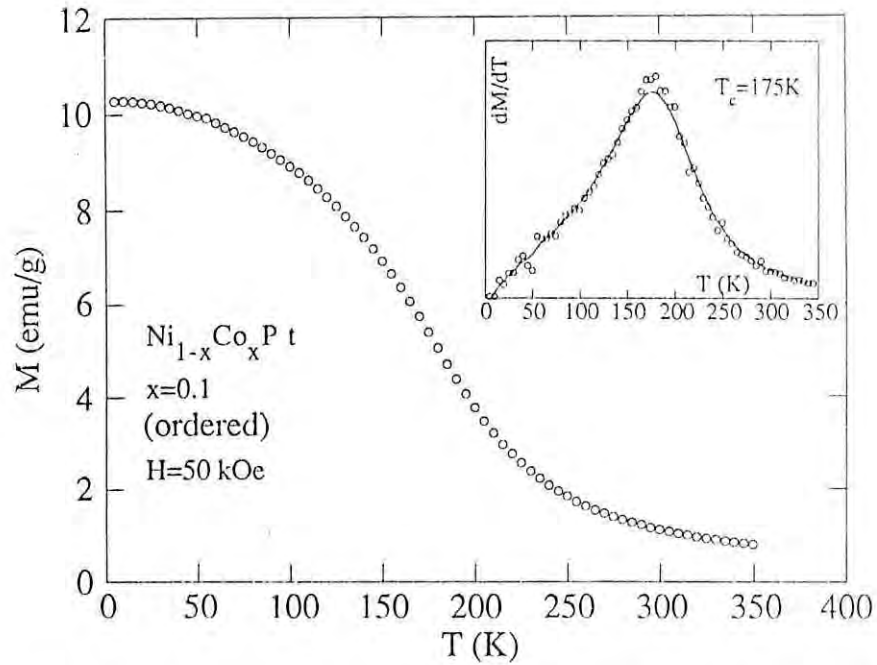


Fig.7.22. Temperature dependence of magnetization of the ordered $\text{Ni}_{1-x}\text{Co}_x\text{Pt}$ with $x=0.1$ with applied field $H=50 \text{ kOe}$; inset: the first derivative of the magnetization with respect to temperature.

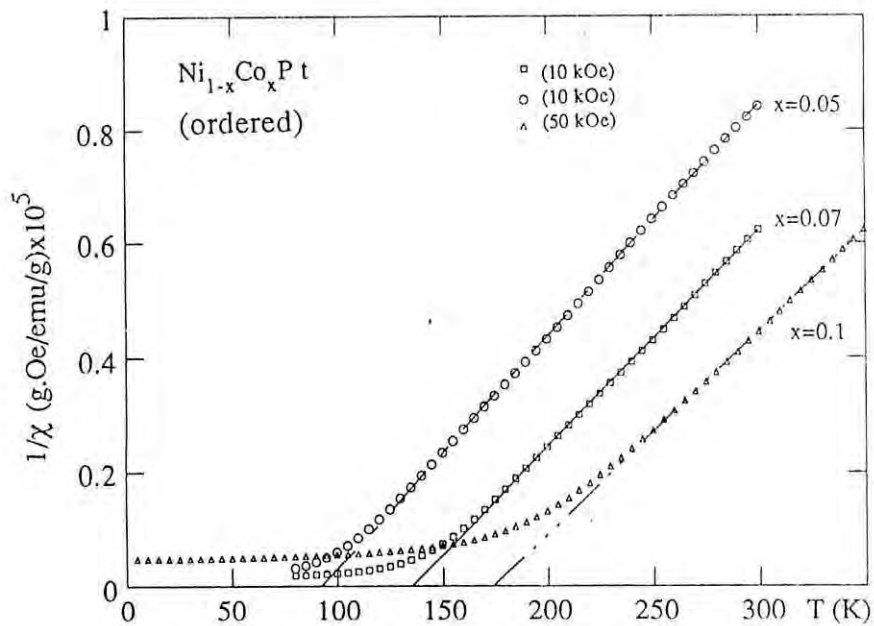


Fig.7.23. Temperature dependence of the inverse susceptibility of the ordered $\text{Ni}_{1-x}\text{Co}_x\text{Pt}$ with $x=0.05$ and 0.07 with $H=10 \text{ kOe}$ and with 0.1 with $H=50 \text{ kOe}$.

temperatures of the samples have been determined from the maxima of the $\frac{d\chi}{dT}$ of these curves. It is observed from the curves that the Curie temperatures of the composition having two ferromagnetic phases can be determined more accurately than the DC magnetization measurement. Figs. 7.24a and b show that the magnitude of χ' and χ'' are dependent on the frequency which increase with increasing frequency. But the Curie temperature of the sample remains unchanged varying the frequency from 15 Hz to 1000 Hz. It is also observed that the alloy with $x=0.01$ shows a single transition temperature while $x=0.02$ and 0.05 have two well defined Curie temperatures, i.e., they have at least two phases and both of them are ferromagnetic. It is observed that the AC susceptibility of all the samples increase dramatically with decreasing temperature and after passing through the ferromagnetic transition temperatures they attain their maximum values. Further lowering of the temperature the AC susceptibility decreases sharply to a very low value and remains almost constant upto the lowest temperature. This low temperature decrease of the AC susceptibility suggests that the domain wall movement becomes increasingly difficult with decreasing temperature and also implies that at this low temperature the domain wall is pinned. The domain wall can not move under the excitation of the external AC field, therefore making no contribution to the AC susceptibility. For the sample $x=0.01$ it is observed that χ' decreases at low temperature and again increases below 10 K. This can be explained that at still lower temperature there might be a ferromagnetic state.

Dependence of magnetic moment μ and Curie temperature T_C with Co concentrations are displayed in Figs. 7.27 and 7.28. Addition of Co increases magnetic moment and Curie temperature. The increase of magnetic moment and the Curie temperature is more for the low concentration of Co. It is observed that the substitution of Co for Ni induces giant moments in the ferromagnetic and paramagnetic NiPt alloys. Fig. 7.29 shows the magnetic moment per Co atom as a function of Co concentration x in both the ordered and disordered phases. The values of the giant moments for the disordered phases are large compared to the ordered phases particularly at lower Co concentrations. This is in contrast

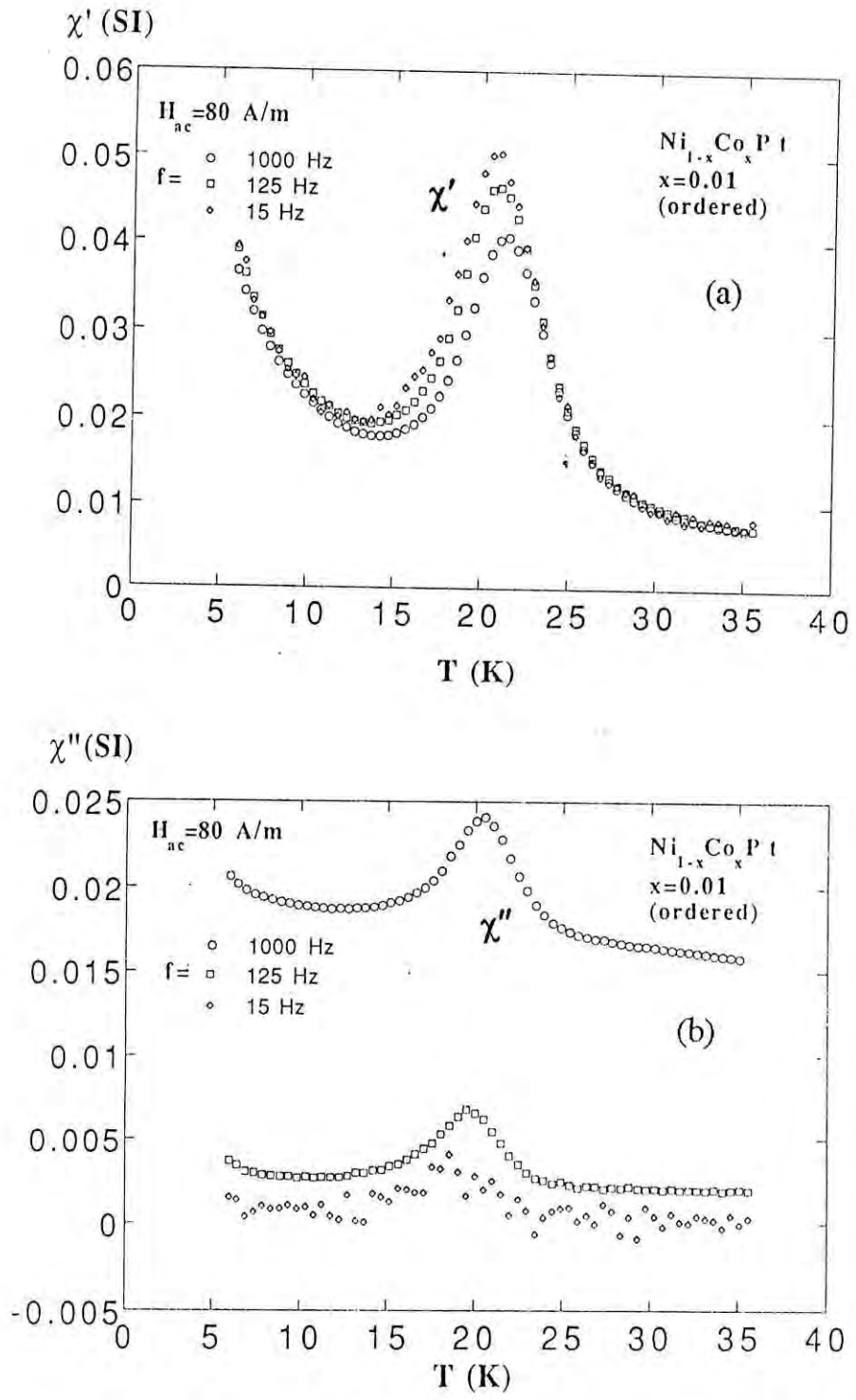


Fig.7.24. Temperature dependence of (a) real component χ' and (b) imaginary component χ'' of the AC susceptibility of the ordered $\text{Ni}_{1-x}\text{Co}_x\text{Pt}$ with $x=0.01$ at an applied AC field of 1 Oe (80 A/m) at different frequencies.

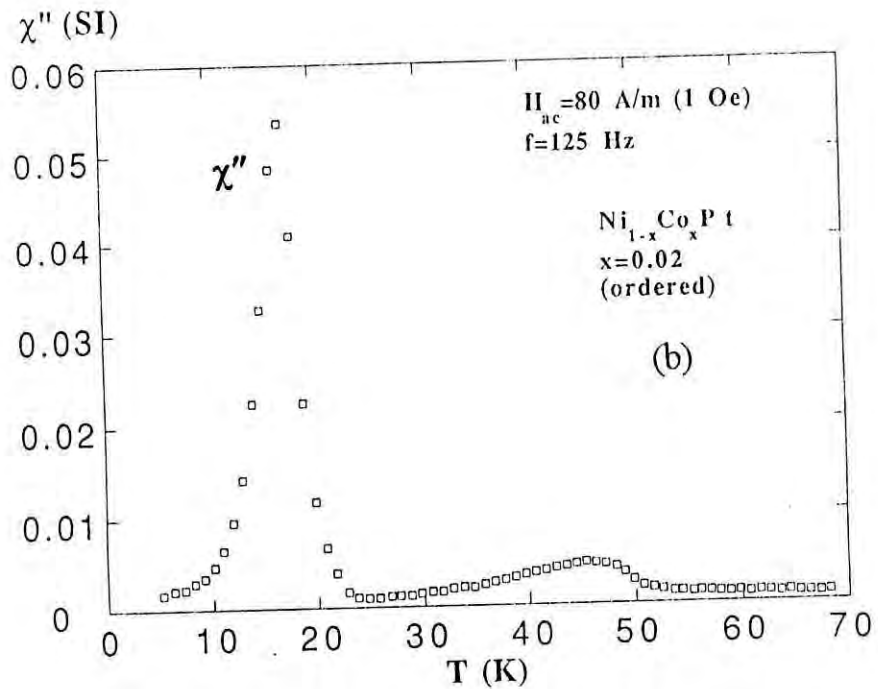
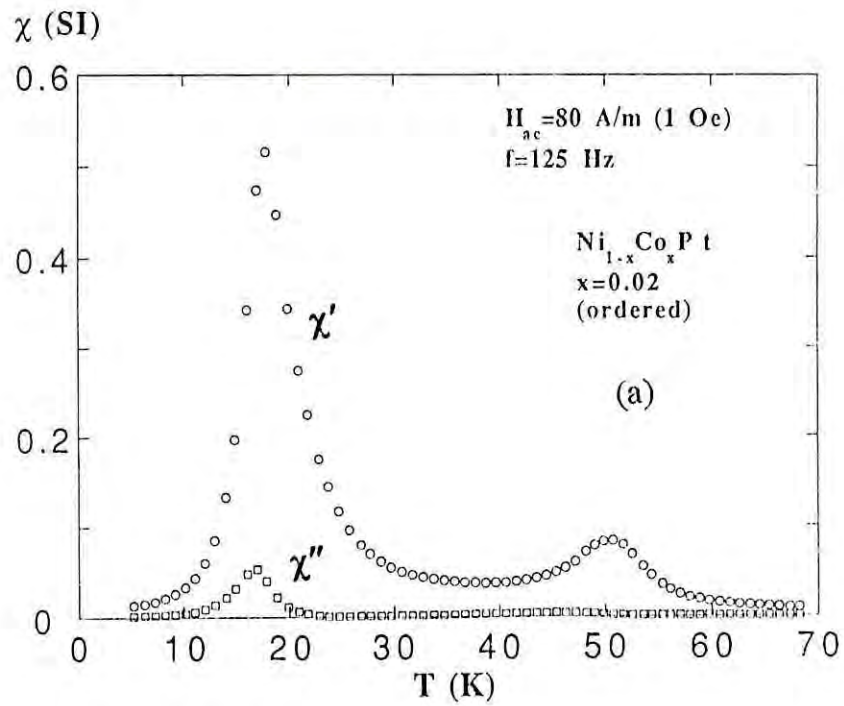


Fig.7.25. Temperature dependence of (a) real χ' and imaginary χ'' component of the AC susceptibility of the ordered $\text{Ni}_{1-x}\text{Co}_x\text{Pt}$ with $x=0.02$ at AC field of 1 Oe (80 A/m) and frequency 125 Hz, (b) χ' and χ'' .

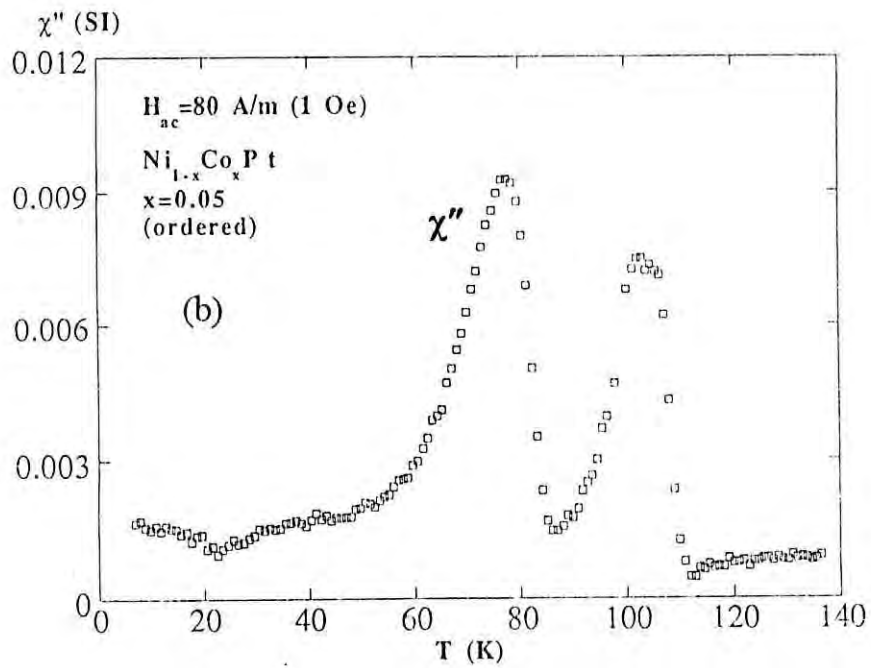
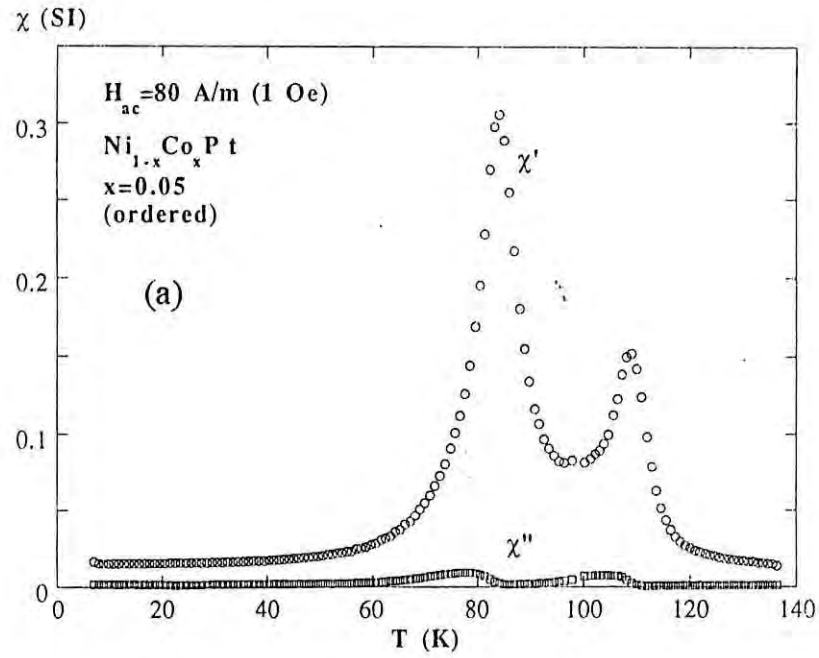


Fig.7.26. Temperature dependence of (a) real χ' and imaginary χ'' component of the AC susceptibility of the ordered $Ni_{1-x}Co_xPt$ with $x=0.05$ at AC field of 1 Oe (80 A/m) and frequency 125 Hz. (b) shows χ'' .

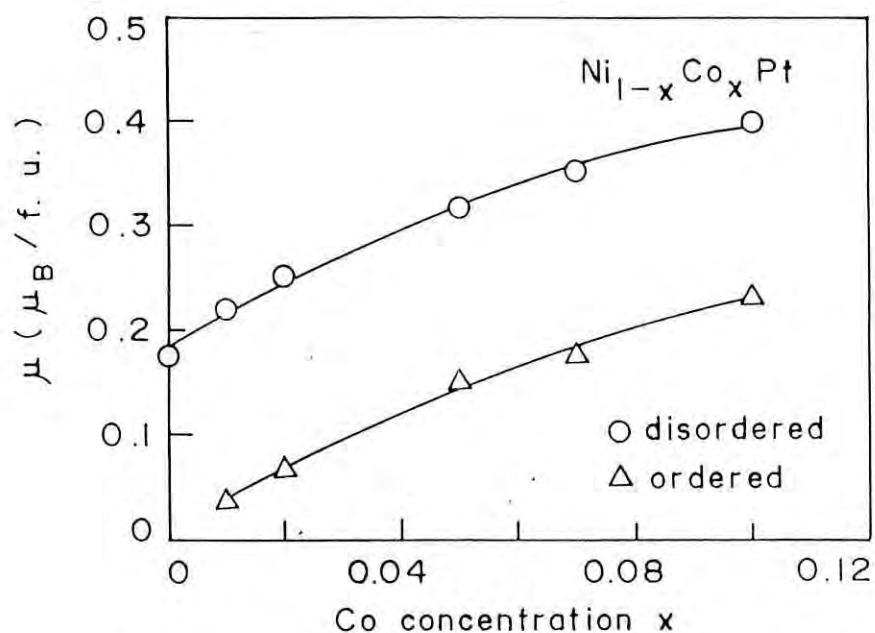


Fig.7.27. Magnetic moment per formula unit of the ordered and disordered $\text{Ni}_{1-x}\text{Co}_x\text{Pt}$ alloys as a function of Co concentration x .

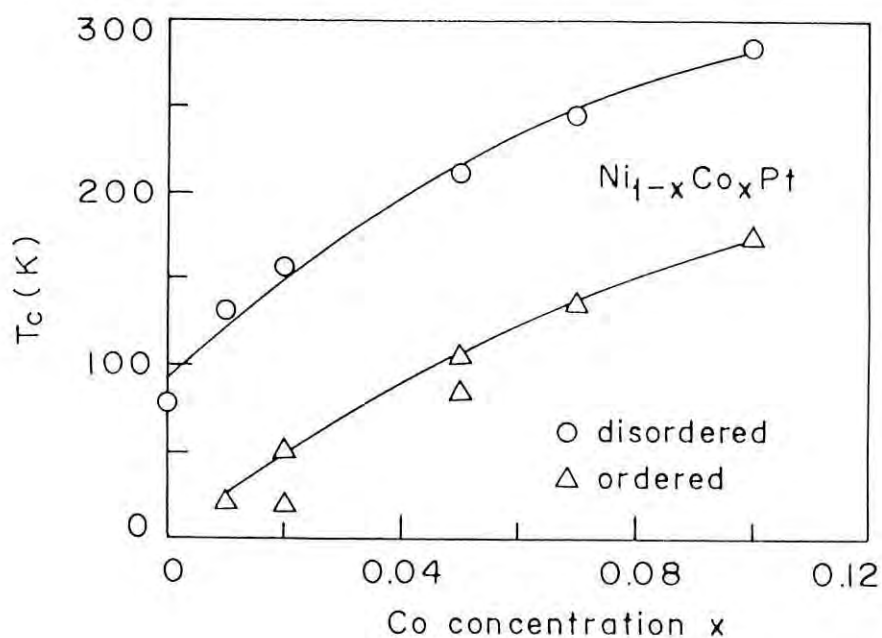


Fig.7.28. Dependence of the Curie temperature of the ordered and disordered $\text{Ni}_{1-x}\text{Co}_x\text{Pt}$ alloys against Co concentration x .

with the result obtained for the Fe doped system. The giant moment per Co atom for both the phases are sensitive to the Co concentrations and have higher values for lower concentrations. This can be explained according to Kim and Schwartz(10) that the polarizability decreases with increasing polarization. The effect has experimentally been observed in Pd and Pt based alloys with Co by a decrease of average magnetic moment per Co atom with increasing its concentration. The giant moment per Co atom in the Co doped alloys is calculated from the increase in magnetic moment due to the replacement of Ni atoms by Co atoms and by attributing net increased moment to the Co atoms taking into account the moment of Ni atoms which are replaced. The giant moment varies from $8 \mu_B$ per Co atom for $x = 0.01$ to $4.68 \mu_B$ per Co atom for $x = 0.1$ for the ordered phases compared to that of $9.28 \mu_B$ and $4.76 \mu_B$ per Co atom for the disordered phases with $x = 0.01$ and 0.1 respectively. This large moment associated with a Co atom is interpreted as due to the polarization of matrix parallel to the Co moment and the net moment is attributed to the Co atom.

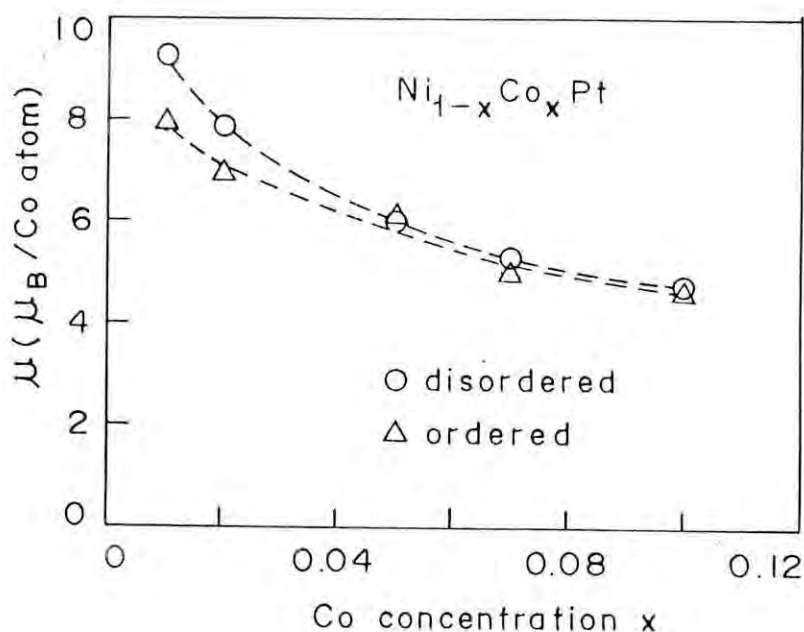


Fig.7.29. Magnetic moment μ per Co atom of the ordered and disordered $Ni_{1-x}Co_xPt$ alloys as a function of Co concentration x .

Table 7.2 Magnetic properties of ordered $\text{Ni}_{1-x}\text{Co}_x\text{Pt}$

Cobalt content x	0	0.01	0.02	0.05	0.07	0.1
M(emu/g) T=5K H=50kOe	0.95	1.17	3.07	6.76	7.8	10.28
M_T (emu/g) T=5K		0.09	1.53	5.41	5.71	8.56
μ (μ_B /f.u.)		0.04	0.07	0.154	0.177	0.234
T_c (K)		22	20 52	85 106	137	175
θ (K)		-87	19	92	135	174
C(emuK/mole)		0.36	0.28	0.313	0.338	0.358
P_{eff} (μ_B /f.u.)		1.70	1.50	1.58	1.65	1.69
μ (μ_B /Co)		8.0	7.0	6.16	5.06	4.68

Reference

1. Ododo, J.C., *J.Phys.F: Metal Phys.*, 1979, Vol.9, 1441
2. Crangle, J., and W.R.Scott, *J. Appl. Phys.* 1965, 36, 921
3. Bozorth, R.M., D.D.Davis, and J.H.Wernick, *J.Phys.Soc.Jpn*, 1962, 17, Suppl.B1, 112
4. Foner, S., E.J.McNiff Jr., and R.P.Guertin, *Phys.Letters*, 1970, 31A, 466
5. Swallow, G.A., G.Williams, A.D.C.Grassi, and J.W.Loram, *Phys. Rev.*, 1975. B11, 330
6. Tsiovkin, Y.N., and N.V.Volkenshteyn, *Phys.Metal Metallog. (U.S.S.R) (English translation)*, 1965, 19, 45
7. Rudman, A., 1963, Ph.D. thesis, University of Nottingham, U.K.
8. Stewart, K.H., *J. de Phys. et Radium*, 1951, 12, 325
9. Williams, H. J., M., Goertz, *J. Appl. Phys.* 1952, 23, 316
10. Kim, D.J. and B. Schwartz, *Phys., Rev, Lett.*, 1968, 20, 201

CHAPTER-8

Conclusion:

Nickel-platinum system has been widely studied mainly for the disordered phases inspite of the fact that it undergoes order-disorder transition. Even for the disordered phases the understanding of whether the magnetization is homogeneous or inhomogeneous near the critical concentration is incomplete. Moreover the existing reports on the concentration dependence of the Curie temperature for the disordered alloys have given rise to a controversial picture. It appears that the values of the Curie temperatures as determined by previous workers for the disordered alloys near the critical concentration are also in disagreements. In the present state of the above mentioned discrepancies and also for an understanding of the effect of atomic ordering on the magnetic properties, which hitherto has not been studied in much detail, Ni-Pt system offers a good opportunity to investigate in detail the magnetic properties in both the ordered and disordered phases.

A systematic investigation of the magnetic properties of $\text{Ni}_{1-x}\text{Pt}_x$ alloys with $x=0.14, 0.24, 0.30, 0.44, 0.50$ and 0.57 has been performed on polycrystalline samples by means of magnetization measurements in the ordered and disordered phases using SQUID magnetometer , Vibrating Sample Magnetometer and AC Susceptometer in the temperature range of 2 K and above the Curie temperature and magnetic field upto 50 kOe. Particular attention has been given to the alloys near the critical concentration. The very high sensitivity of the SQUID magnetometer opens new possibilities for the study of magnetic phenomena than have been possible until now. Special emphasis is laid on the determination of the Curie temperatures in which different methods like AC susceptibility, kink point method and Arrott plots are employed for a good comparison of these diverse techniques.

Magnetic moments in Bohr magneton and Curie temperatures for the alloys in both the phases have been determined. From the concentration dependence of magnetic moments and Curie temperatures, critical concentration for the disordered phases is determined and found to be approximately equal to 57 at.% Pt. It is found that the magnetic moment decreases continuously and non linearly with Pt concentration and vanishes at around 57 at.% Pt. A linear dependence of Curie temperature with Pt concentration is observed. Linear extrapolation of the Curie temperature $T_C=0$ indicates a critical concentration of 57.2 at.% Pt. Two independent methods employed for determining the critical concentration provide a consistent picture by giving identical values. The linear dependence of the Curie temperature with concentration is valid over the whole ferromagnetic regime upto pure nickel. This linear dependence of T_C with concentration agrees well with the proposed localized model and disagrees with the square root dependence proposed for an weak itinerant model as reported by previous workers for the disordered Ni-Pt system. The magnetic isotherms for the ordered alloy with $x=0.44$ have been analyzed in terms of Arrott plots and show that this alloy must be very close to the critical concentration for the onset of ferromagnetism. The value of this critical concentration for the ordered Ni-Pt alloys is in agreement with the value shown in the recent phase diagram. Clustering effects have been observed from the analyses of the magnetic isotherms for the alloys near the critical concentration for the ordered and disordered alloys. This implies that the magnetization appears inhomogeneously at the critical concentration region for both the phases and disagrees with the previous reported results where the appearance of homogeneous magnetization have been claimed for the disordered alloys near the critical concentration from the observed linearity of the Arrott plots. However, the present result is in conformity with the Ni-Pd and many other nickel based binary alloys in which magnetization appears inhomogeneously in the form of ferromagnetic clusters near the critical concentration. For the Ni-Pd alloys near the critical concentration it is therefore claimed that linear Arrott plots have been observed

inspite of inhomogeneous magnetization. It has been demonstrated in the present study that the inconsistent values of the Curie temperatures for the alloys near the critical concentration are due to the use of high magnetic fields in measuring the Curie temperatures. This shows why it is essential to use very low field for the determination of the Curie temperatures of the alloys close to the critical concentration.

The depression of the magnetic moment and the Curie temperature in $L1_2$ phase and the vanishing of the ferromagnetism in the $L1_0$ phase around the stoichiometric compositions Ni_3Pt and $NiPt$ respectively on ordering have been explained in terms of the change in local environment. In an ordered phase a Ni atom has nearest neighbour number of Ni atoms which is always less than that in the disordered phase. Assuming Ni-Ni interactions dominant, a reduced value of the molecular field coefficient is expected on ordering with a consequent reduction in T_C . In the $L1_0$ phase of the equiatomic $NiPt$, a Ni atom has 4 Ni nearest neighbours. Since at the critical concentration of the disordered alloy a Ni atom has on the average 5 Ni nearest neighbours, it is understood that the nearest neighbour number of a Ni atom must exceed four to have ferromagnetism in $NiPt$ system. In other words Ni atoms belonging to nearest neighbour groups of approximately 5 Ni atoms or more get ferromagnetically ordered.

Pseudobinary $Ni_{1-x}Fe_xPt$ alloys with $x=0.02, 0.05, 0.1$ and 0.2 and $Ni_{1-x}Co_xPt$ alloys with $x=0.01, 0.02, 0.05, 0.07$ and 0.1 have been studied for the disordered and ordered phases together to see the effect of an Fe or Co atom in terms of exchange interaction and moment disturbance in the equiatomic $NiPt$ and also the behaviour of these 3d atoms in the inducement of giant moments as expected.

In the pseudobinary $Ni_{1-x}Fe_xPt$ and $Ni_{1-x}Co_xPt$ alloys, substitution of small amount of Fe or Co rapidly increases magnetic moment and the Curie temperature in the ordered and disordered states and is interpreted as due to the polarization of the host matrix by the substituting elements and enhanced exchange interactions among the

magnetic moments. This increase in magnetic moment and Curie temperature is faster for the lower concentrations of Fe or Co than for the higher concentrations. Giant moments have been observed in both the ordered and disordered phases of Fe and Co doped systems. These giant moments are sensitive to Fe and Co concentrations and have higher values per atom for lower concentrations. This is understandable from the fact that the polarizability decreases with increasing polarization. As the concentration of Fe or Co increases the substituted atoms find themselves in a region which are already polarized and can not contribute more to the polarization. As a result the magnetic moment per Fe or Co atom decreases. Disordered Fe and Co doped pseudobinary alloys behave as soft magnetic materials with no hysteresis effect and the magnetization is saturated with magnetizing field $H < 4$ kOe. But the ordered alloys show hysteresis effect and the magnetization is not saturated with magnetic field of 50 kOe implying that high anisotropy energy is associated with the ordered alloys and consequently have narrow domain walls.

Domain wall pinning effect is found in the pseudobinary $\text{Ni}_{1-x}\text{Fe}_x\text{Pt}$ and $\text{Ni}_{1-x}\text{Co}_x\text{Pt}$ alloys. Precipitated phase as identified by X-ray and SEM studies is considered as the source of pinning centres. Initial magnetization behaviour and the field dependence of coercive field and the remanence of the ordered $\text{Ni}_{1-x}\text{Fe}_x\text{Pt}$ alloys strongly suggest that the domain walls are pinned upto the value of coercive field after which magnetization increases sharply and approaches toward saturation indicating that the magnetization process is governed by domain wall pinning. Temperature dependence of coercive field $H_c(T)$ and critical field $H_p(T)$, the field required to free the domain wall from the pinning centers, have been measured and found that they are proportional to each other, i.e., $H_c(T) \propto H_p(T)$ and the constant of proportionality is almost equal to one. Temperature dependence of coercivity of the ordered $\text{Ni}_{1-x}\text{Fe}_x\text{Pt}$ alloys and

$Ni_{1-x}Co_xPt$ with $x=0.07$ is explained as due to thermal activation process of the domain wall unpinning and the temperature dependence of the height of the energy barriers created by the defects in these alloys.

